INFORMATION TO USERS

This manuscript has been reproduced from the microfilm master. UMI films the text directly from the original or copy submitted. Thus, some thesis and dissertation copies are in typewriter face, while others may be from any type of computer printer.

The quality of this reproduction is dependent upon the quality of the copy submitted. Broken or indistinct print, colored or poor quality illustrations and photographs, print bleedthrough, substandard margins, and improper alignment can adversely affect reproduction.

In the unlikely event that the author did not send UMI a complete manuscript and there are missing pages, these will be noted. Also, if unauthorized copyright material had to be removed, a note will indicate the deletion.

Oversize materials (e.g., maps, drawings, charts) are reproduced by sectioning the original, beginning at the upper left-hand corner and continuing from left to right in equal sections with small overlaps. Each original is also photographed in one exposure and is included in reduced form at the back of the book.

Photographs included in the original manuscript have been reproduced xerographically in this copy. Higher quality 6" x 9" black and white photographic prints are available for any photographs or illustrations appearing in this copy for an additional charge. Contact UMI directly to order.

UMI

A Bell & Howell Information Company
300 North Zeeb Road, Ann Arbor MI 48106-1346 USA
313/761-4700 800/521-0600

Université d'Ottawa · University of Ottawa

STRENGTH OF EDGE COLUMN-SLAB CONNECTIONS OF POST-TENSIONED CONCRETE FLAT PLATES

by

© **Haki Sharifi**

A thesis
presented to the University of Ottawa
in partial fulfillment of the
requirements for the degree of
Master of Applied Science in
Civil Engineering

Department of Civil Engineering
University of Ottawa
Ottawa, Ontario, Canada
March 1998

The M.A.Sc. in Civil Engineering is a joint program
with Carleton University administered by
the Ottawa-Carleton Institute for Civil Engineering

ABSTRACT

The strength and behavior of edge column-slab connections of two way unbonded post-tensioned flat slab under uniformly distributed load were investigated. A square flat slab, two bays in each direction was constructed. The span of each bay was 3.2 m (10.5 ft) and the slab 89 mm (3.5 in) thick. The average prestress on the concrete, after deducting losses, was 2.7 MPa in the east-west direction and 2.8 MPa in the north-south direction. The maximum drape of the tendons was 70 mm at mid-span and the interior support and 50 mm at the edge of the slab. No supplementary reinforcement was used. The cylinder compressive strength of the concrete was 45 MPa at 28 days.

Initially the slab behaved elastically and no residual deflections were observed upon releasing the load up to 5.8 kN / m^2 (0.85 psi). Punching shear failure happened at a load of 23.6 kN / m^2 at the edge column-slab connection #2. The failed connection(s) were repaired and shored, tendons re-tensioned and the slab reloaded to fail the next connection. The edge column slab connections failed at 26.27 kN / m^2 for connection # 8, 25.70 kN / m^2 for connection # 6 and 23.94 kN / m^2 for connection # 4 respectively. Progressive collapse occurred in Test # 5. The interior connection failed due to loss of force in the tendons passing through connection # 6 which failed at a load of 29.20 kN/ m^2. To investigate the behaviour of corner column-slab connections all edge and the interior connections were shored. The slab failed by punching shear at a shored, previously failed edge connection at a load of 32.1 kN/ m^2. All the corner connections survived this test.

The measured moments and axial forces transferred to edge and corner columns were compared with those calculated by the Direct Design Method and Equivalent Frame Analysis. It was found that these two linear methods give values close to the test results.

The shear strength obtained from the analysis of the experimental work was compared with previous research work, ACI 318-95 and CSA A23.3-94 concrete design codes and the 1995 Gardner proposed equation.

In spite of the fact that no bonded reinforcement was provided, the slab behaved smoothly right to the point of punching shear failure. In most codes supplementary steel is required and can be justified as back up in case of unexpected failure in the tendons due to corrosion or anchorage damage. Bonded reinforcement also helps in controlling cracks as well as prevents or reduces slab stiffness degradation.

ACKNOWLEDGMENTS

The author would like to express his deepest gratitude to his supervisor Professor Dr. N. J. Gardner for his untiring advice, encouragement and support during the M. A. Sc. degree program.

The author thanks the technical staff of the Civil Engineering Department, especially Mr. Mongi Grira and Mr. Robert Moore for their help during the experimental work.

The author is grateful to the friends who contributed their help and support, especially Derek Mess, Jungsuck Huh and Jamal Kurdi who provided their valuable assistance and time during casting and testing of the slab.

The author is grateful to his dear parents and sisters for their unlimited love and support during his whole life.

Last, but certainly not least, the author expresses his deep appreciation to his fiancée, Majd for her understanding and encouragement to finish writing the thesis.

To

My Parents

AND

My Fiancée

CONTENTS

NOTATIONS

A_{ps}	Area of prestressing tendons
A_s	Area of bonded reinforcement
b_o	Perimeter of critical section
c_o	Column perimeter
c_1, c_2	Column side length
d	Average effective depth of tensile reinforcement
d_r	Effective depth of bonded reinforcement
d_{ps}	Effective depth to actual tendon profile
d_b	Reinforcement bar diameter
E_s	Modulus of elasticity of reinforcement
f'_c	Characteristic compressive strength of concrete cylinders
f_{ck}	Specified compressive strength of concrete cylinders
f_{cu}	Characteristic concrete prestress
f_{pc}	Average initial concrete prestress
f_{pcu}	Average ultimate concrete prestress prior to failure
f_r	Modulus of rupture
f_{se}	Effective initial prestressing force in cables
f_{ps}	Stress in prestressing steel developed at ultimate

f_{pu}	Characteristic strength of prestressing tendons
f_y	Yield stress of the reinforcement
h	Overall thickness of slab
J	Polar moment of inertia of the critical section
ls	Distance from the column face to the loaded area
L	Slab span
m	Slab moment per unit width
P_{shear}	Calculated ultimate shear load
P_{flex}	Calculated ultimate flexural load
P_{pb}	Force in tendon at failure
P_{pe}	Initial force in tendon
P_s	Transverse component of prestressing force
P_u	Collapse load
P_o	Decompression load
P_{up}	Ultimate Punching load in prestressed slab
s	Cable spacing
V	Column axial load or punching shear stress in compression zone
V_c	Shear strength of concrete
V_p	Vertical component of all prestress forces crossing the critical section
V_u	Ultimate shear force
V_d	Shear carried by dowel force

T_o	Total forces in both bonded and prestress reinforcement
x_p	Depth of neutral axis in a reinforced concrete slab
β	Fraction of slab span
ϕ_o	Ratio of P_{shear} / P_{flex}
ρ	Average percentage of tensile reinforcement
ρ_s	Ratio of ordinary bonded reinforcement
ρ_{ps}	Ratio of prestressed reinforcement
ρ_e	Equivalent reinforcement ratio
ρ_l	Reinforcement in the longitudinal direction
ρ_t	Reinforcement in the transverse direction
κ	Ratio of column size to slab thickness
ϵ_{cc}	Strain in concrete at failure
ϵ_{ct}	Strain in concrete in tangential direction
ϵ_{cr}	Strain in concrete in radial direction
ϵ_{pe}	Initial strain in tendon
ϵ_{pb}	Strain in tendon at ultimate
γ_p	Level of prestressing
γ_f	Fraction of unbalanced moment transferred by flexure
γ_v	Fraction of unbalanced moment transferred by shear

LIST OF TABLES

LIST OF FIGURES

CHAPTER 1

FLAT PLATES

1.1 Development of flat slabs :-

Flat slabs were first used in the USA at the beginning of this century. They were provided with drop panels and used for warehouses and structures under heavy loads. Punching shear was not a big problem because of the drop panels. Then plates were developed and used without drop panels. They became popular for residential and commercial buildings. Flat plates became popular because of their simple construction and are preferred by architects due to their good esthetics. Although all design codes have empirical regulations for the design of the flat slabs or flat plates, there are some issues in this area where our knowledge is limited, for instance the magnitudes of the moments transferred from the slab to the columns, the effect of load eccentricity on the shear strength of edge column-slab connections and the effect of the concrete compressive strength on the punching shear strength.

Prestressed concrete slabs were developed in the 1950's as alternatives to the then prevalent reinforced concrete flat slabs. Prestressed concrete slabs require less depth than reinforced flat slabs for the same limiting deflection. In prestressed construction, the designer is able to reduce or eliminate the deflection by an appropriate choice of prestress and eccentricity. In addition, prestress reduces cracking in the slab so it can be used for watertight floors. Moreover, greater shear strength can be obtained for the same slab depth.

Prestressed concrete construction can be either post-tensioned or pre-tensioned. In pre-tensioned construction, stress is applied to the steel before the concrete is placed. While in post-tensioned elements, stress is applied to the tendons after the concrete has been cast and cured. Post-tensioning offers more benefits than pre-tensioning in that it permits more effective use of high strength materials, stage stressing and has lower pre-stress losses.

There are two kinds of post-tensioned concrete structures, bonded and unbonded. Bonded post-tensioned strands are located in a sheath that is grouted after the tendons have been stressed. Unbonded tendons consist of a number of strands in a plastic sheath filled with grease. Unbonded tendons have lower friction losses, permit fast placing and do not need to be grouted. In Canada, the USA and Britain most prestressed concrete flat plates are unbonded, while in Australia bonded flat plates are dominant. The disadvantage of unbonded flat slabs is that corrosion or accidental damage to the anchorages would cause the tendon to fail and could endanger the safety of the entire structure. The parameters involved in choosing between bonded or unbonded tendons are based on the method of construction and economic considerations.

Failure of flat slabs can be due to any of the following reasons:

1- Local punching shear failure around a column.

2- Local flexural failure around a column due to moment transferred from slab to column.

3- Development of a yield line mechanism.

4- Flat slabs may also be considered to have lost their utility due to excessive deflections.

5- Combination of one or more of the above phenomenon.

The purpose of this thesis is specifically to investigate the punching shear failure at edge columns of prestressed concrete flat slab structures.

1.2 Punching shear :-

Punching shear failure is considered a catastrophic mode of failure. It happens suddenly and without any warning signs. It is a brittle failure, which can happen to slabs with moderate to heavy loads even when capitals or drop panels are provided. The latest disaster is the punching shear failure of the Sampoong department store on June 29, 1995 in Seoul, Korea, which caused the entire building to progressively collapse killing over 500 people.

Although the problem of punching shear has been studied by many researchers, there is still no complete, convincing theory.

Local shear failure in the vicinity of columns can happen due to one-way beam action, two-way, also called punching shear failure, or can be a combination of these two cases. In the case of punching shear, the loaded area punches through the slab along a truncated cone or a pyramid.

Punching shear strength is affected by many parameters which can vary in their influence. The most important are: perimeter to thickness ratio, the location of the critical section, size effect and concrete strength. Design codes deal completely differently with these parameters and their effects on punching shear. This reveals the uncertainties that exist. More research is required to answer these questions.

1.3 Objective of the Study :-

1- To investigate the punching shear strength of edge column-slab connections in unbonded post-tensioned flat plates, in particular the contribution of the prestress to the punching shear strength.

2- To determine experimentally the loads and moments transferred to columns and compare them to those predicted by analysis.

3- To compare previous experimental research results and the present results with the design code provision predictions and the punching shear design equation proposed by Gardner.

1.4 Outlines :-

- In Chapter 2, a review of the existing literature related to punching shear is presented. Review includes analytical and experimental work.
- In Chapter 3 a detailed description of the experimental investigation is given. The construction of the test slab and details of the instruments used are described. Drawings are included to show the loading system and the measurement locations.
- In Chapter 4, the various tests are discussed. Graphs are provided to relate loads, moments, strains and stresses at different load steps.
- In Chapter 5, the overall behaviour of the slab is discussed. The different parameters affecting punching shear strength are presented. Loads and moments transferred to columns are compared with these predicted by the Refined Direct Design Method and the method of Equivalent Frame Analysis. Test values are compared with ACI 318-95 and CSA A23.3-94 design code provisions and other research work.

- In Chapter 6, conclusions are drawn and recommendations for future research are made.

CHAPTER 2

LITERATURE REVIEW

2.1 Introduction :-

Extensive research is available in the literature describing the behaviour of reinforced and prestressed concrete flat slabs. In general, reinforced and prestressed concrete slabs behave similarly with the distinction that prestressed concrete slabs have in plane compressive forces. Consequently, many of the concepts of reinforced concrete slabs behaviour are found in the analysis of prestressed concrete flat slab research.

Predicting the behaviour of non-elastic redundant structures, such as continuous reinforced or prestressed concrete flat slab systems is extremely difficult. For continuous flat slab structures the shear forces and moments transferred through the slab-column connections need to be determined. These force resultants are then converted into stresses, shear stresses in the case of punching shear, which are compared to the limiting shear strength of the section. Comparing experimental results with code provisions requires examination of each of these items.

This research is an extension of that started by Rezai-Kallage 1993. An extensive literature review up to 1993 can be found in his M.A.Sc. Thesis. Therefore in this chapter, only literature published since 1993 will be reviewed together with the code provisions of ACI 318-95, CSA A23.3-94 and BS 8110-85. Various interest groups have published handbooks based upon one or more of these codes which will be discussed with the parent code.

2.2 ACI 318-95 and CSA A23.3-94 :-

These two codes are identical in their methods of calculating the forces and moments transferred through the slab-column connections.

2.2.1 Equivalent Frame Analysis :-

The slab has regular column layouts. Therefore Equivalent Frame Analysis, referred to as EFA, was used to find moments and shear forces at critical sections. As it is shown in Fig. 2.1, the slab is divided into strips along the mid panel lines. This method is recommended by both North American Codes, ACI 318-95 and CSA A23.3-94 as a tool to find moments at critical sections. First the equivalent column and slab stiffness are found, then the negative moments at the supports can be found using moment distribution.

Technical Report no. 43 published by the Concrete Society (U. K.) suggests that in the case of getting different reactions at a column from the analysis of two orthogonal design strips, the larger value should be taken knowing that a little accuracy will be lost.

2.2.2 Refined Direct Design Method :-

The structure is divided into strips in both directions in a way similar to Fig. 2.1 for the equivalent frame analysis. The total equilibrium moment is calculated for each span:

$$M_o = \frac{W l_2 l_n^{\,2}}{8} \qquad (2.1)$$

W = Applied Load (KPa)

l_2 = Width of design strip (m)

l_n = Clear span (face to face of columns) (m)

Defined factors are used to allocate moments at critical sections. ACI code allows 10% of moment distribution between negative and positive moment areas. While CSA A23.3-94 in clause 13.10.3.3 mentions that negative and positive moments can be modified by 15% provided equilibrium is satisfied.

There are some limitations to use this simplified method, one of them is the number of spans in each design strip should be three or more. Gardner in 1997 suggested a Refined Direct Design Method, **RDDM** will be used to identify this method, to be used with two bay spans equal in dimensions. Using $0.85M_o$ at interior column and $0.275M_o$ at an edge column, 30%, 12.5% and 5% of the total applied load are carried by the middle, edge and corner columns respectively.

2.2.3 Moment transfer provisions :-

Clause 11.12.6 ACI 318-95 mentions that in the case of transfer of unbalanced moment between a slab and column, a portion of this moment is transferred by non-uniform shear stress as shown in Fig. 2.2 and the rest is transferred by moment. The shear force V and the unbalanced moment M are determined at the centroid of the critical section. The shear stress is the maximum of the following two equations:

$$\gamma_{AB} = \frac{V}{A} + \frac{\gamma_v M e_1}{J} \qquad (2.2)$$

$$\gamma_{CD} = \frac{V}{A} - \frac{\gamma_v M e_2}{J} \qquad (2.3)$$

e_1, e_2 distances from the centroid of the critical section to the face of the critical section.

γ_v = portion of unbalanced moment which is resisted by shear.

J = property of assumed critical section analogous to the polar moment of inertia.

A = area of critical section

These parameters can be calculated using the following formulas:

Interior Column:

$$A = 2d(c_1 + c_2 + 2d)$$

$$e = \frac{c_1 + d}{2}$$

$$\gamma_v = 1 - \frac{1}{1 + \frac{2}{3}\sqrt{\frac{c_1 + d}{c_2 + d}}}$$

$$J = \frac{(c_1 + d)d^3}{6} + \frac{(c_1 + d)^3 d}{6} + \frac{d(c_2 + d)(c_1 + d)^2}{2}$$

Edge Column:

$$A = d(2c_1 + c_2 + 2d)$$

$$e = \frac{(c_1 + \frac{d}{2})^2}{2(c_1 + c_2 + 2d)}$$

$$\gamma_v = 1 - \frac{1}{1 + \frac{2}{3}\sqrt{\frac{c_1 + \frac{d}{2}}{c_2 + d}}}$$

$$J = \frac{(c_1 + \frac{d}{2})d^3 + (c_1 + \frac{d}{2})^3 d}{6} + (c_2 + d)de^2 + 2(c_1 + \frac{d}{2})d(\frac{c_1 + \frac{d}{2}}{2} - e)^2$$

Corner Column:

$$A = d(c_1 + c_2 + d)$$

$$e = \frac{(c_1 + \frac{d}{2})^2}{2(c_1 + c_2 + d)}$$

$$\gamma_v = 1 - \frac{1}{1 + \frac{2}{3}\sqrt{\frac{c_1 + \frac{d}{2}}{c_2 + \frac{d}{2}}}}$$

$$J = \frac{(c_1 - \frac{d}{2})d^3 + (c_1 + \frac{d}{2})^3 d}{12} + (c_2 + \frac{d}{2})de^2 + (c_1 + \frac{d}{2})d(\frac{c_1 + \frac{d}{2}}{2} - e)^2$$

The geometric expressions for these terms are illustrated in Fig. 2.3

In reference 11.49 of ACI, 60% of moment should be considered to be transferred by flexure across the perimeter of the critical section, and 40% by eccentricity of shear. Elgabry (1991) used finite element analysis to investigate the shear distribution. He concluded that 38% of the unbalanced moment M is resisted by flexure, 12% by torsion and 50% by shear.

2.2.4 ACI provision of punching shear strength :-

ACI 318-95 proposes an empirical equation to calculate punching shear strength which takes into consideration the influence of the compressive strength of concrete, the axial compressive force due to prestressing and ratio of the column perimeter to the effective depth of the slab c/d. The ACI uses the following equation to calculate the

punching shear strength of interior slab-column connections in two-way prestressing flat slabs:

$$V_c = (\beta_p \sqrt{f_c'} + 0.3 f_{pc}) b_o d + V_p \qquad SI \qquad (2.4)$$

β_p The smaller of $\alpha_s d / b_o + 0.13$ or 0.29 for prestressed slab

α_s 3.3 for interior column, 2.50 for edge columns and 1.67 for corner columns.

d The distance from the extreme compression fiber to the centroid of the prestressing tendons, but need not to be taken less than 0.8h.

b_o The perimeter of pseudo-critical section located at a distance d/2 from the periphery of the concentrated load.

f_{pc} The average value of prestress, P/A, for the two directions.

f'_c Specified compressive strength of concrete.

V_p The vertical component of all effective prestressing forces crossing the critical section. It may be conservatively taken as zero. If V_p is to be included, the tendon profile assumed in the calculations must be specified.

ACI allows equation (2.4) to be used if the following conditions are satisfied:

- The distance between slab edge and column face closer to the discontinuous edge must be larger than 4 times the slab thickness. ACI comment on this condition saying that for exterior columns where the distance to the edge is less than 4 times the slab thickness, the prestress is not fully effective around the total perimeter b_o of the

critical section. Shear strength in this case is conservatively taken the same as for a non-prestressed slab.

- f'_c shall not be taken greater than 35 MPa.
- f_{pc} in each direction shall not be less than 0.86 MPa nor greater than 3.45 MPa. If f_{pc} is less than 0.86 MPa, the slab is treated as an ordinary reinforced concrete slab.

Design values for f'_c and f_{pc} are restricted due to limited test data available for higher values.

V_p can be calculated using the following equation where βL and h are defined in Fig. 2.4

$$V_p = \frac{2Fh}{(\beta L)^2}(c+d) \qquad (2.5)$$

2.2.5 CSA provision of punching shear strength :-

The CSA and ACI design codes use an ultimate limit state approach to check punching shear. The combined effect of load factor and material safety factor for CSA is about 26% more conservative than the ACI load factor and behaviour factor. Therefore when the Canadians developed their own equation from the American Equation (2.4), they tried to overcome the 26% discrepancy, so they increased the punching shear resistance by the same factor and used 0.4 instead of 0.33 in CSA A23.3-77.

$$V_c = 0.4\lambda\phi_c\sqrt{f_{ck}}\sqrt{1+\frac{\phi_p f_{cp}}{0.4\lambda\phi_c\sqrt{f_{ck}}}}b_o d + V_p \qquad (2.6)$$

λ = factor to account for concrete density

All other terms and conditions are the same as in the ACI equation (2.4).

2.3 BS 8110-85 provision :-

BS 8110-85 Structural Use of Concrete is an extensively used code which was based in turn upon the 1970 CEB Model Code.

The British code uses a rectangular control perimeter 1.5d from the loaded area for both circular and rectangular loaded areas. For reinforced concrete flat slabs the available shear force can be calculated from;

$$\frac{V_{eff}}{b_0 d} < v_{cbs} = 0.79\left(100\rho\frac{f_{cu}}{25}\right)^{1/3}\left(\frac{400}{d}\right)^{1/4} < 5.0 < 0.8\sqrt{f_{cu}} \quad MPa \quad (2.7)$$

where f_{cu} is the specified concrete cube strength (taken as 1.25 f_{ck}), MPa.

$b_0 = 4\,(c + 3d)$ for circular loaded areas, mm

$b_0 = 4\,(b + 3d)$ for square loaded areas, mm

$\rho = (\rho_x + \rho_y)/2$ calculated for a width equal to $(c + 3d)$ or $(b + 3d)$

BS 8110-85 distinguishes between punching shear due to an applied load and punching shear around a column. To make allowance for moment transfer at an interior column the calculated applied factored shear force is increased by 15%.

BS 8110-85 does not have any provisions to estimate the punching shear capacity of prestressed concrete flat slabs. The Handbook to the Code suggests the punching shear capacity of slabs with bonded tendons can be calculated as an ordinary reinforced concrete slab using the actual area of tendons, and to add the decompression load; the load required to annul the prestress in the extreme fibres put into tension by the applied loading. For

unbonded tendons the punching resistance would be 10% less. This method was first developed by Regan for one-way bonded prestressed slabs, and extended to two-way slabs.

For interior column slab connections with moment transfer and edge and corner column slab connections BS 8110-85 magnifies the applied shear force and simply uses the magnified, or effective, shear force in equation (2.7).

For corner columns and edge columns with bending about an axis parallel to the free edge

$$V_{eff} = 1.25\, V_t$$

2.3.1 Post-tensioned concrete floors design handbook :-

Technical Report no. 43 published by Concrete Society in 1994 allows for tension in the slab. However this leads to more unbonded reinforcement in the slab. Some of the important outlines in this report are:

i. The distribution of tendons in the slab is not a critical issue, providing the slab has an adequate number of tendons passing through the column zone to prevent punching shear and avoid progressive collapse. The author does not agree with this point, as mentioned in chapter 5 the distribution of the tendons has a big impact on punching shear resistance.

ii. The minimum average prestress to be considered effective should be at least 0.7 N/mm^2. The maximum stresses in the unbonded tendons shall not exceed 0.85 f_{pu}. This ensures that the anchorages are not over stressed.

iii. Untensioned reinforcement greater than a minimum of 0.75% of the cross-section area of concrete of should be concentrated in column zones between lines of 1.5 times slab depth on either side of the column. This reinforcement shall extend 0.2 of span length or as far as necessary by calculation.

BS 8110 does not provide a specific design procedure for checking punching shear of prestressed flat slabs, therefore the Technical Report no. 43 suggest some steps to satisfy this requirement:

- Punching shear should be checked using other international standards.
- Punching shear strength can be improved by concentrating tendons in the column vicinity.
- Design procedures should be followed as far it complements BS 8110.

2.4 Gardner 1996 equation :-

Gardner proposed a prediction equation for the punching shear strength of interior slab column connections of reinforced and prestressed concrete flat slabs, by extending the work of Shehata and Regan (1989), and Shehata (1990). Gardner examined the dependence of the punching shear strength to the concrete strength, for reinforced and prestressed concrete slabs, using a control perimeter at the periphery of the loaded area and a Shehata and Shehata (1989) type strength enhancement expression. Columns with circular or rectangular cross sections were analysed as square columns of the same cross sectional area. A sensitivity analysis, using the coefficient of variation of the equation coefficient as the criterion of goodness, was used to confirm that the one third power of concrete strength and steel force were close to optimal.

For the unbonded post-tensioned slabs the prestressed reinforcement ratio was calculated from the initial precompression at the column i.e. $\rho_p = f_{pc} h \quad f_{se} d_p$.

The shear force, V_d, appropriate to the decompression moment, was calculated by $V_d \cong 2\pi \rho_p d_p f_{ps}(d_p - h/3)$; (developed from the yield line expression for punching shear $V_{yield} = 2\pi M$, M = yield moment per unit width, Wood (page 69). This avoids the problem of determining the inclination of the prestressing tendons crossing the failure surface required to calculate the vertical component of the prestressing force. For design purposes the decompression shear force is multiplied by 0.75 to represent the lower 95%

$$V_c = 0.55 \lambda u d_{eff} \left[1 - \left(\frac{250}{h}\right)^{0.5}\right]\left(\frac{h}{4c}\right)^{0.5}\left[\frac{\rho f_y d^3 - \rho_p f_{ps} d_p^3}{d_{eff}^3}\right]^{1/3}[f_{ck}^{1/3}] - 0.75 V_d\left[\frac{u}{4c}\right] \quad (2.8)$$

c = dimension of square column of same cross sectional area as the actual column, (mm).

d = effective slab depth to reinforcement, (mm).

d_p = effective slab depth to prestressed reinforcement, (mm).

$d_{eff} = (\rho f_y d^2 + \rho_p f_{se} d_p^2)/(\rho f_y d + \rho_p f_{se} d_p)$

f_{ck} = specified concrete cylinder strength, (MPa).

f_{se} = effective stress in prestressed reinforcement after losses, (MPa).

f_{pc} = precompression in concrete calculated at the centroid of the slab, (MPa)

f_{ps} = stress in prestressed reinforcement at ultimate load, (assumed = 1.1 f_{se})

f_y = yield strength of flexural reinforcement, (MPa)

h = slab thickness, (mm).

λ = 1 for normal density concrete, 0.85 for lightweight concrete

u = perimeter of equivalent square column attached to slab, (mm)

ρ = ratio of flexural tensile reinforcement calculated over a width c+6d

ρ_p = ratio of prestressed steel calculated from $\rho_p = f_{pc} h \quad f_{se} d_p$

$V_d \cong 2\pi \rho_p d_p f_{ps} (d_p - h/3), \quad (N)$

For continuous reinforced concrete flat slabs Gardner and Shao (1996) suggested two alternative methods for combined shear and moment transfer; using the ACI eccentric shear method with a control perimeter around the loaded area or a simple BS 8110 type multiplier for slabs under gravity loads.

For edge and corner column slab connections of slabs subjected to gravity loads the nominal shear force is multiplied by a factor to obtain an effective shear force which is used in equation (2.8).

For edge connections subjected to moments perpendicular to the slab edge

$$V_{eff} = 1.5 V_u$$

For corner column slab connections

$$V_{eff} = 2.0 V_u$$

2.5 Long and Cleland's experimental work :-

In 1993, Long and Cleland conducted experimental work to investigate the strength of post-tensioned flat slabs at edge columns. They tested five models that represented 1/4 scale edge panels. Fig. 2.5 shows plan and sketch of the models used in the experiment. The dimensions and thickness were kept the same for all models. The average prestress, distribution of prestressed steel, bonded steel and tendon drapes are given in Table 2.1.

The primary variables investigated were the distribution of the tendons and the magnitude of the average prestress. The failure zone extended 1/6 of the span length in the direction of moment transfer. It extended to the location where bonded reinforcement terminated. Tendons in the failure zone lost most or all of their forces.

Long and Cleland observed the following:

- Comparing models E1 and E2, banding of tendons in E2 caused a small increase in ultimate load capacity. This could be because E1 had 50% more bonded reinforcement in the direction of moment transfer.
- Increasing the drape of the tendons in the direction of moment transfer from 20 mm in E2 to 28 mm in E5 caused only a small increase in the ultimate load capacity in E5.
- E2, E3 and E4 were used to study the influence of average prestress on ultimate load capacity. It was found that increasing the average prestress 300% would improve the shear capacity by only 37%.

Long and Cleland drew the following conclusions:

- Post-tensioned flat slabs should have bonded reinforcement to control cracks and improve ductility.
- Banding of tendons in one direction causes a small increase in the ultimate punching shear strength of edge columns.
- The ratio of prestress at failure to initial prestress is in the range of 105 to 110%.
- The ACI-ASCE committee 423 equation is too conservative in its prediction of punching shear strength at edge columns. Using local prestress rather than average

prestress will improve punching shear capacity particularly in slabs provided with banded prestress in one direction.

2.6 Gardner and Rezai 1998 :-

In 1993 Rezai constructed and tested to failure a 2 bay x 2 bay unbonded post-tensioned flat slab. The distribution of tendons is shown in Fig. 2.6. The circular columns were 203 mm in diameter and the square columns 203 mm x 203 mm. The purpose was to study the column shape and perimeter effect on punching shear resistance. Tendons were banded in one direction and uniformly distributed in the other direction, as if the slab was spanning onto beams spanning between columns. In Table 2.2, the ultimate load capacities at which the punching shear failure happened in the three tests are illustrated.

The load that caused punching shear failure of interior column is 9% less than the load the column was able to carry in the first test. That was explained by the authors, because of

1) Load redistribution after the first test failure.
2) The prestress reduced in the tendons passing through the failed edge column.
3) Punching shear is preceded by internal diagonal cracks reducing connection stiffness.

The authors compared experimental work results reported in literature with ACI 318-95, BS 8110-85 and the proposed method by Gardner. The code values were calculated using $f_{ck} = 0.8\ f_{cm}$ and the prestress at failure was assumed 10% higher than the initial prestress. V_p was taken as zero to reduce the calculated load. Gardner and Rezai noted that:

- Neglecting the vertical component of the prestressing force in calculation attributed to ACI 318-95, or the decompression shear in BS 8110-85 and the proposed method, will be conservative. The decompression shear forces can be as large as 25% of the calculated shear strength.
- The punching shear provisions of ACI 318-95 for slabs with only precompression, or precompression and bonded reinforcement, even ignoring the vertical component Vp is less conservative than those for reinforced flat slabs.
- The precompression is effective to the edge of the slab and can be used in calculations estimating punching shear strength.

2.7 Sherif's experimental work :-

In 1996 Sherif under the supervision of W. Dilger and in partial fulfillment of the requirement for his Ph.D. research conducted experimental work on two continuous reinforced concrete slabs and four full scale isolated edge column-slab connections containing shear studs. In Fig. 2.7 plan of the full scale slabs, in Fig. 2.8 dimensions of slab-column connections SC-1 and SC-2 and in Fig. 2.9 plan of slab-column connections SC-3 and SC-4 are shown. The objective was to investigate the behaviour of continuous flat slabs. The parameters investigated in this research load eccentricity and the distribution of the flexural reinforcement on the shear strength. Three main topics were the focus of the thesis: Analysis of flat slabs, deflections of flat slabs and shear strength of slab-column connections.

Sherif made the following conclusions:

- Different analysis methods such as direct design, equivalent frame and prismatic member of the flexural strain at interior column give approximately the same results.

- Direct design method gives better results for moments transferred to columns compared with test results than other analysis methods.
- The increase of slab-column moment with load decreases at higher loads. This can be explained due to decreasing torsional stiffness of the slab because of cracks around edge columns.
- The relationship between concrete compressive strength and shear strength is more realistic to be expressed as a function of $(f'c)^{1/3}$ instead of $(f'c)^{1/2}$ especially for higher strength concrete.
- A formula was proposed which is:

$$V_c = 0.7\,(100\,\rho\,f'c\,)^{1/3} \qquad (2.9)$$

This equation relates flexural reinforcement ratios and concrete strength to shear strength of slab-column connection. This equation is more realistic than the current CSA A23.3-94 provisions. $v_c = 0.4\sqrt{f'c}$ (2.10)

which does not consider reinforcement ratio and can be unsafe for ρ less than 1%.

Model no.	Level of Average Prestress psi	No. of Tendons In x Direction	No. of Tendons In y Direction	Bonded reinforcement Over column In x-direction	Tendon Drape in x-direction in.
E1	340	18	20	6#2	0.80
E2	340	16	18	4#2	0.80
E3	510	26	26	4#2	0.53
E4	170	8	7	4#2	0.80
E5	340	15	18	4#2	1.10

1 psi = 6895 N/m^2, 1 in = 25.4mm

Table 2-1 Summary of test program in 1993 Long's research

	Edge#2 Circular	Interior Square	Corner#9 Circular
Experiment* Load(kN/m^2)	32.9 100%	30.1[1] 91%	43.6 133%
Shear Force(kN)	135	297	57
dp(mm)	50	70	50

*includes slab self load of 2.1 kN/m^2

1 considered anomalous as previously supported 32.9 kN/m^2

Table 2-2 Experimental results in Gardner and Rezai's research

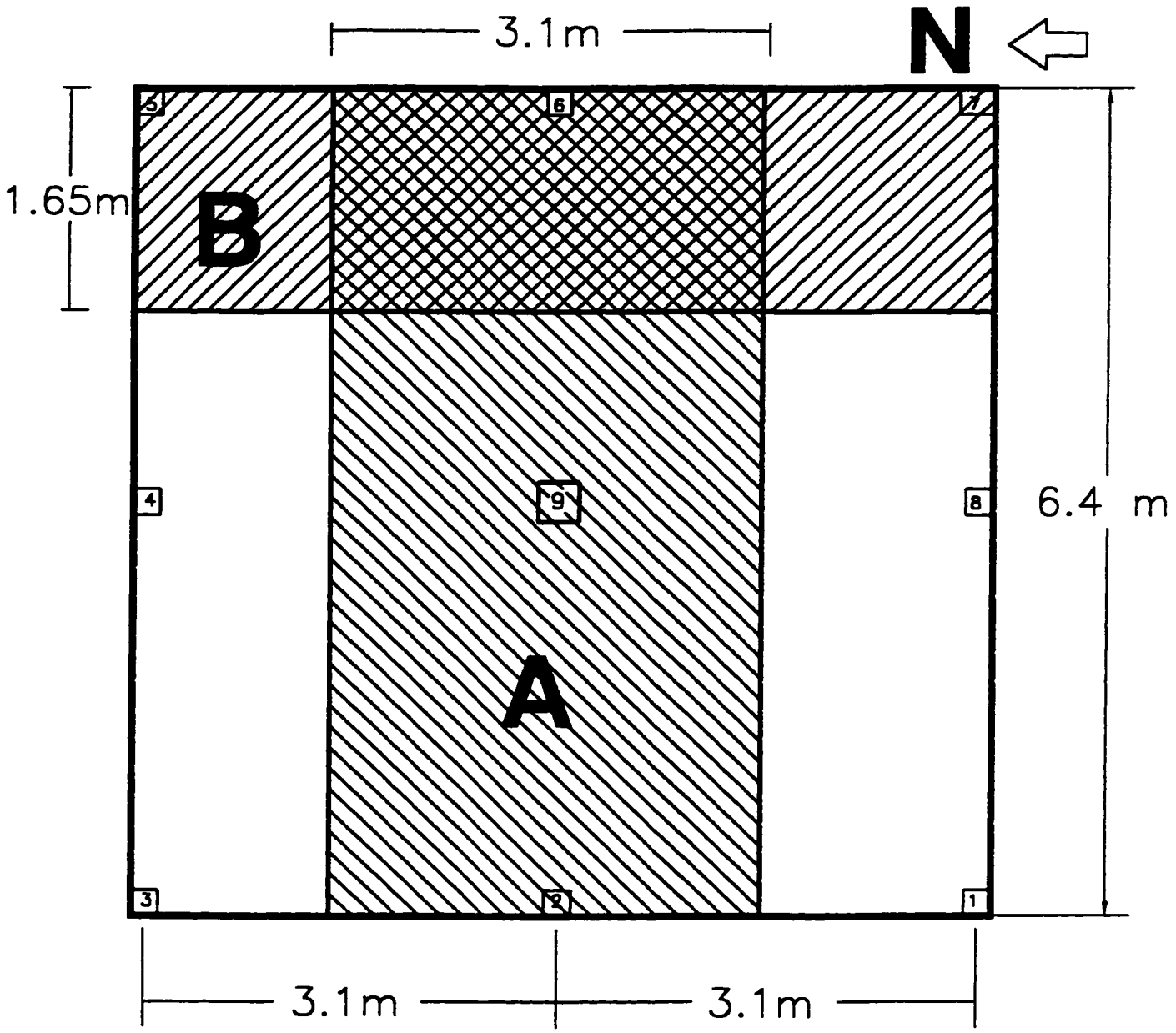

Fig. 2-1 Design strips in the equivalent frame analysis

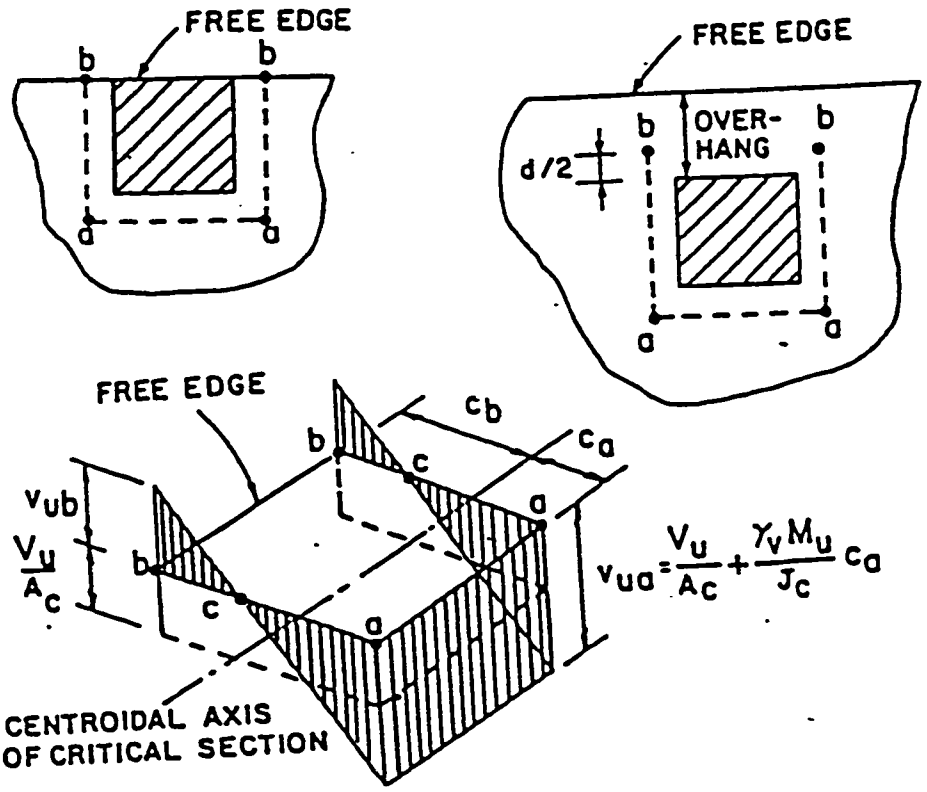

Fig. 2.2 Assumed distribution of shear stresses

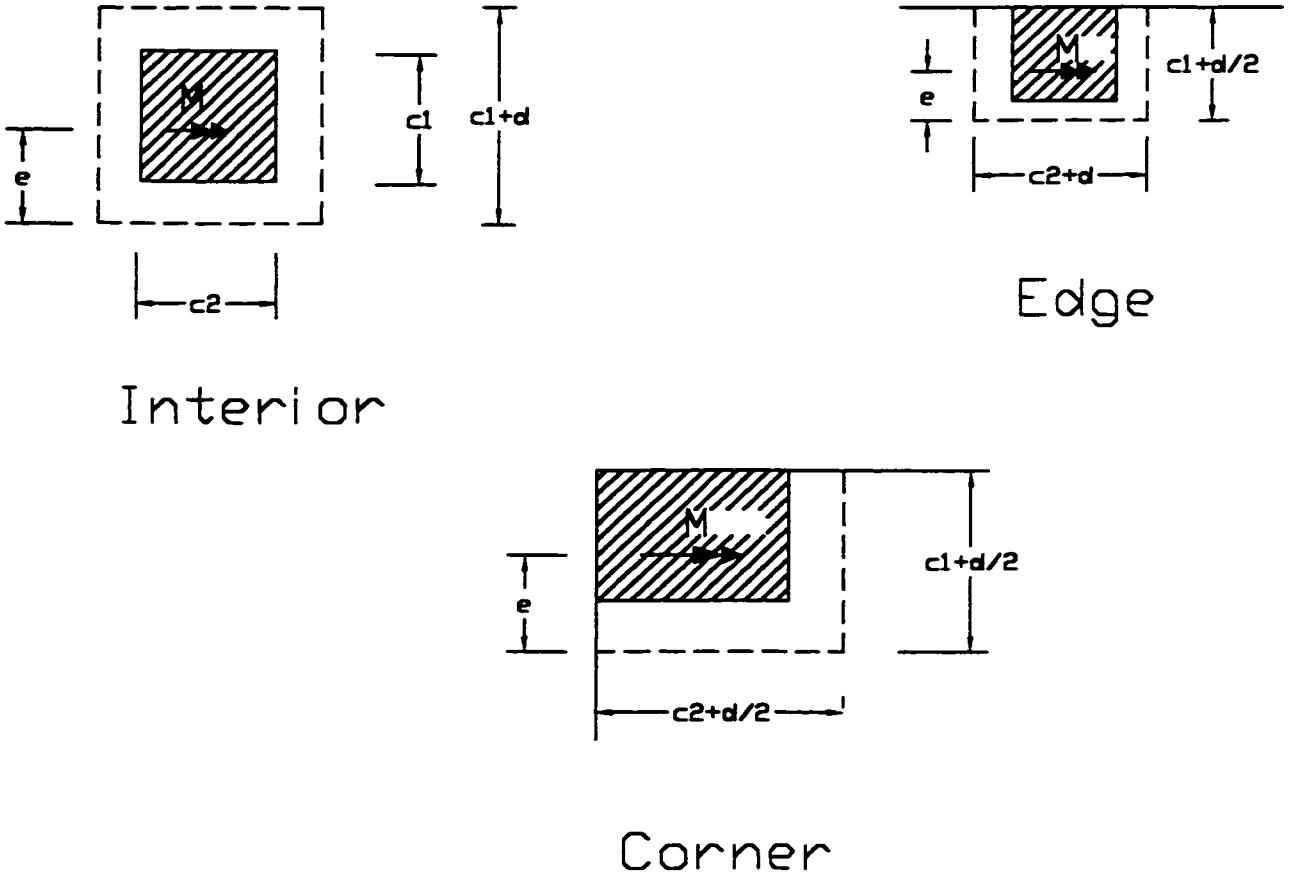

Fig. 2-3 Geometric expressions for shear-moment transfer

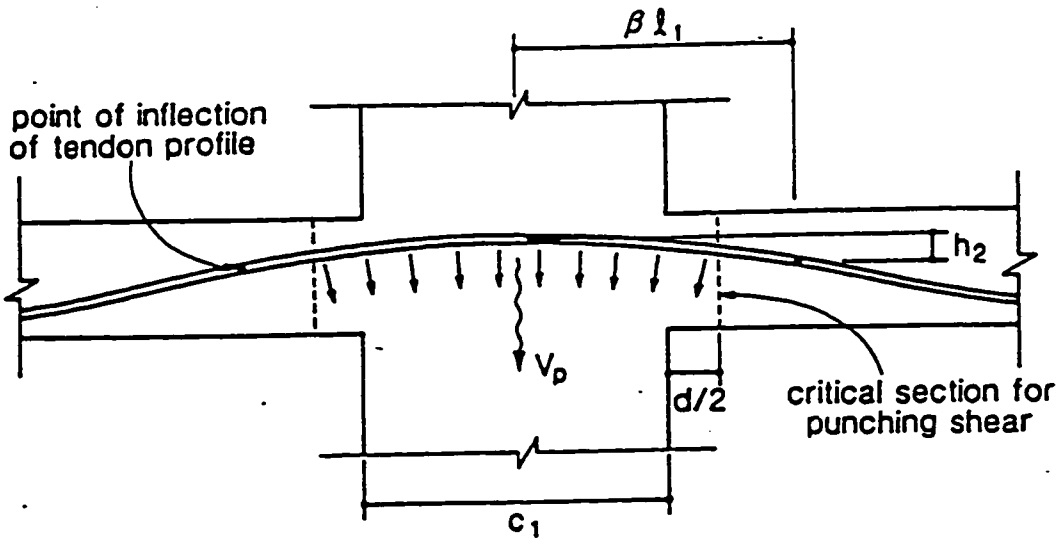

(a) Tendon profile through column region

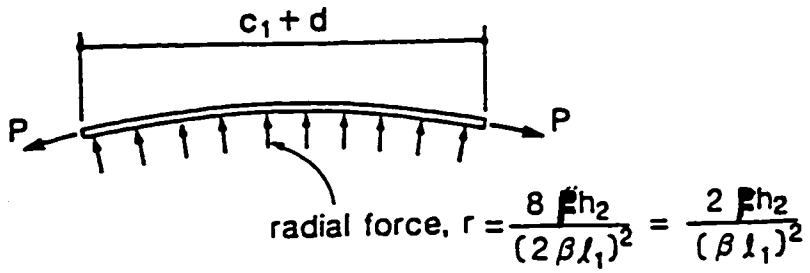

Fig. 2.4 Calculation of the vertical component of the prestressed cables, Vp

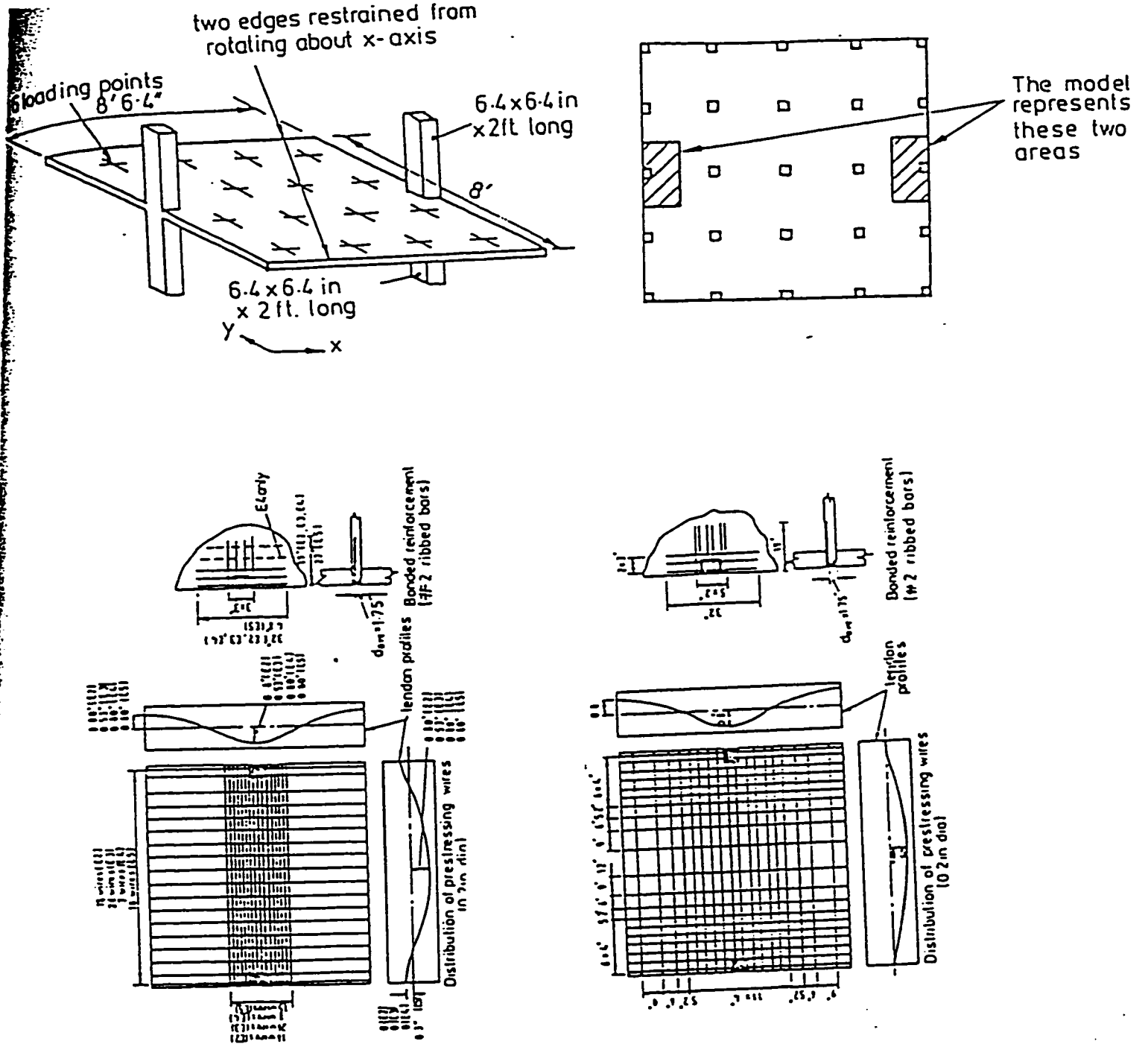

Fig. 2.5 Plan and sketch of the models used in Long's experiment

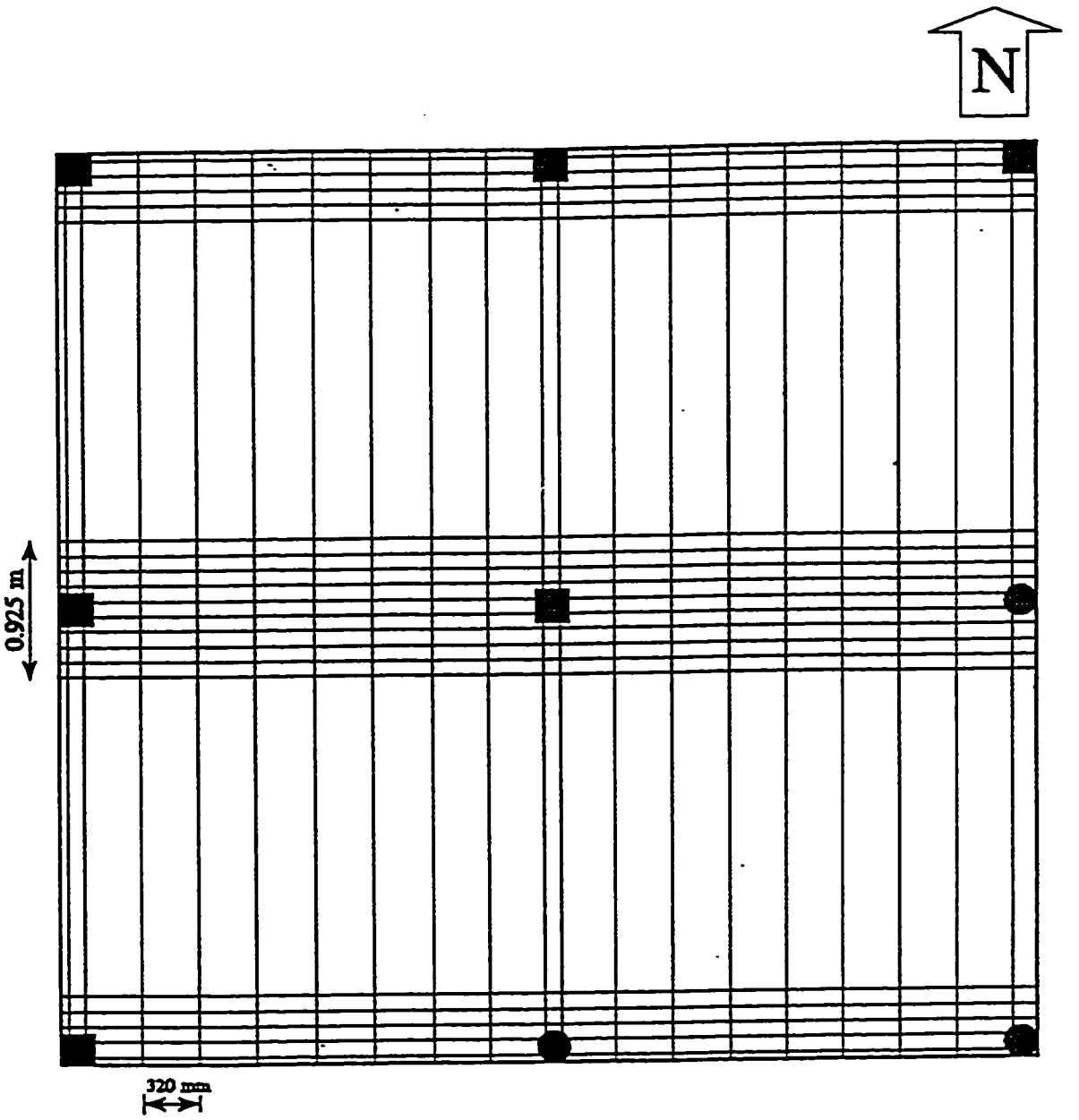

Fig. 2.6 Plan of the distribution of tendons in Rezai's experimental work

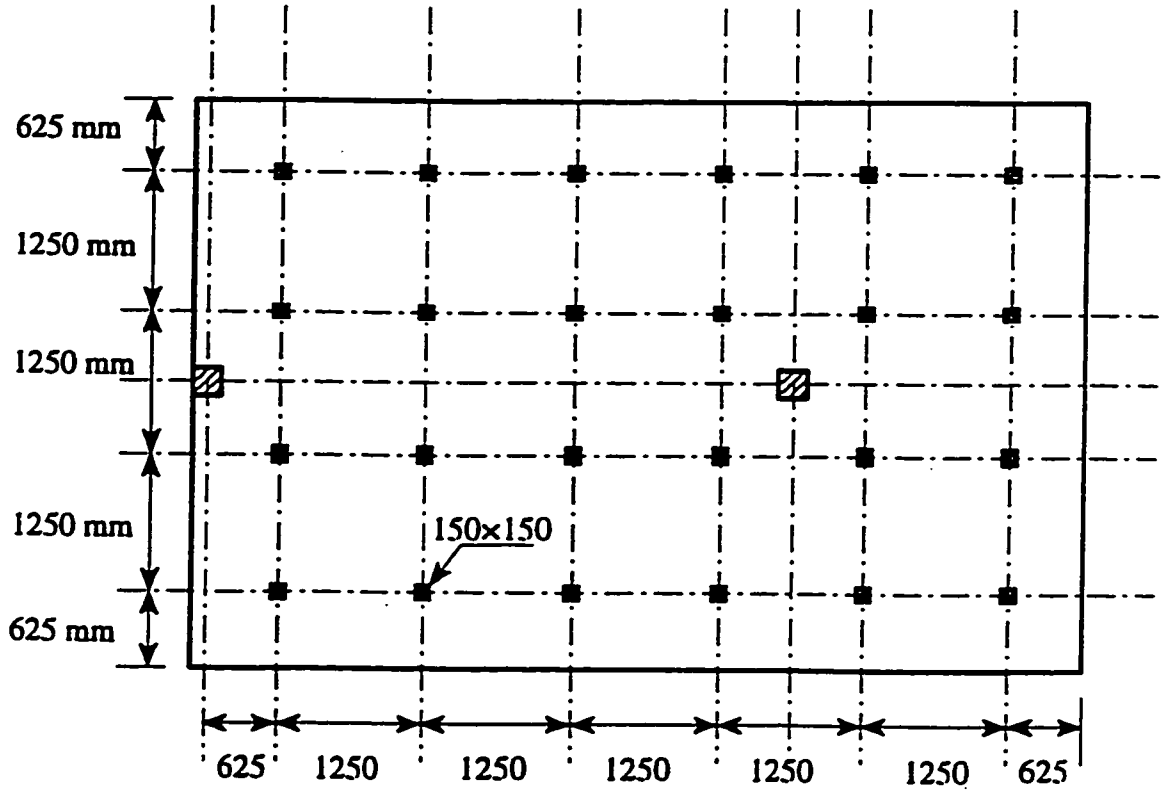

Fig. 2-7 Plan of the full scale slabs in Sherif's work

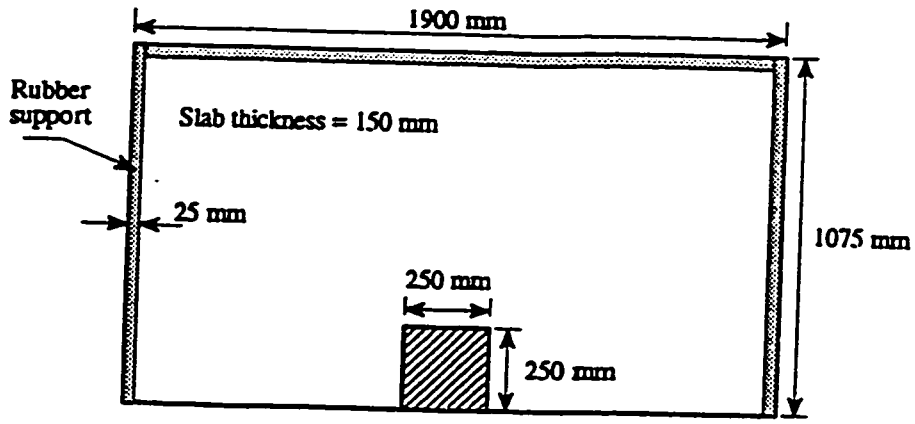

Fig. 2.8 Dimensions of slab-column connections SC-1 and SC-2 in Sherif's work

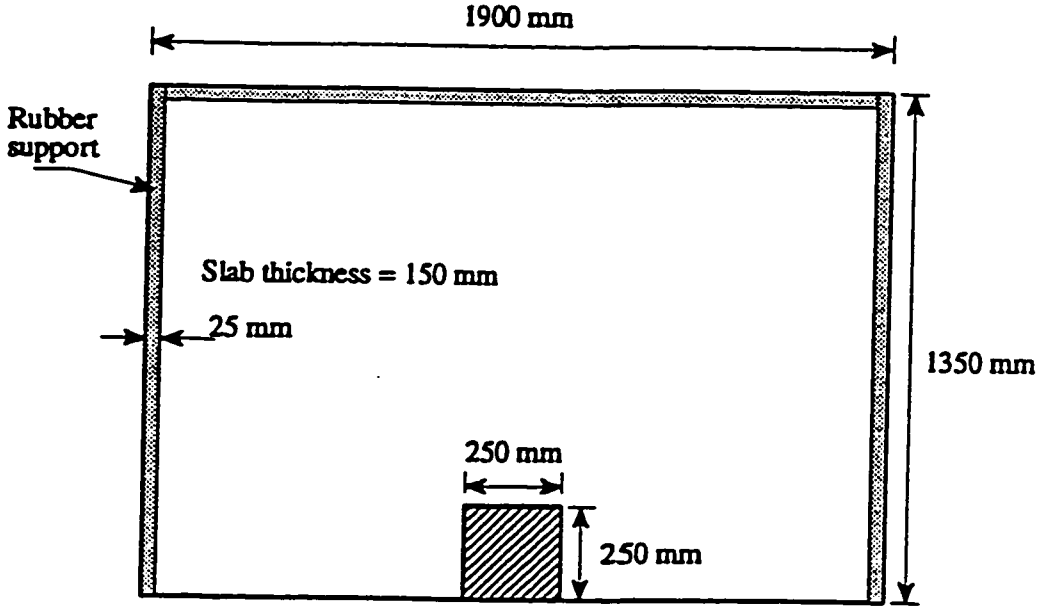

Fig. 2.9 Plan of slab-column connections SC-3 and SC-4 in Sherif's work

CHAPTER 3

EXPERIMENTAL SET UP

3.1 Introduction :-

The primary purpose of the research was to investigate experimentally the effect of the level of precompression on the punching shear behaviour of edge slab-column connections. A two bay by two bay, unbonded post-tensioned flat slab with different tendon distributions in the edge columns regions was constructed. Vibrating wire gauges were cast at mid-depth of the slab to measure the precompression in the concrete. The edge and corner columns were supported on load cells to measure vertical reactions and by horizontal load cells to measure column moments. Tendon forces were also measured. No supplementary bonded reinforcement was used. The slab had equal dimensions in each direction. The outside dimensions of the slab were 6.4 m x 6.4 m with centre to centre column distances of 3.1 m. The thickness of the slab was 90 mm. The dimensions of the edge and corner columns were 203 x 203 mm (8 x 8 inch) and the interior column 305 x 305 mm (12 x 12 inch). Fig. 3.1 shows a plan of the slab identifying each column by a number and each panel by a letter. The dimensions of the slab were chosen as a compromise between the space available in the structural laboratory and to be as close as possible to full scale to eliminate, or reduce, the effect of scale factor. Three reasons were considered in choosing 90 mm thickness of the slab, first to control deflection and to be in the range span / (35 – 45). Second the smaller the thickness the smaller the load required to fail the slab, especially knowing that the

applied load is limited by the maximum force available from the jacks. Thirdly the thickness must be sufficient to permit the required drape of the tendons.

3.2 Formwork Construction :-

The plywood casting surface for the slab was supported on eighteen aluminum I-beams 6.4 m (21 ft.) long. Fig. 3.2 shows the distribution of the beams, 8 in the north–south direction and 10 in the east-west direction. The beams were supported on concrete blocks. Plywood sheets were nailed to the supporting beams and covered with polyethylene to avoid bond between the formwork and concrete and to prevent the wood from absorbing the hydration water.

3.3 Building The Columns :-

The edge and corner columns were 203 mm square; which is the smallest practical size that can be constructed with relatively no difficulty in placing the concrete. The size of the interior column was 305 mm square to avoid having a shear failure around the internal column.

To replicate the points of contraflexure the columns were supported on balls and rollers to eliminate any moment or horizontal restraint. The length of the columns below the slab was chosen to represent the distance to the points of contraflexure ie to represent the half height of the column. In addition, to facilitate working and setting the instruments under the slab, the height from the bottom of the slab to the floor was 940 mm (37 inch). To prevent any horizontal restraint the edge and corner columns were also mounted on rollers. Fig. 3.3A shows the steel plates and the rollers for the columns without load cells. The first plate, positioned under the column, was provided with small notch to locate the steel roller which provided the free rotation to the columns. Four 25

mm (1 inch) diameter rollers were used to enable the horizontal movement of the columns. Fig. 3.3B shows the set up of the columns with load cells. The top 25-mm (1 inch) thick plate was fixed to the load cell by a 6.4-mm (1/4 inch) diameter bolt. The ends of the load cells were provided with a curved bearing surface so the column-load cell system could rotate. Steel reinforcement cages were built using 4 #20M bars for the 203 x 203 mm columns and 8 no. 20 bars for the 305 x 305 mm interior column; #10M bars were used for the stirrups, the specified yield strength of the bars was 400 MPa. The cages were located in the column formwork using side spacers to provide 20 mm cover. Horizontal movements of the edge and corner concrete columns were prevented by threaded rods which were anchored to 8 steel columns of HSS 203 x 203 (8 x 8 x 3/8 inch). Fig. 3.4 shows one of these columns which were fixed by prestressing bolts to the laboratory floor. The lower threaded rod load cells, which were in compression, of the corner columns buckled during the first test and were replaced before the second test by hollow circular tubes OD = 21.1 mm and ID = 15.9 mm having larger moments of inertia than the threaded rods. Preliminary testing showed that the steel columns were not stiff enough to prevent the slab columns from movement. Therefore, 76 x 76 x 9 mm (3 x 3 x 3/8 inch) HSS beams were welded from the top of each 203X203 mm column to the opposite column. These restraints are shown in Fig. 3.5. To reduce the effective length of these restraints they were all welded to a 12.7 mm steel plate bolted to the interior column. Fig. 3.6 details the way the beams were welded at the middle of the slab.

3.4 Distribution of the Cables :-

Thirteen mm, sheathed, seven-wire strand tendons were used. The manufacture's stated ultimate strength was fpu = 1860 MPa. The strands were supplied inside plastic sheaths filled with grease to avoid any bonding with the concrete and for corrosion protection. Fig. 3.7 shows the design drape of the tendons in each direction. Eighteen cables were placed in the east – west direction first and then 19 cables were positioned in the north – south direction. Plastic chairs were used to provide the drape shown in Fig. 3.7. The distribution of tendons in both directions can be seen in Fig. 3.8.

The tendon distributions were chosen so that the local precompression calculated at the faces of the edge and corner columns were different but the average precompressions calculated over the width of the slab were similar.

3.5 Casting the Slab :-

Five cubic meters of ready mix concrete with a maximum aggregate size of 10 mm, specified concrete strength f'_c = 35 MPa and a slump of 70 mm was delivered from a local company. A retardar was used. The columns were cast with the slab. Placing started from panel B and the columns around it using steel bucket moved by a crane. The casting took approximately 3.5 hours, 12 standard 150 x 300 mm cylinders were cast to determine the value of f'c. The slab was covered by burlap and moist cured for two weeks. Three cylinders tested at 10 days gave an average compressive strength of 37 MPa. At 28 days, more cylinders were tested and it was found that the compressive strength was 45 MPa. The side formwork was removed 10 days after casting.

3.6 Pre-stressing the Cables :-

To avoid concentration of stress in one area, alternate cables were stressed to 50 kN in both directions starting at the middle of north-south direction. These prestresses were enough to counteract the self-weight of the slab. The slab formwork was removed. The second step was to post-tension the remaining tendons to 50 kN force. Finally, the last step was to post-tension all the cables to 100 kN. It was estimated that the force in each tendon after all losses was 85 kN or stress equal to 859 MPa. The average compression after losses in the east–west direction was 2.7 MPa and 2.8 MPa in the north–south direction.

Two hydraulic jacks, steel trestle, two pumps and pressure gauge were used to post – tension the cables. Once everything was set up the tendon was stressed by the large jack to the required force from the pressure gauge. Then the small jack was used to push the grips inside the anchorage against the bearing steel plate and pressure would be released. Some tendons were provided with load cells to measure the tendon force. The anchorage slippage loses were measured to give an average reading of 7 kN. Fig. 3.9 shows the steel plates, anchorage, grips and load cells.

After the cables had been stressed, the steel plates and rollers were removed, one at a time, from beneath the edge and corner columns. These bearings were exposed to corrosion because of the water used to cure the slab. The plates and rollers were removed and cleaned using high-pressure air. They were then replaced in their original positions.

3.7 The Loading System :-

The loads were applied through 48 rods penetrating the slab spaced at 0.915 m (3 ft) from each other. These rods passed through the floor of the laboratory. Each pair of rods was connected by 101 x 101 mm (4 x 4 inch) steel box–section 1.2 m long beam. In total twenty-four 101 x 101 mm beams were used. At the middle of each beam, a hydraulic jack was located. Twenty-four hydraulic jacks, maximum pressure of 69 MPa (10000 psi) and an area of 1445 mm^2 were used. Fig. 3.10 shows part of the loading system under the slab floor. The jacks react against the floor causing the rods to be pulled. Each rod would transfer half of the jack force to the slab. Fig. 3.11 shows a schematic of the loading system and the way the load is applied on the slab. To center the rod at the middle of the hole two wooden washers, one on the floor and the other underneath the floor, were used. All the jacks were calibrated and the hoses checked for leakage using a compression machine before installation. To avoid lateral movement of the beams during loading, the beams were supported laterally by steel box–section beams. The beams carrying the jacks and those providing the lateral support are shown in Fig. 3.10. Fig. 3.12 shows the distribution of these beams.

The slab loads were measured from the pressure gauge of the pump multiplied by the number of jacks used in the test, and by their ram areas. divided by the slab area, unless otherwise mentioned. Rezai used a finite element program and determined that the discrepancy between this loading system and a uniformly distributed load system as assumed is less than 3%.

3.8 Instrumentation :-

Aluminum load cells were used on 18 selected tendons to measure the tendon forces. Fig. 3.13 shows the locations of these load cells. Two strain gauges were attached to each load cell to take the average reading, they were connected to strain connection boxes, and then were wired to strain indicators. Variations of tendon forces were measured at various load steps in tests. In addition, they were used to quantify change of force in the tendons passing through failure zones. Before use, all of the load cells were calibrated using a universal testing machine. Calibrations of the aluminum load cells can be found in Appendix A.

Five load cells were used under some selected columns. Two small load cells with a maximum capacity of 75 kN were used under corner columns no. 7 and 3. Two load cells with a maximum capacity of 200 kN were used under edge columns 6 and 8. A large load cell of 450 kN maximum capacity was used to measure the load transferred to internal column #9. Load cell calibrations are given in Appendix A.

To measure the forces in the threaded rod load cells two strain gauges were glued on flats machined on opposite sides of each rod. In total, thirty-two 10 mm long strain gauges were used to measure readings in these rods. After the corner threaded rods buckled in compression, all the lower threaded rods were replaced with tube rods having bigger moment of inertia. Calibrations of the threaded rods and the tube load cells are given in Appendix A. These strain gauges were wired to strain connection box and to a strain indicator.

Nineteen vibrating wire gauges were installed inside the slab. Fig. 3.14 shows their positions at different locations in both directions. Two of them broke during

casting. Fig. 3.15 shows the vibrating wire gauges placed on chairs and tightened to the formwork to prevent movement. These VWGs were used to measure strains in the concrete after each load step.

Sixteen dial gauges were used to measure deflections at the cardinal points of the slab. Fig. 3.16 shows the positions of these dial gauges, the readings taken during tests were due to external loads and did not include the self–weight of the slab. Fig. 3.17 shows dial gauges 11, 14 and 10 in the panel C.

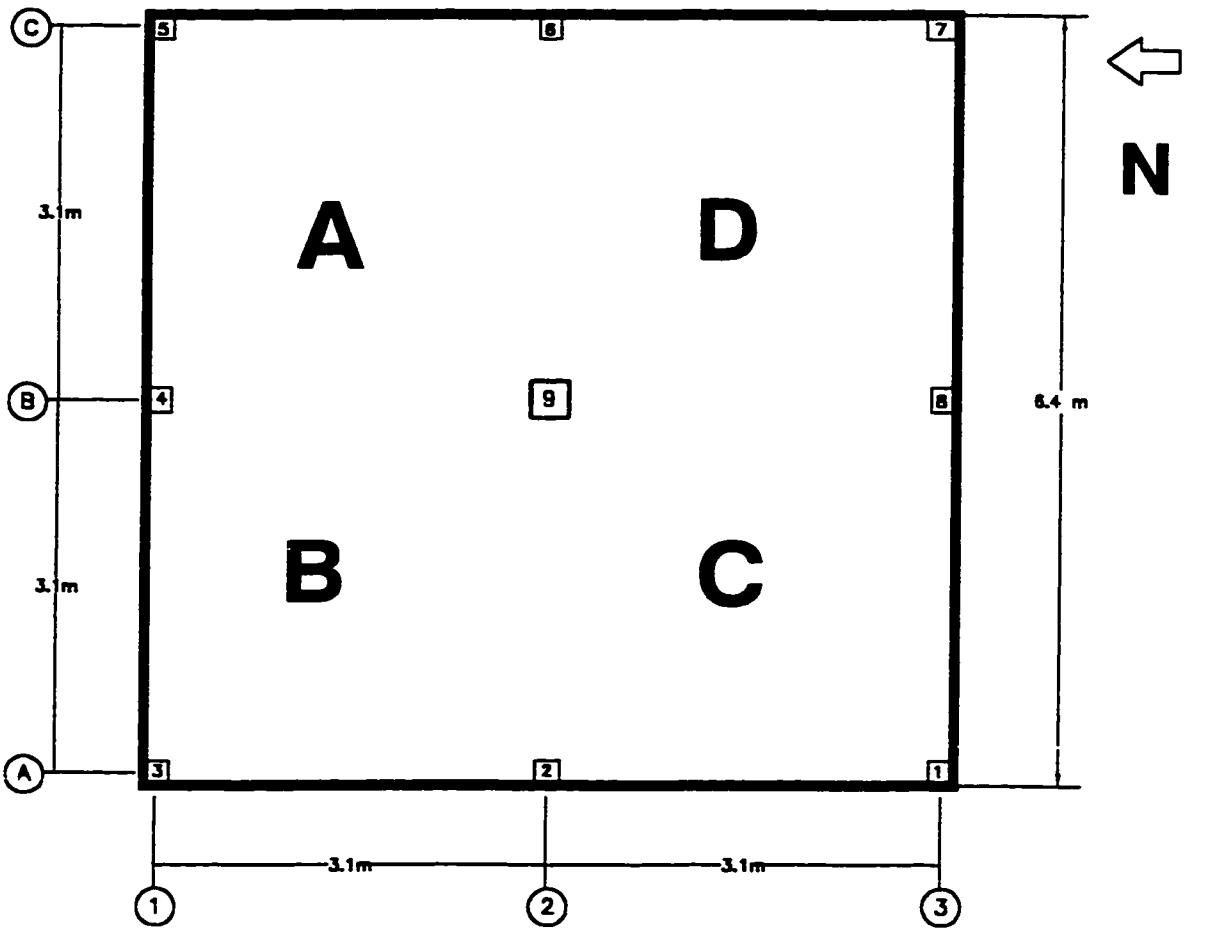

Fig. 3-1 Plan of the test slab

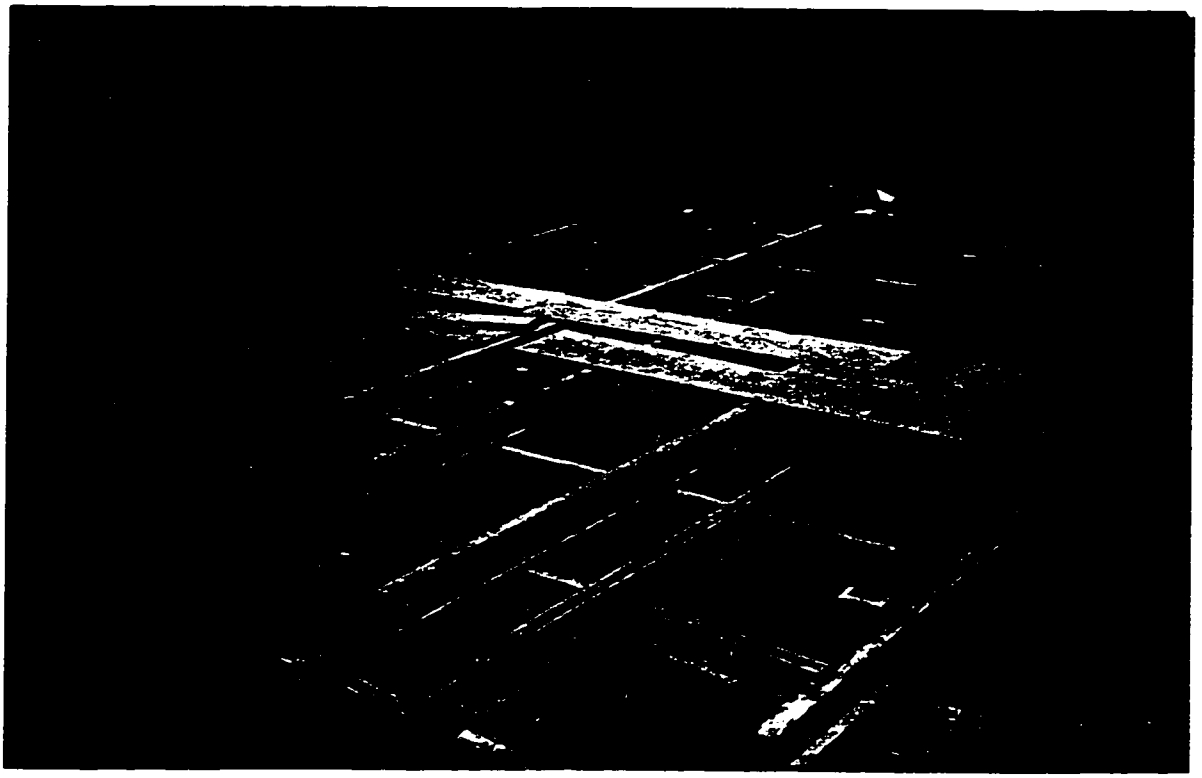

Fig. 3.2 The distribution of the I-beams used in the formwork

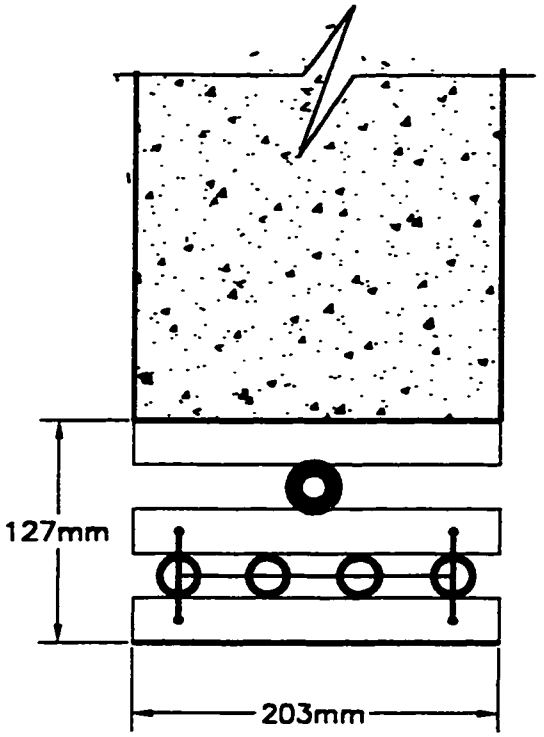

Fig. 3-3A Column Base

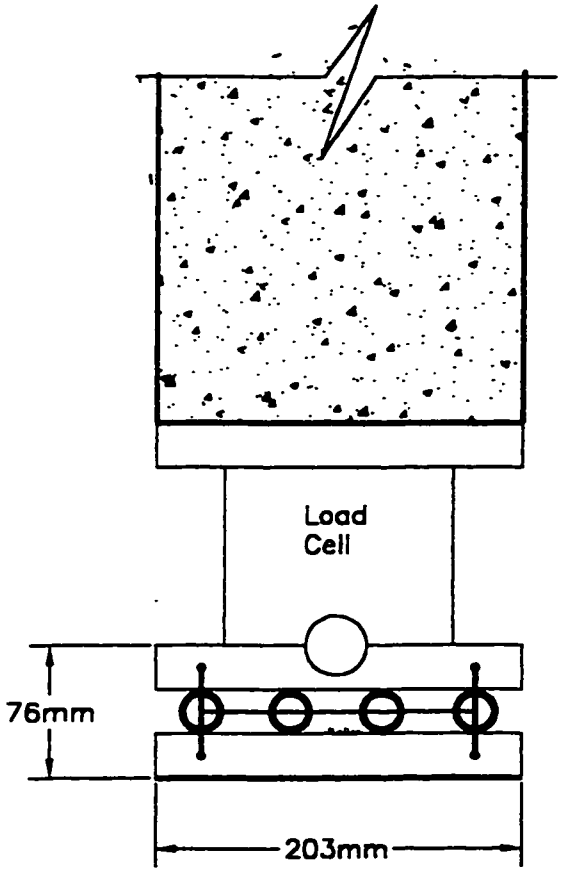

Fig. 3-3B Column Base with Load Cell

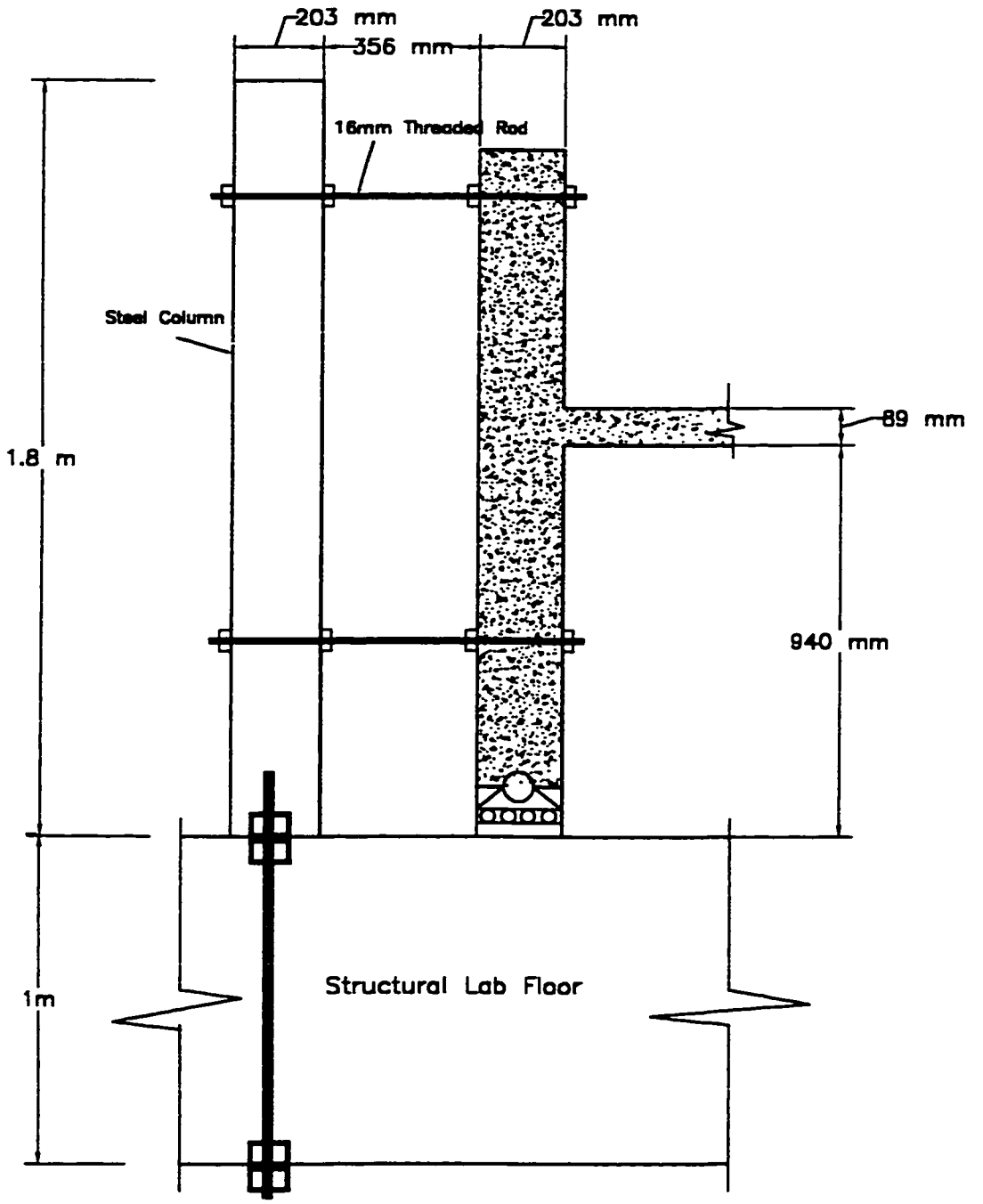

Fig. 3-4 The restraining steel column connected to the slab column

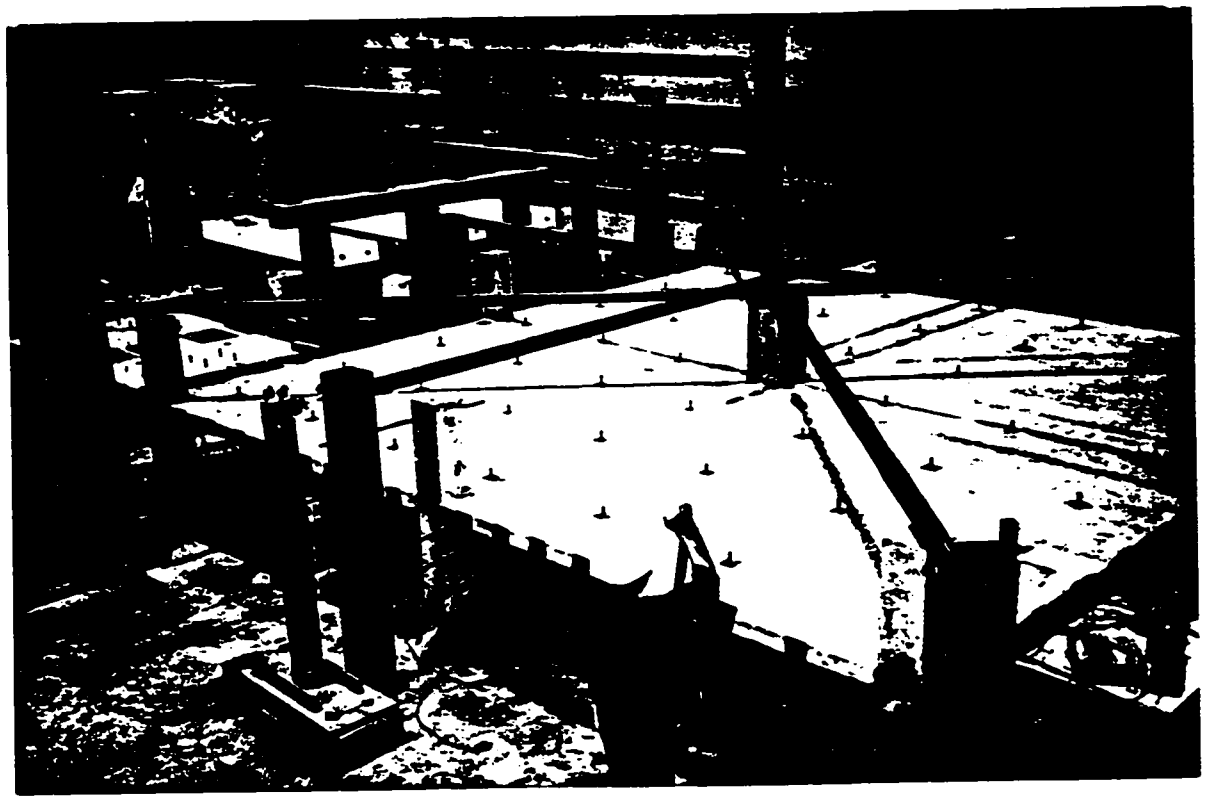

Fig. 3.5 HSS beams used to restrain columns from movements

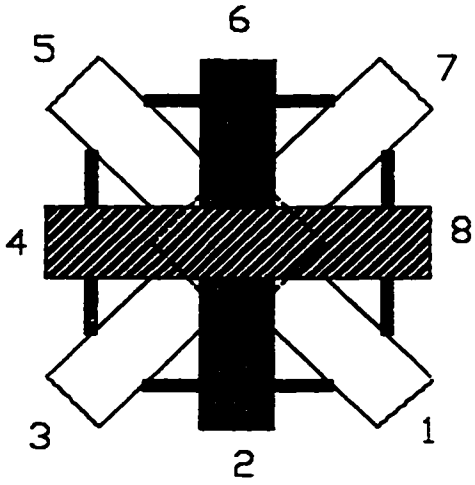

Fig. 3-6 Box-section Beams connected at the interior column

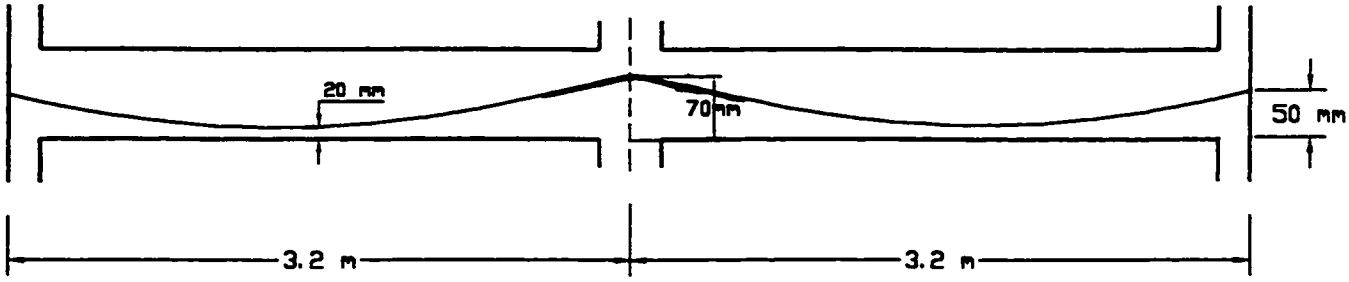

Fig. 3-7 Tendon profile in the slab (not to scale)

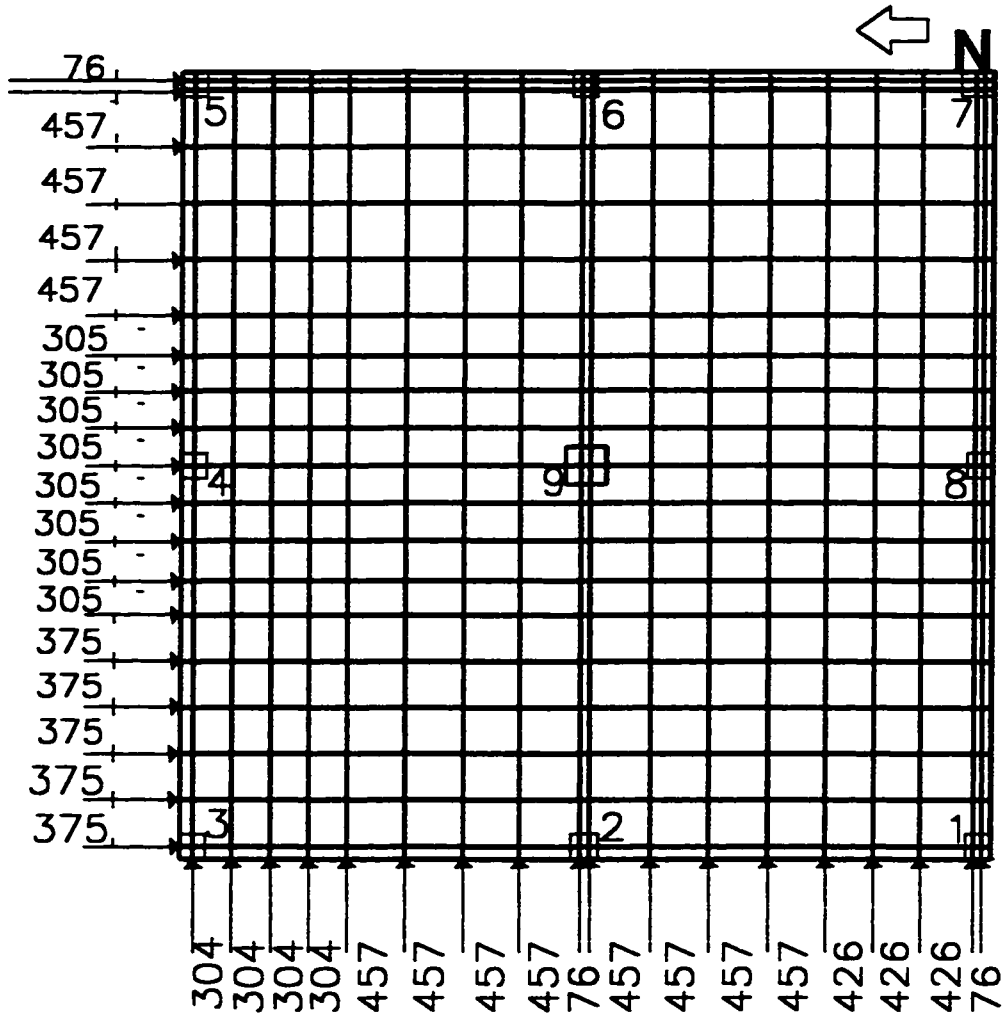

Fig. 3-8 Distribution and distance between tendons in mm

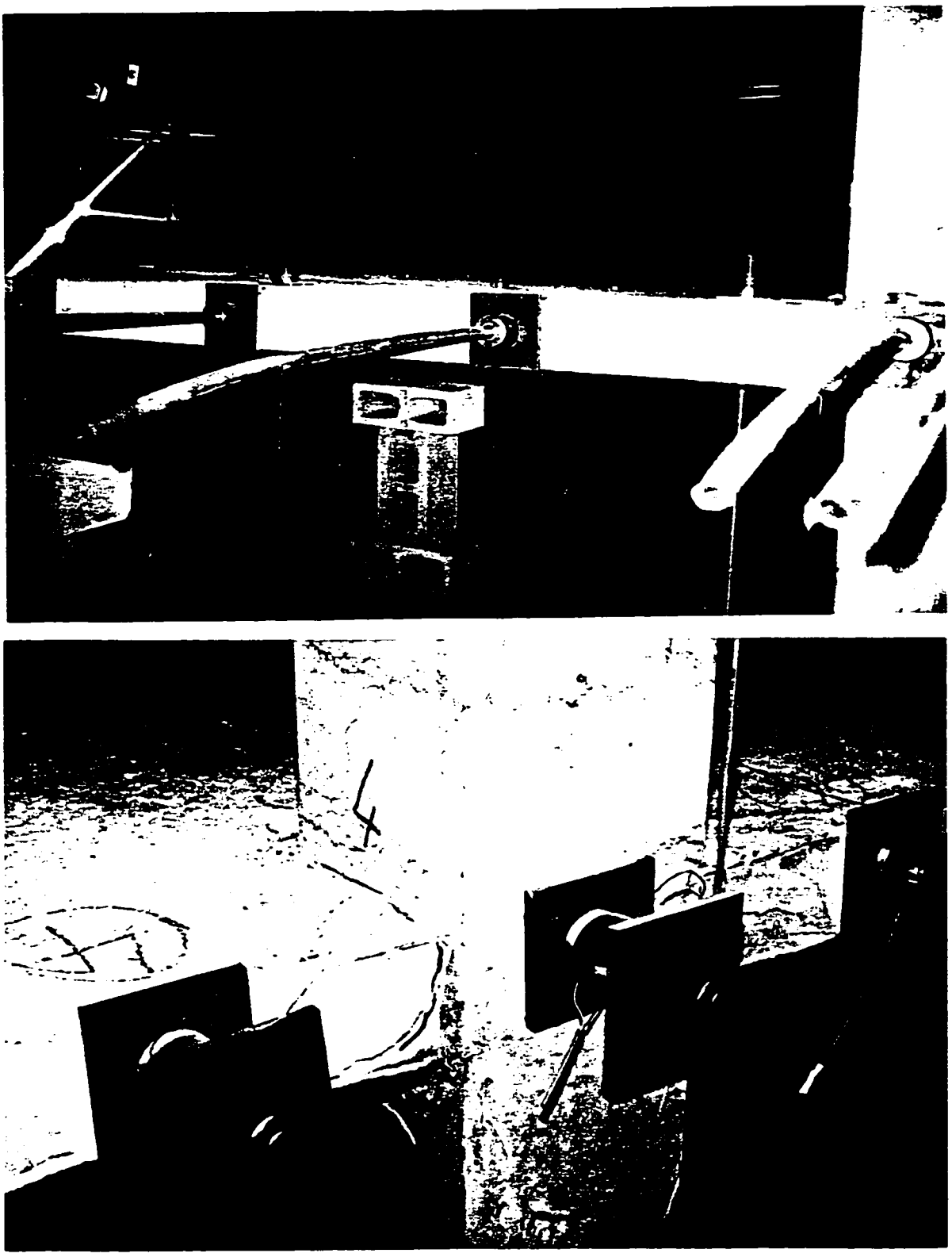

Fig. 3.9 The steel plates, anchorage grips and load cells used in the experiment

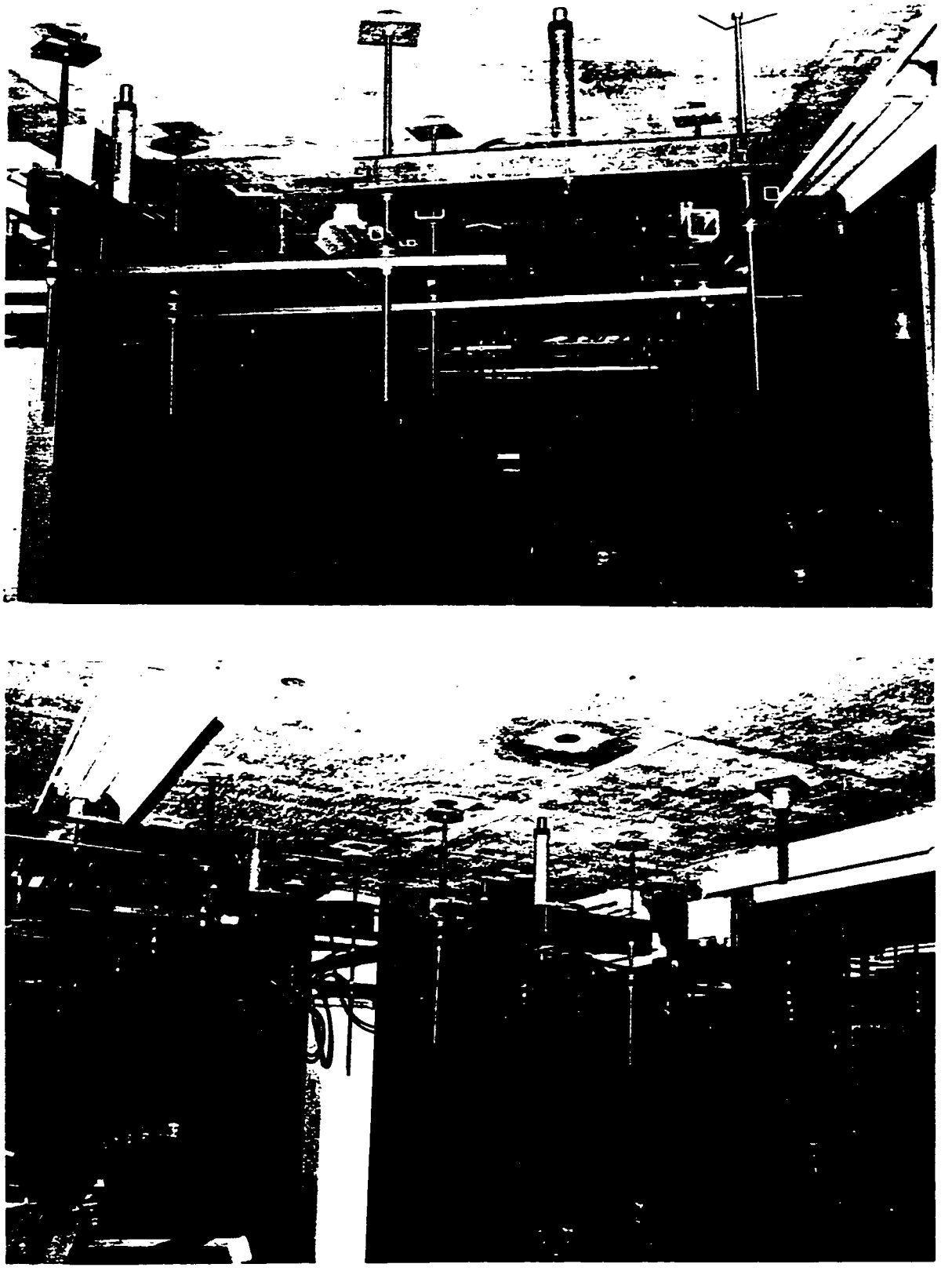

Fig. 3.10 The part of the loading system erected in the basement of the laboratory

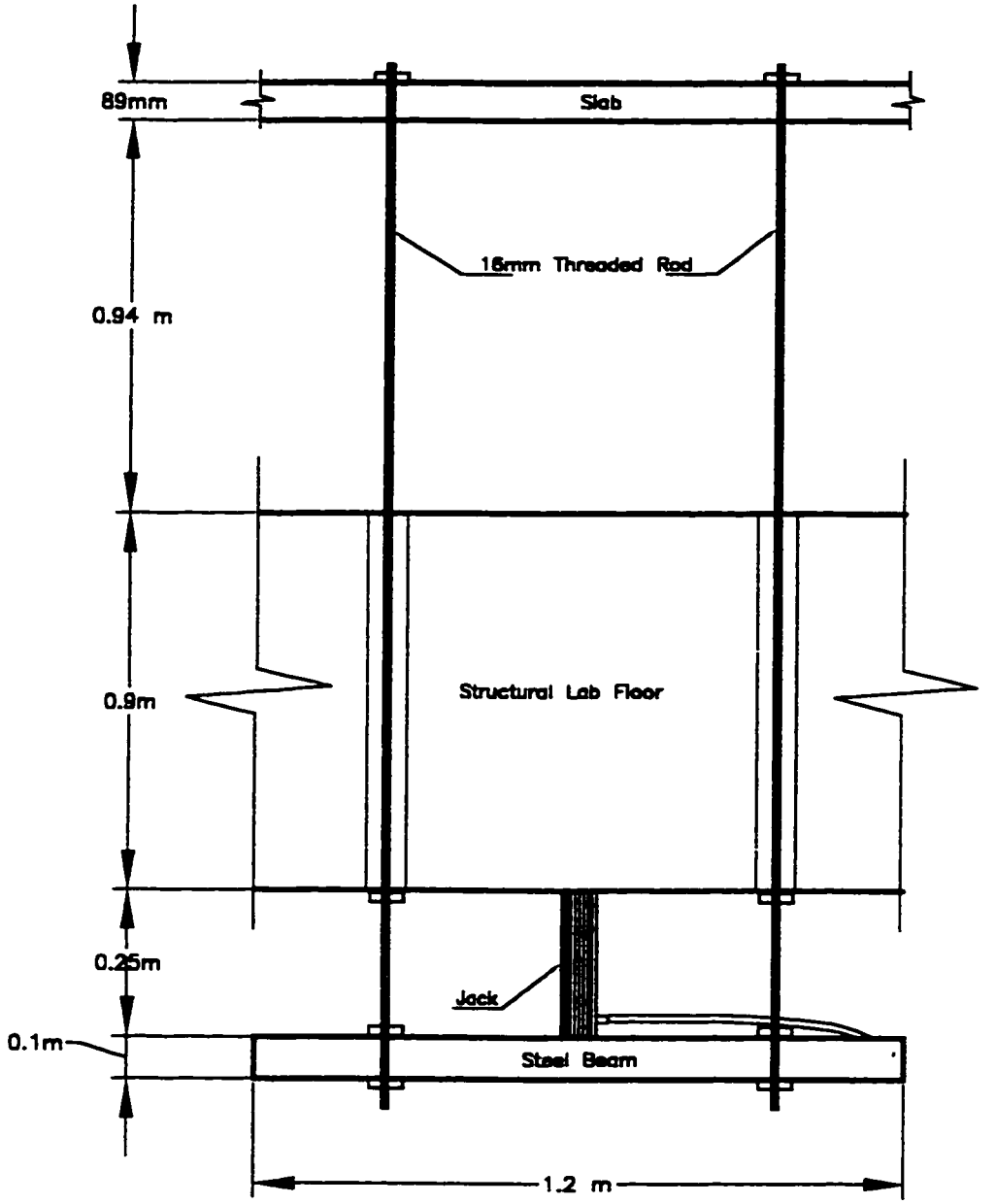

Fig. 3-11 Schematic of the loading system

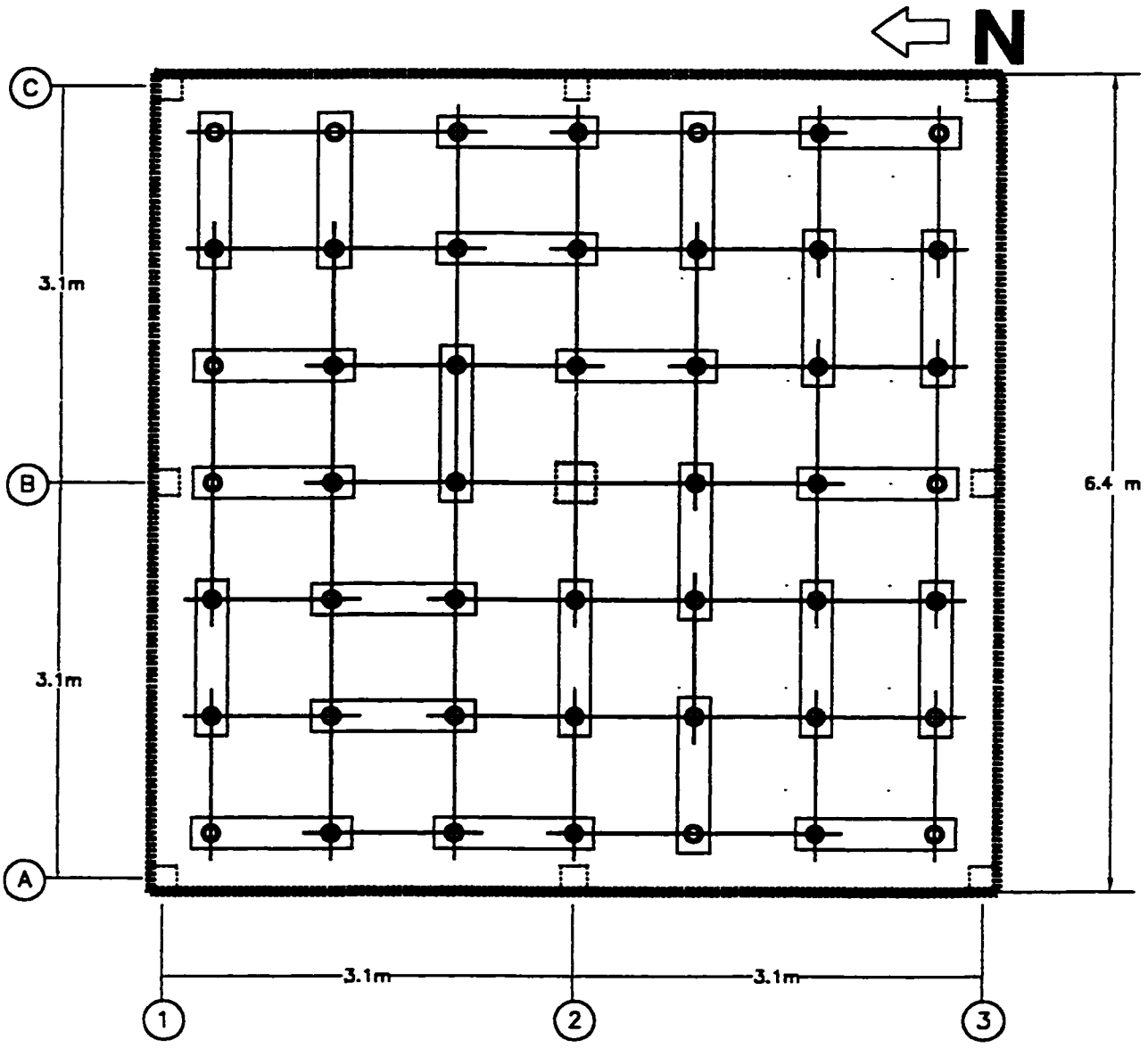

Fig. 3-12 Distribution of beams in the loading system

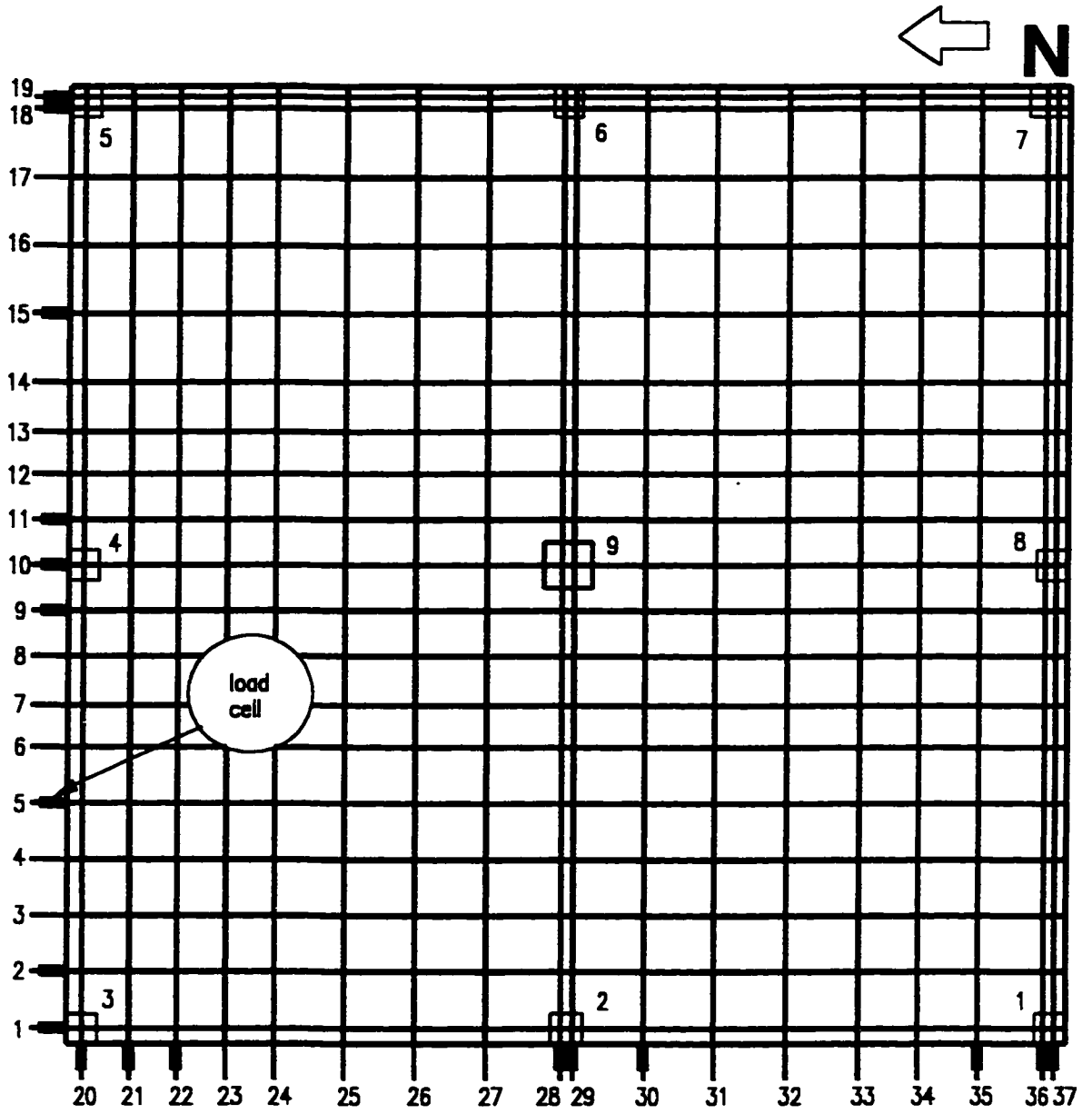

Fig. 3-13 Positions of tendon load cells

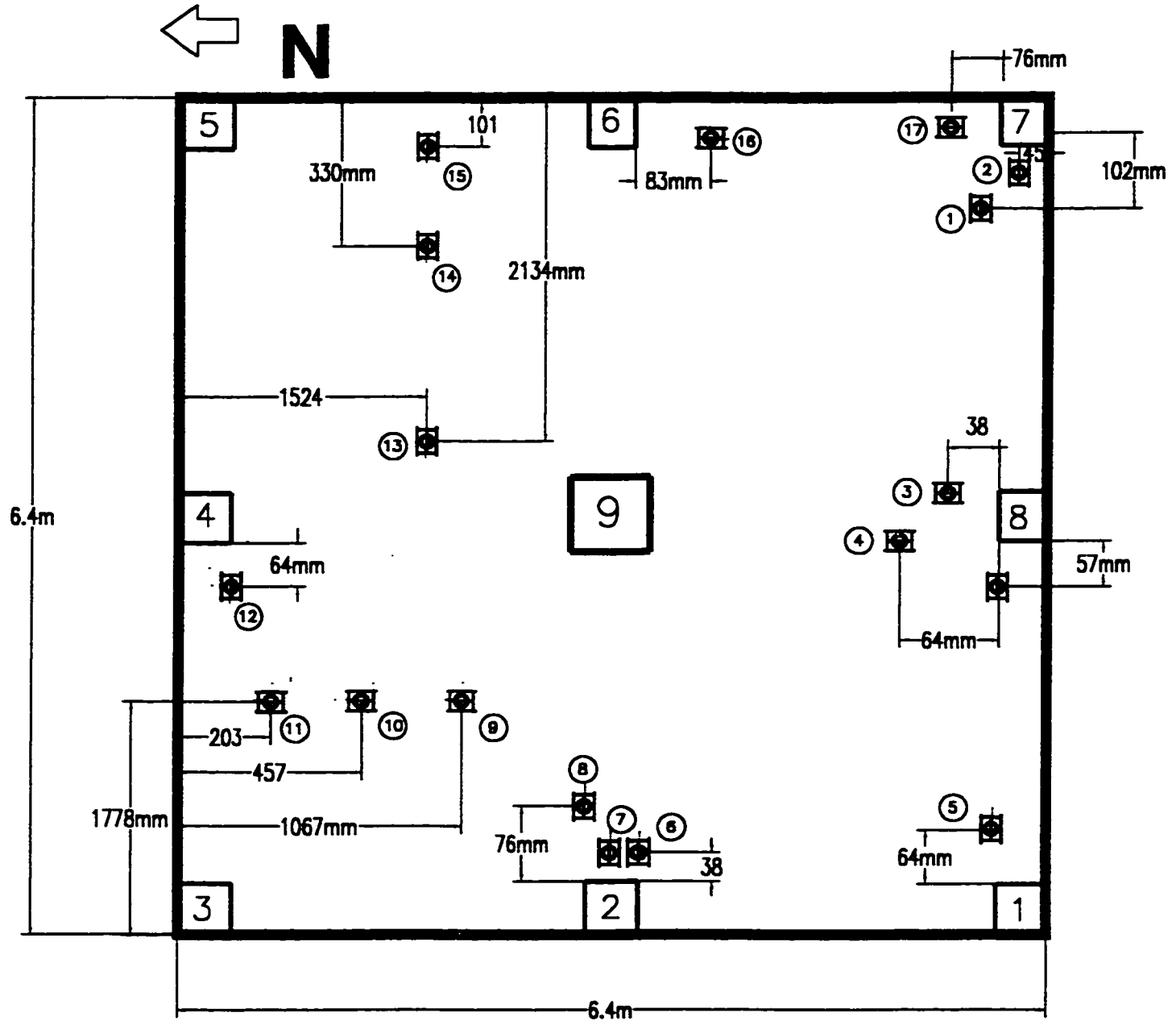

Fig. 3-14 Positions of the vibrating wire gauges(VWG) in the slab

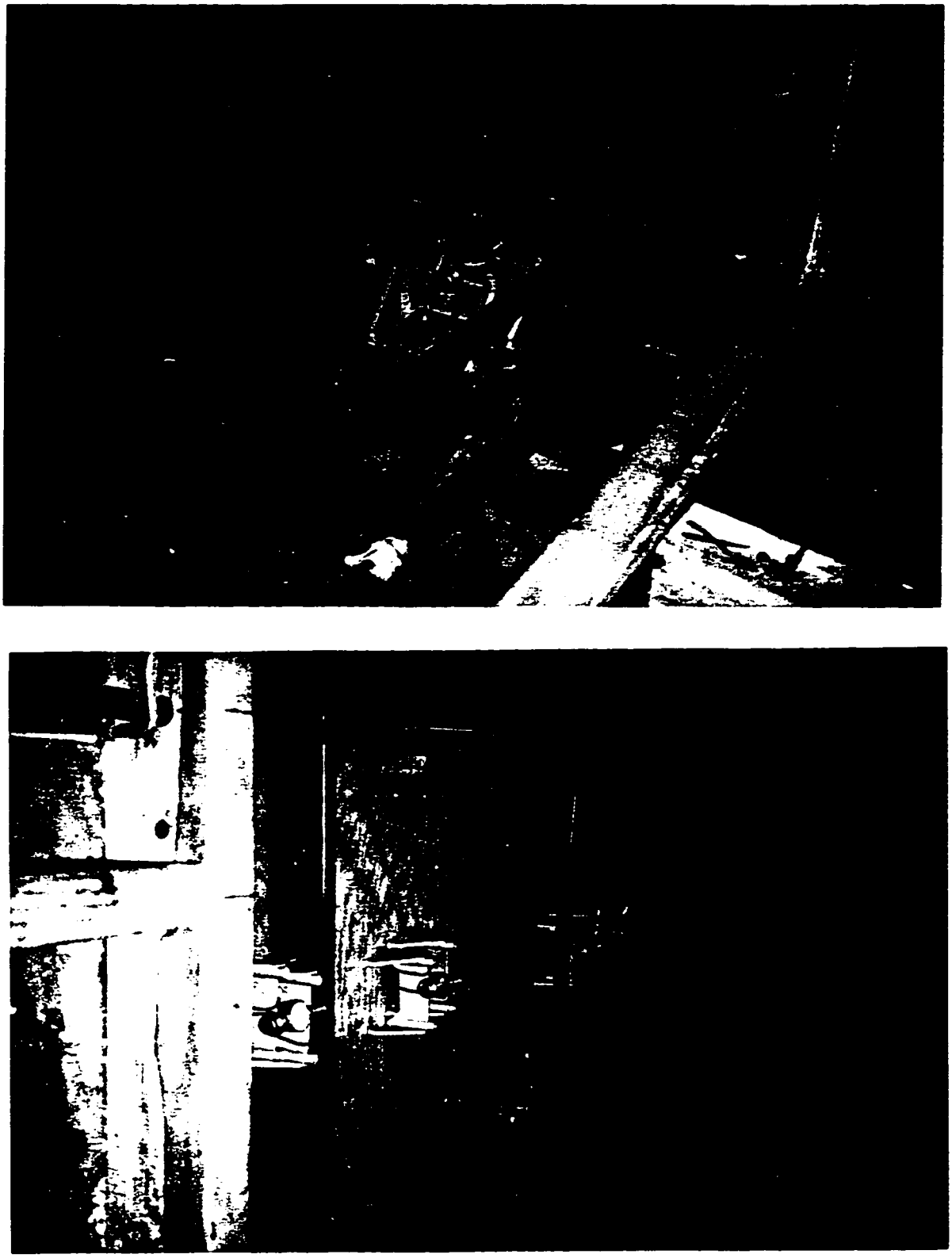

Fig 3.15 The vibrating wire gauges placed on chairs and tightened to the formwork to prevent them from movement

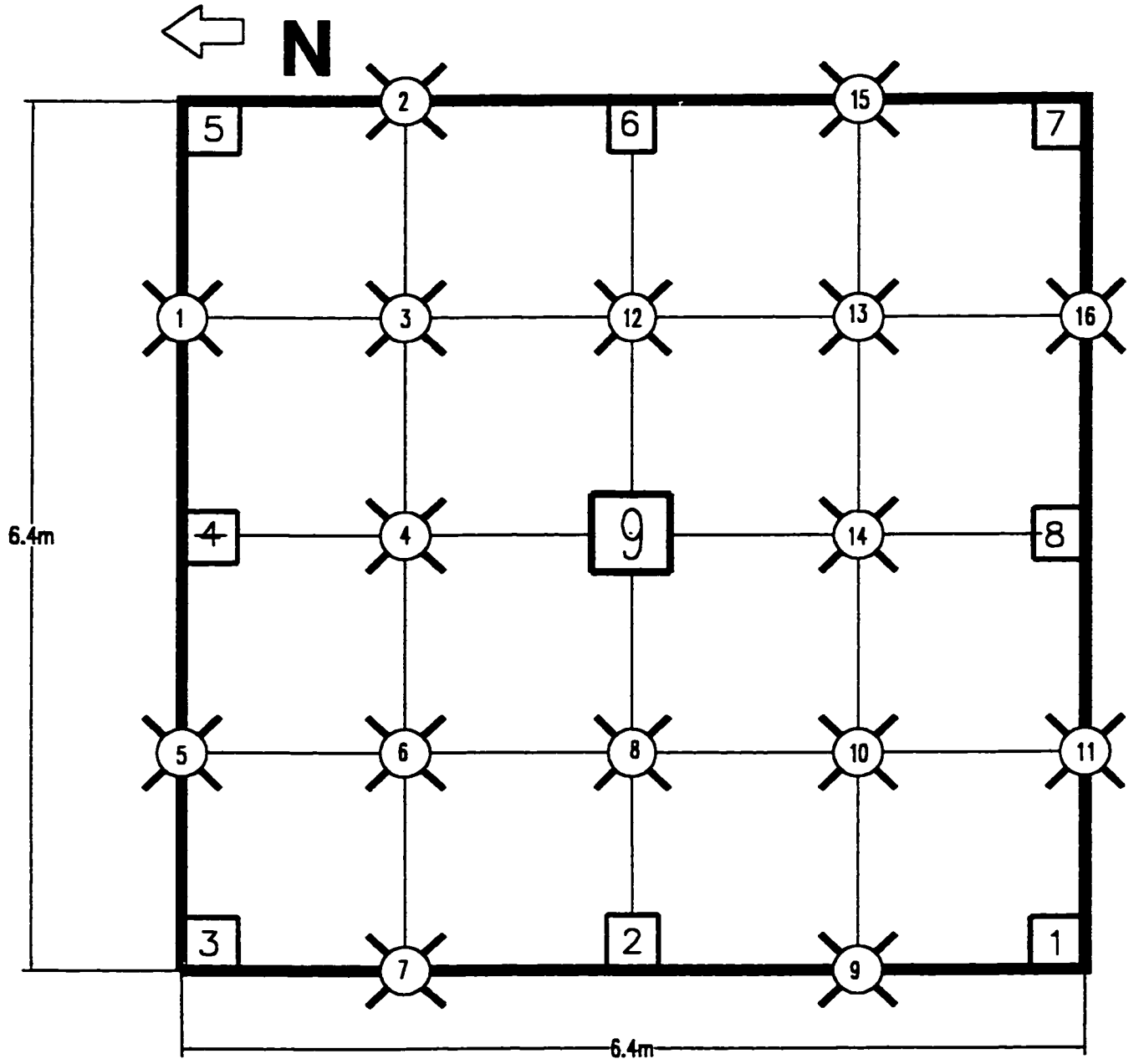

Fig. 3-16 The positions of deflection dial gauges under the slab

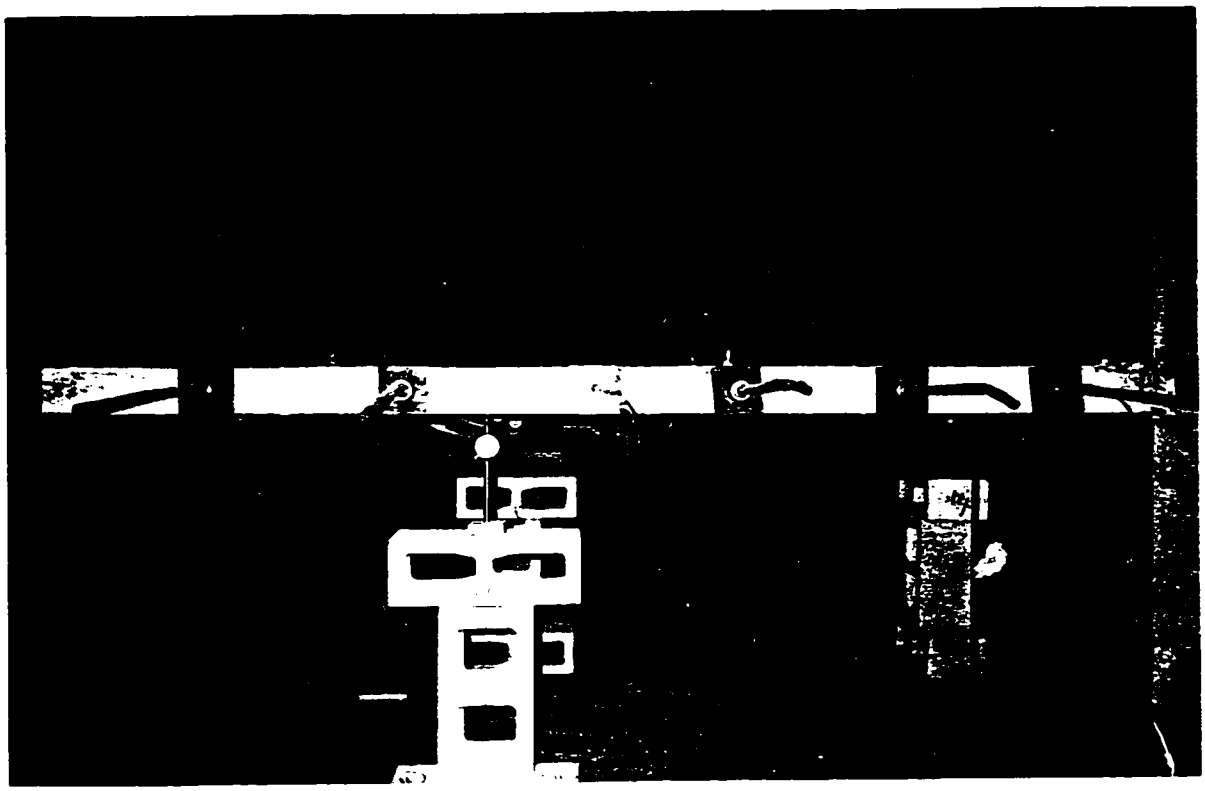

Fig. 3.17 Dial gauges no. 10, 11 and 14 in panel C

CHAPTER 4

SLAB TESTS

4.1 Pretests :-

Three pretests were performed to make sure that the system worked well. All hoses, jacks and connections were checked during these pretests. Leakage at connections, jacks and hoses were fixed. The distribution of oil to all jacks was checked. The electrical pump was tested and the pressure gauge was calibrated. Initial readings were taken for the dial gauges under the slab and the load cells located under columns 3, 6, 7, 8 and 9. A live load of 2.9 kN/ m^2 was applied, readings were taken. The load was increased to 5.84 kN / m^2 and the gauges were reread. Most of the readings doubled indicating elastic behaviour. When the load was released the readings returned to their initial values. At this step, the linearity of the slab was checked and it was found that the system was ready for the first test to failure.

4.2 TEST # 1 : -

Initial readings were taken of the load cells used to measure tendons forces, the strain gauges on rods connecting the slab columns with steel box – section columns, the vibrating wire gauges in the slab, the load cells under columns 3, 6, 7, 8 and 9 and the 16 dial gauges under the slab.

An initial 5.83 kN / m^2 load was applied and no visible cracks were seen. The load was increased to 8.76 kN/ m^2. Top surface cracks were observed in the negative moment regions in the column–slab connections. The cracks were tangential around

columns 2, 4 and 9. The cracks were less visible around columns 6 and 8. No cracks were noticed at the corner columns.

The load was increased by increments of 2.92 kN / m^2 until it reached 17.51 kN/ m^2. The cracks became wider and the radial cracks around the columns became longer, the average length of the radial crack passing by the corner of the interior column was 320 mm. No change happened to the forces in the tendons. The biggest increase in the strains in the vibrating wire gauges was noticed in VWG no. 7, which was at the middle of column number 2 at distance 38 mm from the column in the east–west direction. The change in strain at this stage was 230 με. Fig. 4.1 shows that the average of the mid panel deflection in the four panels was 7.75 mm at an applied load of 17.5 kN/ m^2. The deflection started to enter the inelastic range at this load step. As the test progressed, the cracks became more visible in the negative moment regions and it was decided to reduce the increment of the load increase.

At a load of 20.43 kN/ m^2 one of the jacks, close to column 4 started leaking, but it was decided to continue the test because the problem was not considered serious. The next load step was 22.48 kN/ m^2. Fig. 4.2A shows that moments transferred from slab to edge columns at this applied load ranged from 19.5 to 21.1 kN.m. While Fig. 4.2B shows that the moments at the corner columns at an applied load of 22.48 kN/ m^2 ranged from 15.9 to 18.0 kN.m.

As the load was increased to 23.65 kN/ m^2, the radial cracks around the columns became longer and deeper and positive moment cracks were obvious at the bottom of the slab. Fig. 4.3 shows the distribution of cracks at this load step. As the dial gauges were being read, punching shear failure happened at column 2, on the west side, accompanied

with loud bang. The failure was sudden, the load dropped to 18.7 kN/ m^2. Fig. 4.4 shows the failure zone as a truncated cone forming an angle of 18^o with the surface of the slab. The column moved horizontally into the failed slab. Prior to failure the moments transferred to edge columns were around 23 kN.m and the moments transferred to corner columns were around 18 kN.m.

Fig. 4.5 shows the increase in force in the two tendons passing through column 2 in the east–west direction. The forces in these two tendons dropped by 20 kN after the punching shear failure (not shown in the graph). The tendons lost almost 23 % of their force. Fig. 4.6 shows the change in force in the tendon passing through column 2 in the north–south direction. No drop in the force was recorded in this direction. The maximum deflection prior to failure was 22 mm. Fig. 4.7 shows the change in the vibrating wire gauges no.7 strain in the east–west direction.

The slab was unloaded and the damaged deflection gauges under the slab were replaced. The compression threaded rods connecting the steel box–section columns with the slab columns had buckled as a consequence of the punching shear failure. These threaded rod load cells were replaced with tube load cells with higher buckling resistance. The tubes were provided with new strain gauges. Cutting the rods connecting column #2 to the steel anchors caused more force to be released from the two tendons passing through this column and column # 6, the loss was about 20 kN. The failure area was cleaned and the crushed pieces of concrete were removed. Formwork of steel sheets were put under the failed area. The two tendons were restressed to regain part of their losses. Fig. 4.8 shows the reshores around the repaired column. The wooden reshores were 102 mm x 102 mm in section. The damaged area was patched using concrete with

maximum 10-mm gravel. It was cured for 10 days. All 16 deflection gauges were reset in their positions. Because of the reduction in stress in the tendons passing through columns 2 and 6 in the east–west direction, column 6 was reshored in a similar manner to column 2 to prevent it from failure.

4.3 TEST # 2 :-

Initial readings were taken for the deflection dial gauges, the strain gauges on the connecting rods, the vibrating wire gauges, the tendon load cells and the load cells under columns. Because columns 2 and 6 were reshored, it was expected that failure would occur around either column 4 or 8. It was decided to start with load equal to 4.67 kN/ m^2 because it is relatively small and easy to read from the pressure gauge. After the readings had been taken the applied load was doubled to 9.33 kN/ m^2 but the mid panel deflections increased 2.3 times, indicating the deflection had already entered the inelastic range. The load was increased in increments to 14 kN/ m^2. By comparing Figs. 4.1 and 4.9, it can be observed that at the same load, deflections in the second test are 2mm larger at 14 kN/ m^2 applied load due to the residual cracks from Test 1. The location and distribution of cracks were the same as in the first test, but in the second test the cracks were wider and deeper. All the tendons, in both directions, experienced some increase to their forces. At this applied load, the loads measured at corner columns were 27 kN, 175 kN to middle column and the load transferred to edge column eight 64 kN. These values are close to the values obtained in Test 1. If it was assumed that the loads transferred to corner columns and to edge columns were 27 kN and 64 kN respectively we would get 9.4 % less loads transferred to columns than the applied loads which is exactly the same

difference between the applied and the transferred load in Test 1. It can be concluded that the precision in the instrument readings is about 90%.

At a load of 18.68 kN/ m^2, the cracks became wider and torsional cracks were visible around edge columns, so it was decided to decrease the increment to 2.33 kN/ m^2. The next step was 21 kN/ m^2 (3600 psi on the pressure gauge knowing that there are 24 jacks), the maximum deflection was 18 mm at mid panels A and B. To record changes close to the failure load it was decided to reduce the increment to 1.12 kN/ m^2. It was possible to take the last reading of the vibrating strain gauge 3 which was located at 38 mm (1.5 inch) from the corner of column 8, then the vibrating wire gauge failed. It is compared in Fig. 4.10 with vibrating wire gauge 4, which was at the other corner of column 8 and located at 64mm (2.5 inch).

From the previous test it was known that the failure load would be approximately 23 kN/ m^2, it was decided to take readings every 0.6 kN/ m^2. At load equal to 23.35 kN/ m^2 a problem happened to the electrical pump causing the entire load to be released. The pump was repaired and the test resumed keeping the previous load increments. When the load reached to 23.35 kN/ m^2, it was obvious that the moments transferred to column 8 were larger than the moments transferred to column 4 which is illustrated clearly in Fig. 4.11A. This could be explained because the top bar connecting column 8, which was supposed to be subjected to tension, did not experience any load until prior to failure when it showed some tensile force equal to 7.7 kN while the bottom bar was subjected to high compression force. In contrast at column 4, the top bar which was under tension from the beginning of the test, the tension force started decreasing until two load steps before failure when the bar became under compression instead of tension while the

bottom bar was under compression in all load steps with constant increase in its force. This phenomena could be explained by movement of the two restraining columns and steel beam of 4" x 4" box–section connecting them, causing column 8 to move inward and column 4 outward of the slab and the distribution of moments to be changed causing column 8 to fail instead of 4.

Fig. 4.11 B shows the moments transferred to corner columns. The moments ranged from 12 to 15 kN.m. Comparing these values with those measured in Test 1, at an equivalent load step, corner moments in the second test were less than the corner moments in the first test. This could be due to movement of concrete columns or reduction of slab stiffness because of cracks, which caused less moments to be transferred from the slab to the columns.

As the test continued, with load increments of 0.6 kN/ m^2, cracks and sounds indicated that column 8 was very close to failure. At a load of 26.27 kN/ m^2, was decided to take the deflection readings only at mid–panels because it was very dangerous to go under the slab. The slab had wide cracks in the both negative and positive moment regions. At this load a punching shear failure happened around column 8 accompanied with a large explosion and pieces of concrete thrown distances exceeding 7 m. The damaged area was about 0.6 m around the column. The damage was larger and more severe than in the first test. The load immediately dropped to 18 kN/ m^2. The tube bar load cell at the bottom of column 8 had buckled. The column had moved inward by more than 15 mm. Fig. 4.12 shows the change in force in tendons 9, 10 and 11 in the north–south direction, while Fig. 4.13 shows changes in the east-west direction. The losses in force in the tendons passing through the failure zone in the north–south direction were as

follows: Tendon T9 broke out of the slab at the south end and lost all its force. Tendon T10 which passed through the middle of column 8 lost 15 kN, and T11 lost 25 kN. No losses were recorded for the tendons in the perpendicular direction. Maximum deflection prior to failure was 33 mm at mid–panels A and B and 30 mm at mid-panels C and D.

After the test the crushed pieces of concrete were removed and the damaged area around column 8 was cleaned. The failure area was lifted by a jack. Metal sheet formwork was used. The formwork was shored by two layers of 102 mm x 102 mm (4" x 4") pieces of wood. Because the damaged area was larger than in the first test, it was provided with two layers of support. Then the jack was released to let the formwork sit on the supports. Fig. 4.14 shows the reshored zone ready for patching. Because of the damage of the concrete at the bottom of the slab, this time no gravel was used. After patching, it was cured for 10 days. Tendon 9 was stressed again to regain the force it had lost at failure. It was estimated that it regained the full 100 kN. Tendon 10 was stressed again using 305 mm (12") square plates with 12.7 mm (0.5") thickness, as it can be seen in Fig 4.14 and by using 25.4 mm (1") diameter threaded rods. By tensioning the plates against the steel columns at both ends pulled the tendon outward, causing it to be under tension, regaining it's initial force. Because of losses in stresses in the three tendons, column 4 was reshored using 5 pieces of 102 mm x 102 mm wood, located at a perimeter of 100 mm from the face of the column, the area of the slab around the column lifted 10 mm by a jack, the supports located in their positions and the pressure released to let the area sit on the reshores.

The damaged dial gauges were replaced with new ones, any broken wires were repaired, all the instruments set to their initial readings, the hydraulic system was checked and two hoses and jack connections were changed. The slab was ready for another test.

4.4 TEST # 3 :-

At this test three of the edge columns were reshored, and it was known that the ultimate load would range between 23 to 26 kN/ m^2. Before the test, the supports around column 6 were removed, by lifting the slab around this column using a jack. As usual the initial readings for all instruments were taken and a load of 4.7 kN/ m^2 was applied. The load was doubled to 9.33 kN/ m^2 then to 14 kN/ m^2. Comparing Figs 4.9 and 4.15, it can be concluded that at a load of 14 kN/ m^2 , the deflections were similar in the second and third tests. No changes were observed in the tendon forces at this load. The next load step was chosen to be 16.34 kN/ m^2. Then it was followed by steps of 18.68 and 21.01 kN/ m^2. The load steps were reduced first by a half and then by quarter. It was very difficult to keep the pressure constant on the jacks. The load dropped very quickly, so the readings were taken as quick as possible. Later on it was decided to stop the test and investigate the problem. It was found that there was a problem with the valve connecting the pump to the hydraulic system. With the load kept at 22.18 kN/ m^2, the hoses were disconnected from the pump. The valve was replaced and checked for pressure up to 62 MPa (9000 psi). It was then reconnected with the hoses and the test restarted. The next load step was 23.34 kN/ m^2. Fig. 4.16A shows that the moment transferred to column 6 at this load step was 19.8 kN.m. At an applied load of 23.6 kN/ m^2 in Test no. 1 the moment transferred to column 6 was 23 kN.m. It was not possible to measure the moments transferred to other columns because of the reshoring around these columns.

Fig. 4.16B shows that moments transferred to corner columns at this load step were: column no. one 10.9 kN.m, column no. three 12.0 kN.m, column no. five 16.8 and column no. seven 12.3 kN.m. While one load step prior to failure and at an applied of 25.1 kN/ m^2 the moments were as follows; column no. one 13.0 kN.m, column no. three 13.1 kN.m; column no. five 18.0 kN.m and column no. seven 15 kN.m.

As the load was increased by 0.6 kN/ m^2 to 25.70 kN/ m^2 , slab-column connection no. 6 failed due to shear, moment and torsion. Fig. 4.17 illustrates the combination of shear and torsion failure, while the right side failed by shear as shown in Fig. 4.18. Fig. 4.19 shows the crushing of concrete due to moment. Fig. 4.20 shows the changes in tendon force T 29 and T 28 which passed through column 6 and T 30 which was at a distance of 186 mm from the column in the west–east direction. Tendon T 30 did not lose any force after failure while T 29 lost 26 kN and T 28 lost 29 kN. The changes in tendon T18 and T19 forces passing through column 6 in the north–south direction are shown in Fig. 4.21. These tendons did not lose any force due to the connection failure. The maximum mid–panel deflection was 34 mm in panel A.

To speed up the process of tests, it was decided not to patch the failure area this time. It was reshored by two rows of supports in a similar way to column 8. The reshoring was removed from around column 4. Column 4 was the only edge column not previously failed but the tendon forces in the column region had been reduced due to the failure of connection #8 in Test #2. All other edge columns were reshored. The system was checked, all the instruments were set to their initial readings. The slab was ready for new test.

4.5 TEST # 4 : -

This time the aim was slab-column 4 connection. The load steps were the same as in the previous tests starting with load equal to 4.7 kN/ m^2 . Fig. 4.22 shows that at an applied load of 14 kN/ m^2, mid-panel A deflection was 8.3 mm, B 11.7 mm, C 8.4 mm and D 6.9 mm. Generally speaking, in most tests panel B suffered the biggest deflections and panel D the least deflections.

To compare with moments transferred to other columns in previous tests, Fig. 4.23A shows the moments transferred to column 4 up to 23.34 kN/ m^2 of applied load. Fig. 4.23B illustrates moments transferred to corner columns up to this load. The next load step was 23.9 kN/ m^2. At this stage while readings were taken for deflections punching shear failure happened to column 4. Fig. 4.24 shows the changes to VWG no. 12 from the beginning to the end of the test when slab–column 4 connection failed. Fig. 4.25 shows the severe damage of this connection due to punching shear failure.

Fig. 4.26 shows the changes in tendon forces, 9, 10 and 11 in the north–south direction. Tendon T 10 which passes through column 4 lost 10.5 kN of its force after failure. Tendon T 11 which is at 202 mm toward the east side lost 67.27 kN and tore out of the slab at the north side. Tendon T 9 at a distance of 202 mm toward the west side, lost 25.6 kN. Fig. 4.27 shows change in tendon T 20 force in the direction parallel to free edge. The last reading for the deflections was at an applied load of 23.3 kN/ m^2. The biggest deflection was 35 mm in panel B and the smallest 16 mm in panel D. Finally the failure zone around column 4 was lifted up by a jack, and supported by two rows of supports in a similar manner to the previous test. All instruments were set to their initial readings and the hydraulic system was inspected for any problem.

4.6 TEST # 5 : -

This time all the edge columns were supported. All the tendons which passed through the failed edge columns had lost some or all of their prestress. The objective was to see the overall behaviour of the slab after the reshoring of all the edge columns which would cause failure of a corner or the interior slab-column connection. At load equal to 29.20 kN/ m^2 loud bang was heard from column 6, followed by column 2-connection failure. As the load was dropping, after column 2 connection failure, column 9 (interior) connection failed. The slab suffered major damage, columns 2 and 6 moved in about 25 mm. Also the columns in the other side moved toward the slab. The reason of column 2 connection failure was because it was provided with only one row of supports while others were provided with two rows. Losing the force in T 30 caused column 9 connection to fail. Fig. 4.28 shows the changes in tendon forces passing through the failure zone. Surprisingly tendons T29 and T28 did not lose any force after failure while tendon T30 lost 63 kN. The last readings for deflections were taken at a load of 26.27 kN/ m^2 because it was not safe to go under the slab to take the readings. Fig. 4.29 shows deflections being taken. The mid–panels deflections were; panel A 23 mm, panel B 36.3 mm, panel C 28.6 mm and panel D 20 mm. Fig. 4.30 shows the failure zone around column 2 and it shows that T30 pulled out of the slab. Fig. 4.31 shows the punching shear failure around column 9 with perimeter of 60 mm around the column. Fig. 4.32 shows the two failure zones and the severe deflection at panel B which was estimated to be more than 40 mm at failure. Fig. 4.33 shows column 9 and 2 connections after failure.

Column 2 was provided with second row of supports. Column 9 zone was supported with 8 reshores at a distance of 300 mm around the column. Because of leaks,

two jacks were disconnected from the system. Dial gauges were removed from under the slab. The pump was repaired and filled with oil. The slab was ready for a final test.

4.7 TEST # 6 : -

The objective was to investigate the behavior of the corner column-slab connections. Fig. 4.34A shows the changes in tendon forces in the east–west direction at corner columns. In Fig. 4.34B changes in tendon forces at corner columns in the north–south direction are shown. It can be concluded that the tendons passing through column no. 3 experienced the biggest change in their forces. Fig. 4.35 shows the top and side cracks at column 3 periphery while 4.36 shows the severe cracks around column 3 from the bottom which suffered more cracks in its perimeter than other columns. In Fig. 4.37 the axial loads transferred to corner columns provided with load cells are shown. Those loads are less than in previous tests because of reshoring of internal and edge columns making these internal and edge columns absorb more loads and at the same time shortening the span lengths. At a load of 26.76 kN/m^2 column 2 connection failed, the failure was outside the reshores making a large hole inside the failure zone. The failure was because of the tendon losses in the previous test. It was decided to continue the test. At applied load equal to 32.11 kN/m^2 a massive failure happened around column 6 making a big hole in the failure zone. All the corner columns survived the test but column 3 connection suffered severe cracks.

4.8 Summary : -

All edge column connections failed at applied loads in the range 23–26 kN/m^2. Table 4.1 summarizes the loads which caused failure in the first 4 tests. In Test no. 5 all the periphery failed edge column-slab connections were reshored and the load was applied until failure occurred at the outside of the reshored region of edge column #2 and at interior column #9. This occurred at an applied load of 29.20 Kn/m^2. The maximum load was applied in Test no. 6; all the corner columns survived this load of 32.1 kN/m^2. Table 4.2 shows losses in tendons perpendicular to the slab edge passing through the failure zone in the first 5 tests. The tendons in the direction parallel to the slab edge did not lose any force. Table 4.3 gives the mid-panel deflections in the first five tests prior to failure. It must be noted that reshores were used for all tests, except Test #1, reducing span length and presumably deflections. Table 4.4 summarizes the loads transferred to columns 3, 6, 7, 8 and 9 in the 6 tests. Table 4.5 summarizes the moments transferred to edge columns in the first 4 tests. In the last two tests no edge moments were measured. Table 4.6 summarizes the moments transferred to corner columns in the 6 tests.

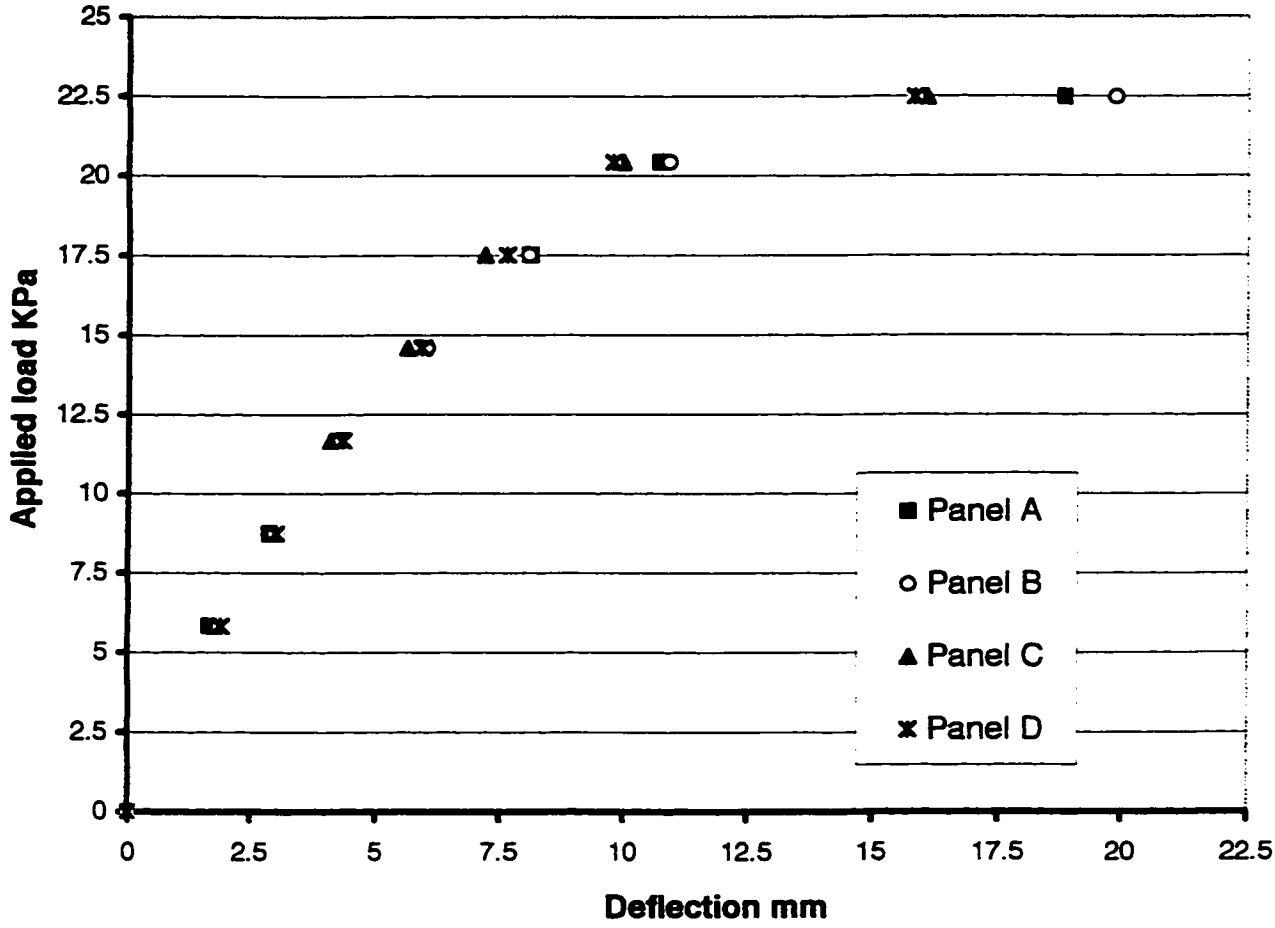

Fig. 4-1 Mid-panel deflections in Test no. 1

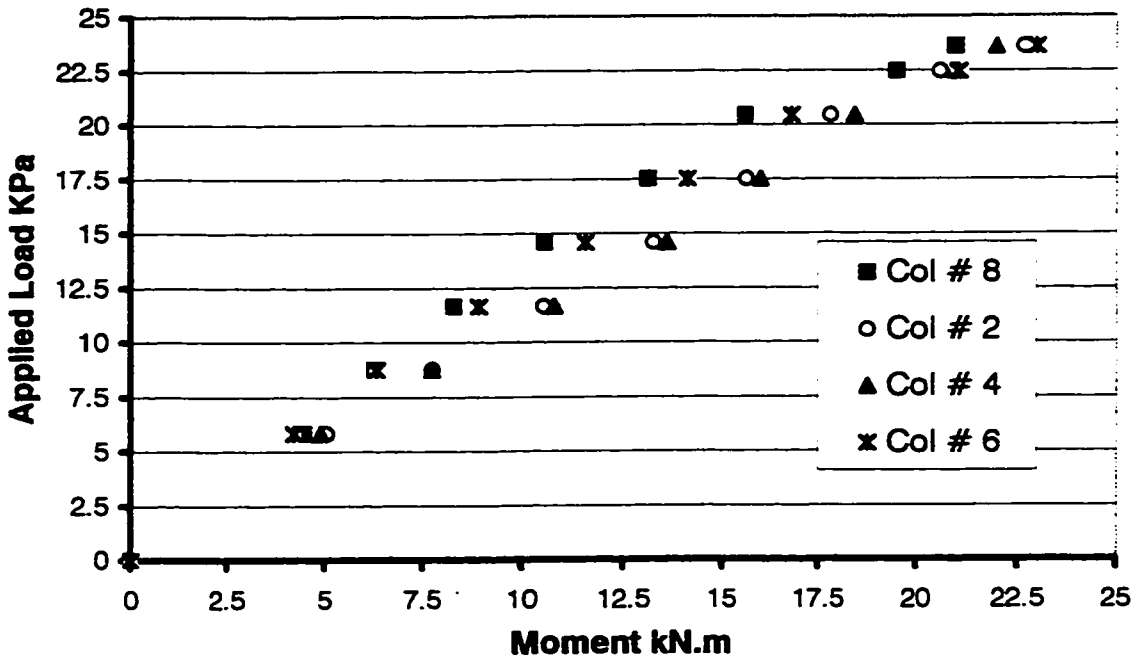

Fig. 4-2A Edge column moments in Test no. 1

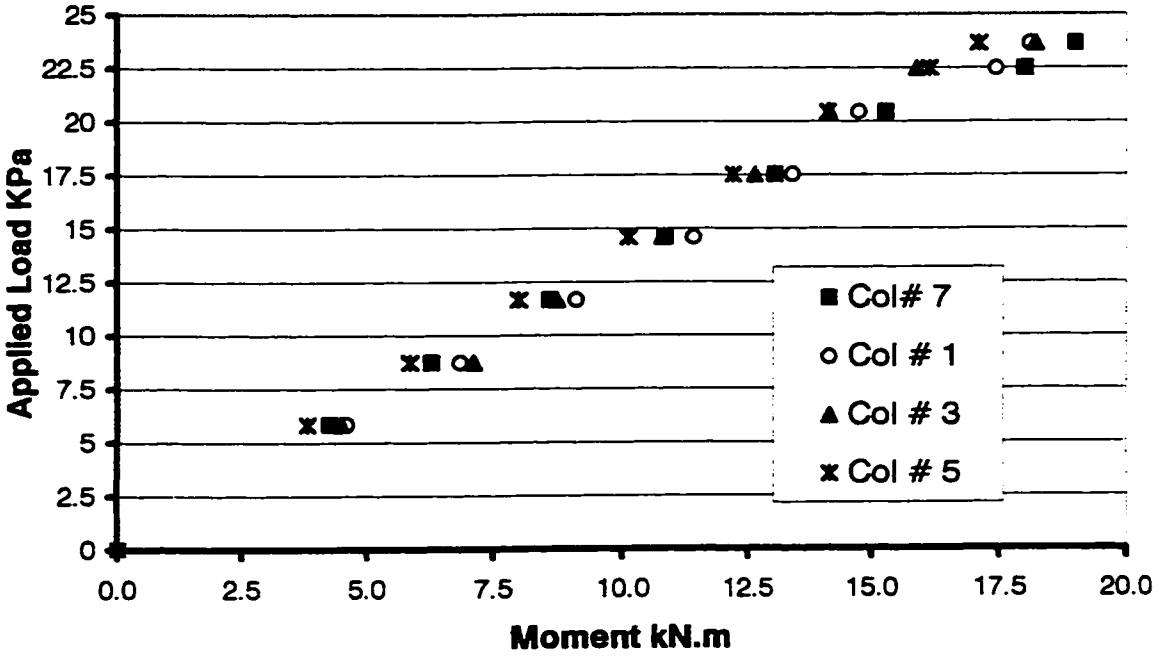

Fig. 4-2B Corner column moments in Test no. 1

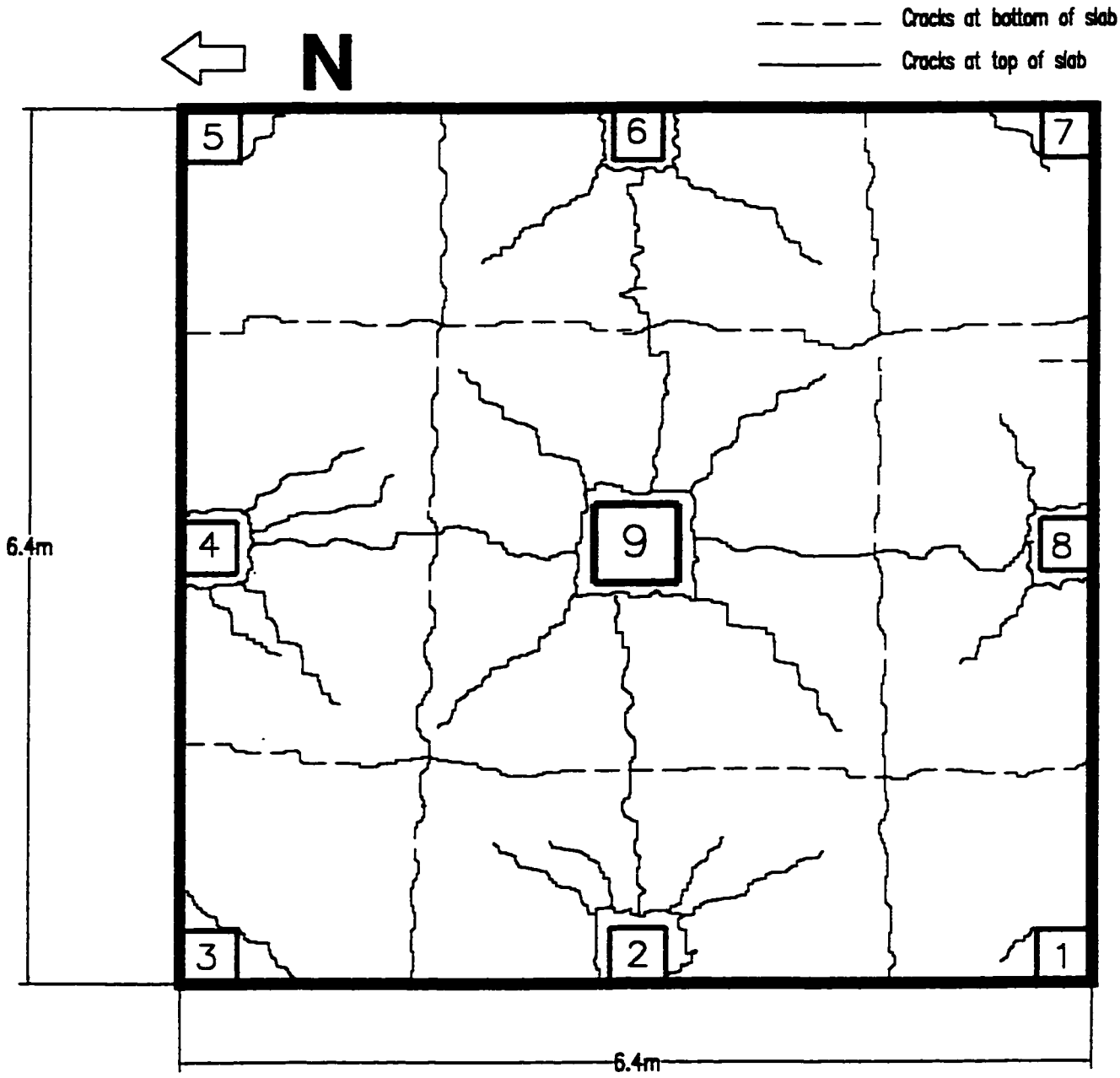

Fig. 4-3 Distribution of cracks immediately prior to failure in Test no. 1

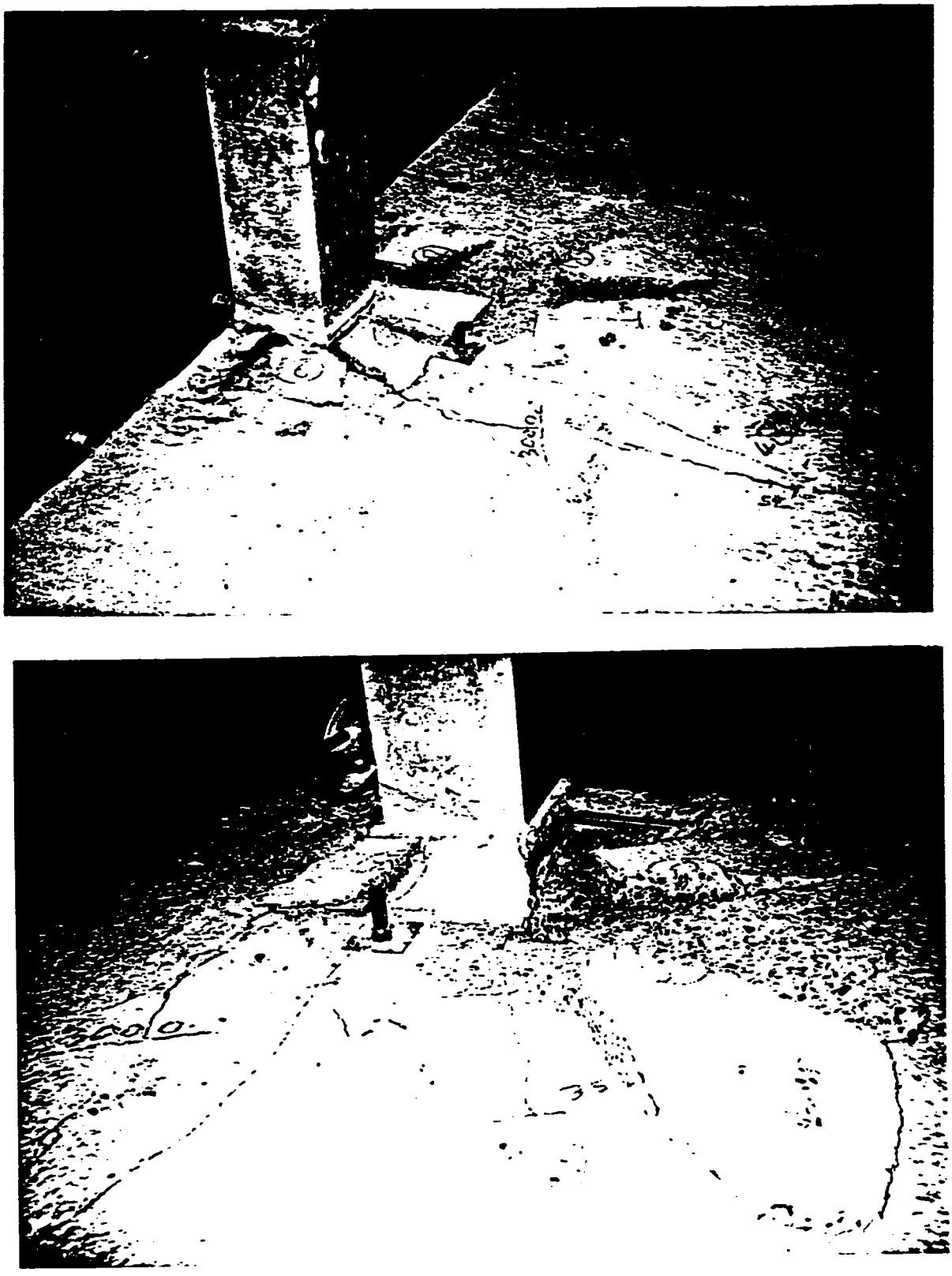

Fig. 4.4 Punching shear failure zone at column no. 2 in Test no. 1

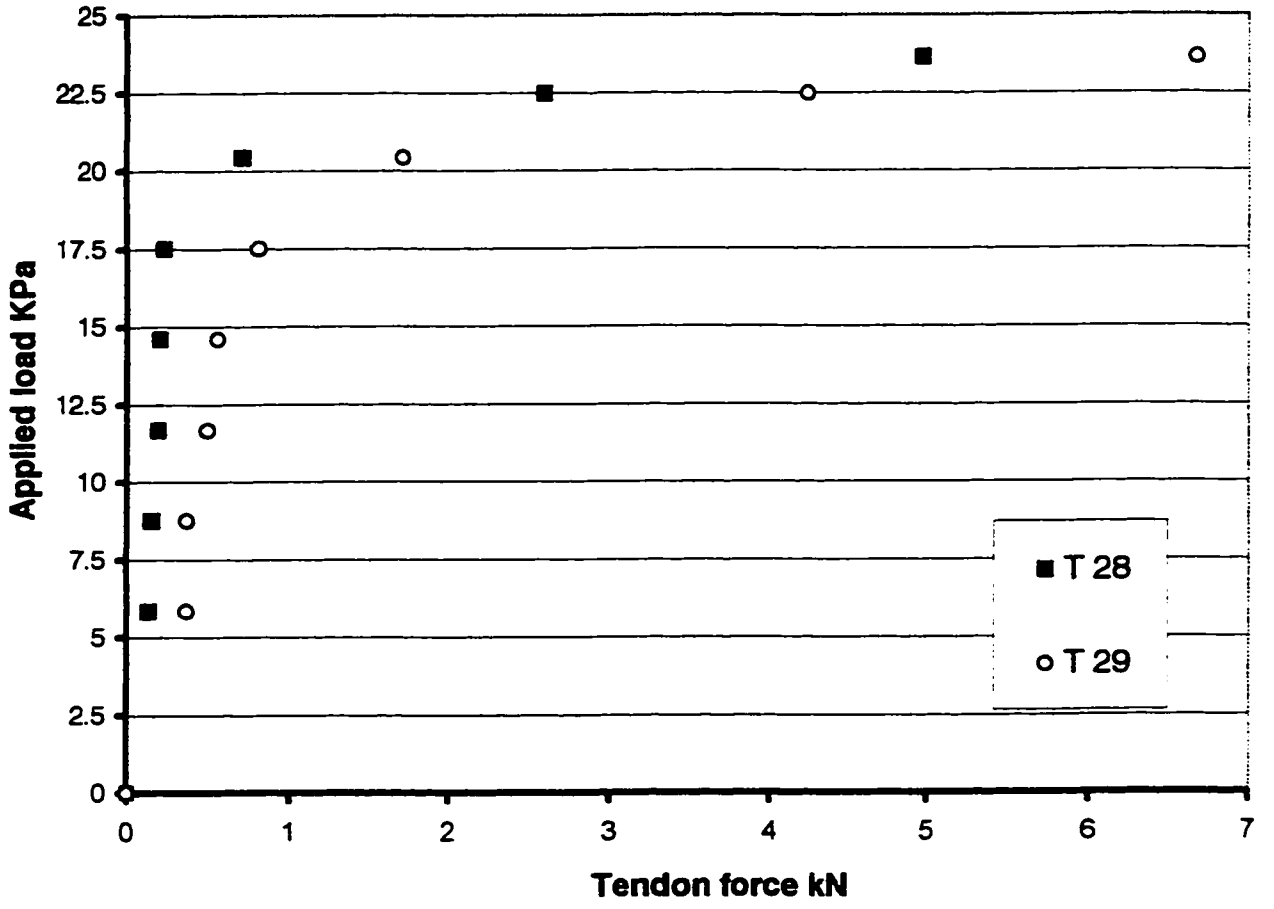

Fig. 4-5 Changes in force in the tendons passing through column 2 in the east-west direction in Test no. 1

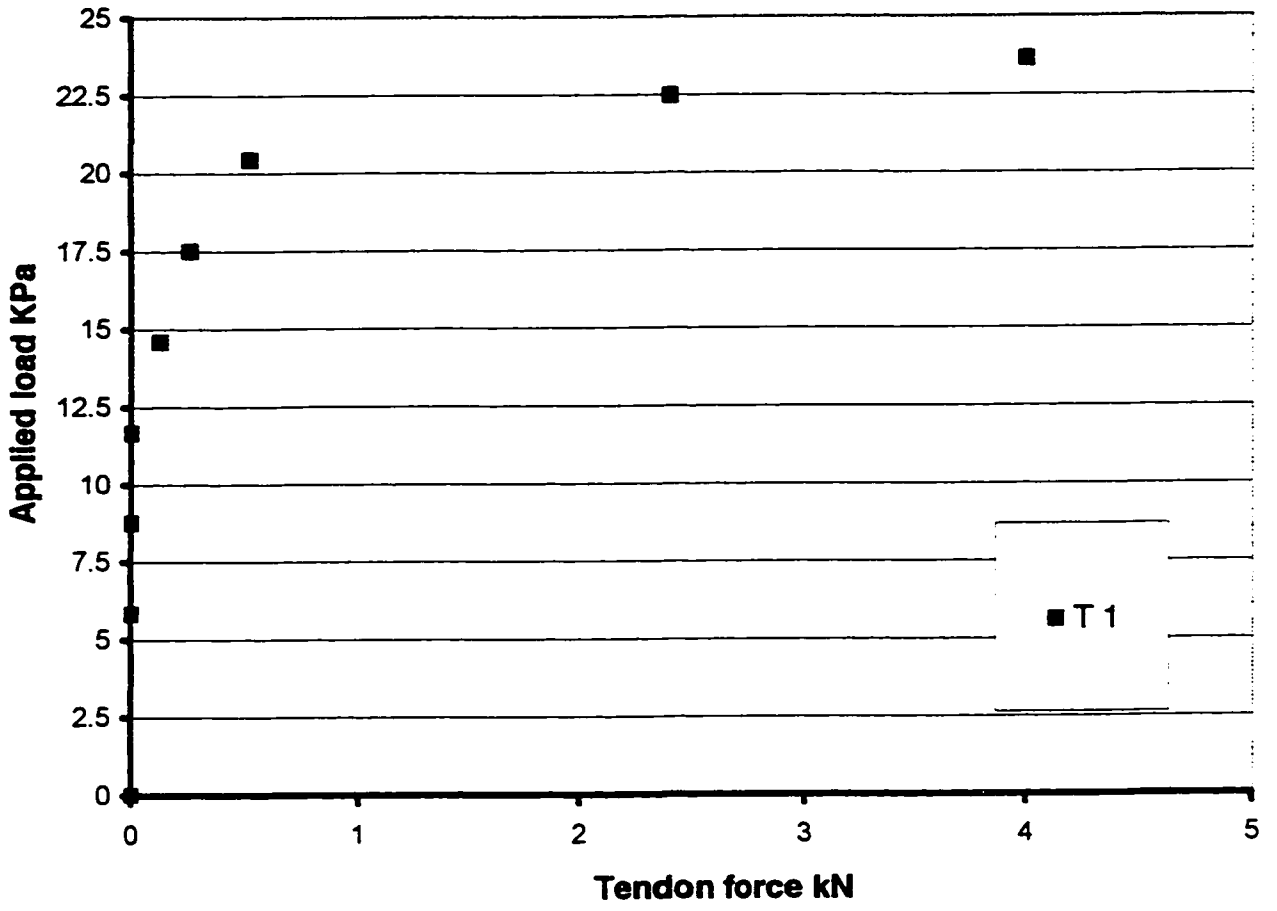

Fig. 4-6 Changes in force in the tendon passing through column 2 in the north-south direction in Test no.1

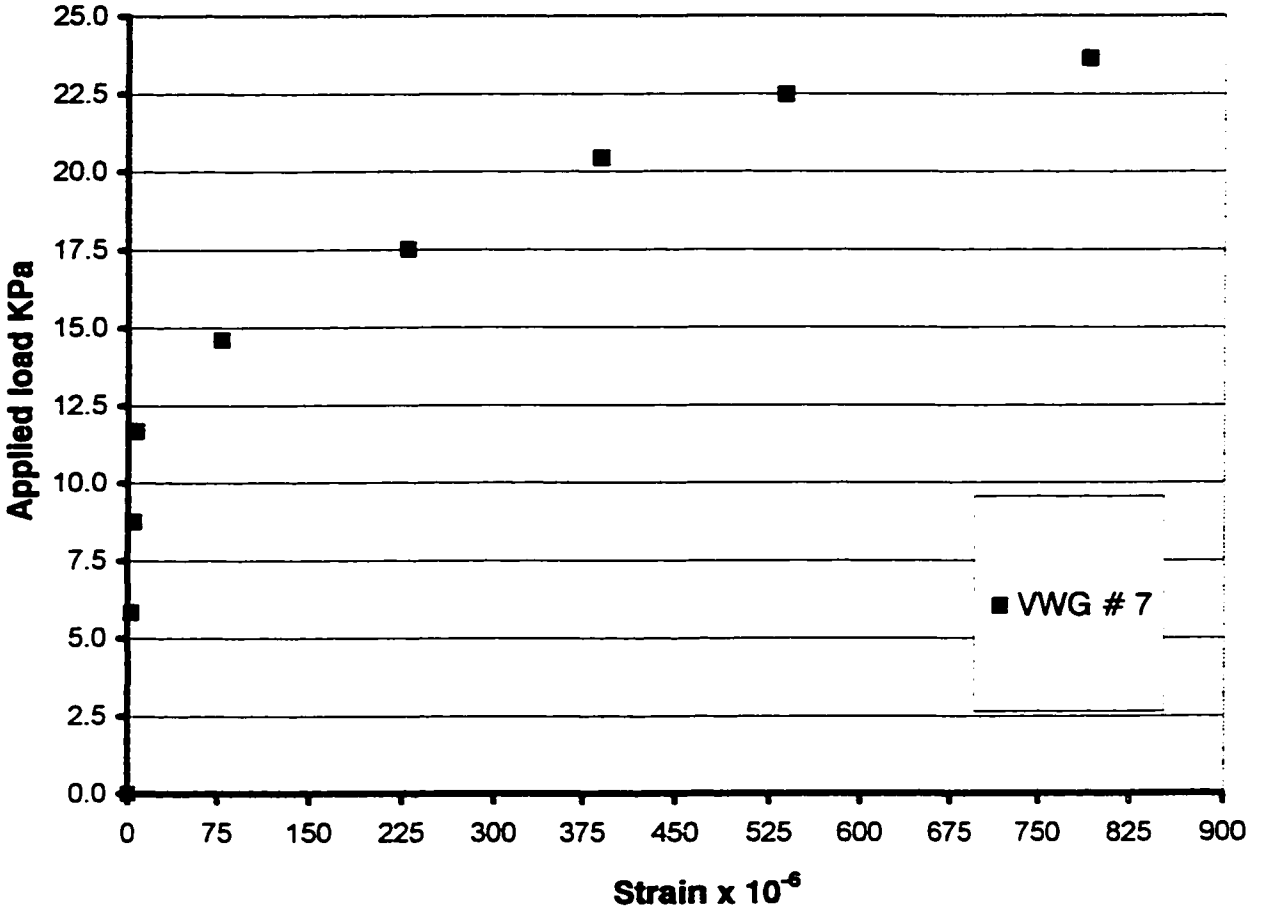

Fig. 4-7 Change in strain in VWG # 7
in Test no.1

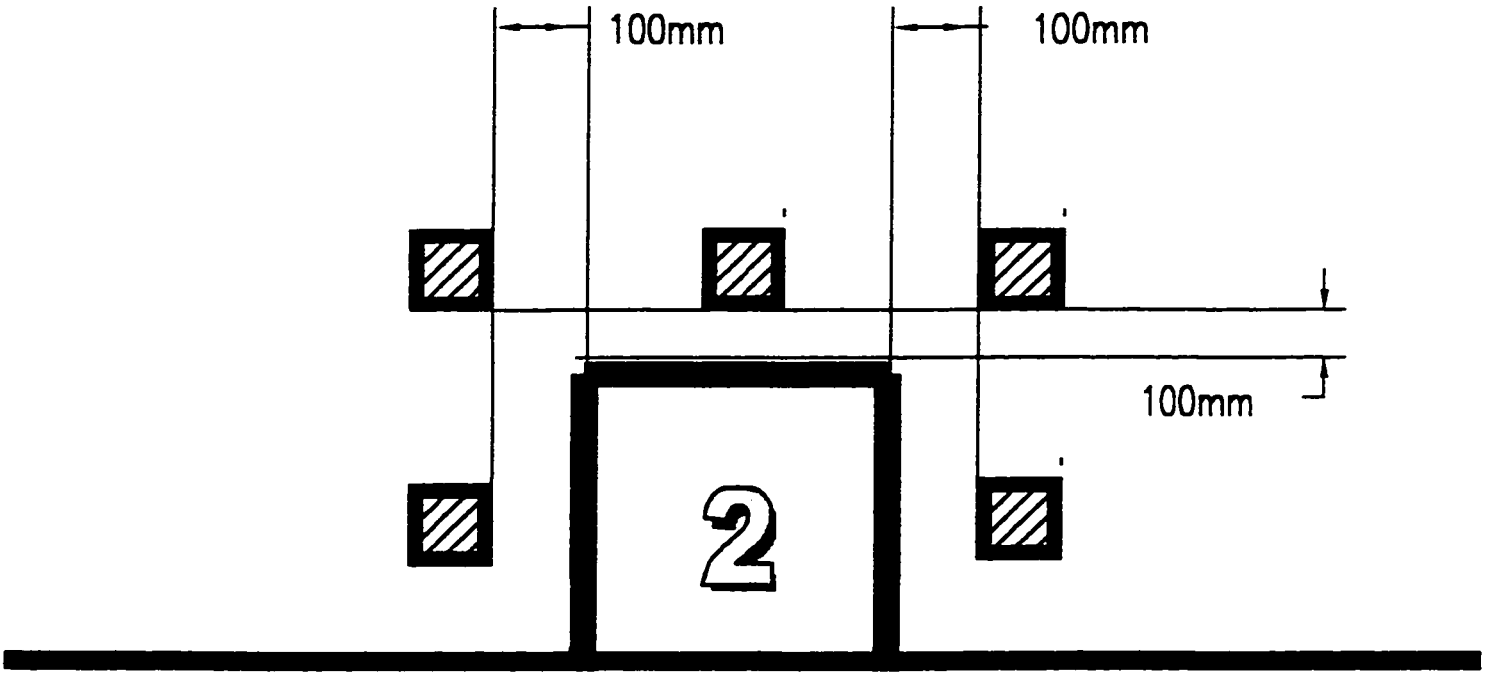

Fig. 4-8 Reshoring of failure zone after column-slab connection failure in the periphery of column 2 in Test no. 1

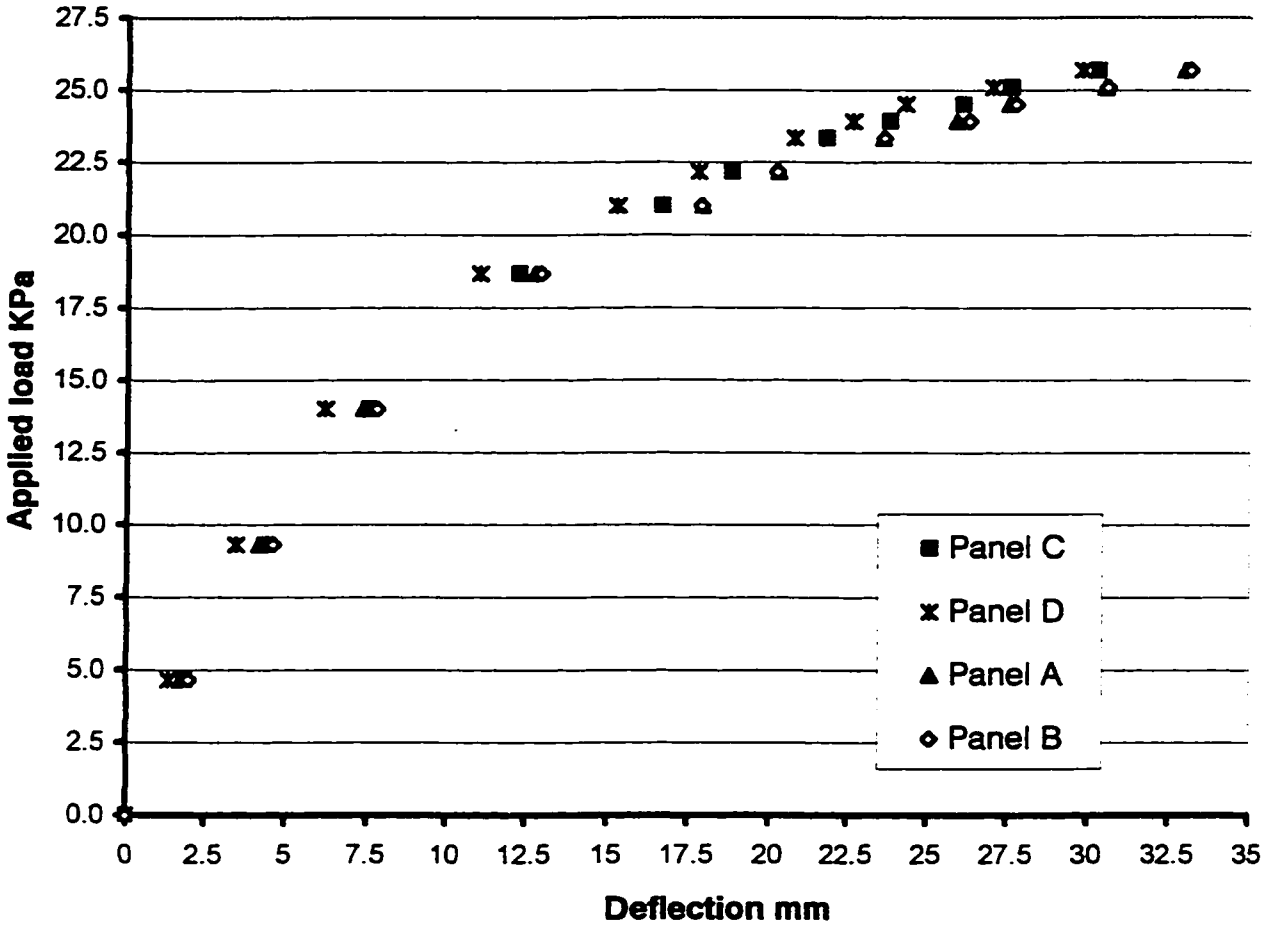

Fig. 4-9 Mid-panel deflections in Test no. 2

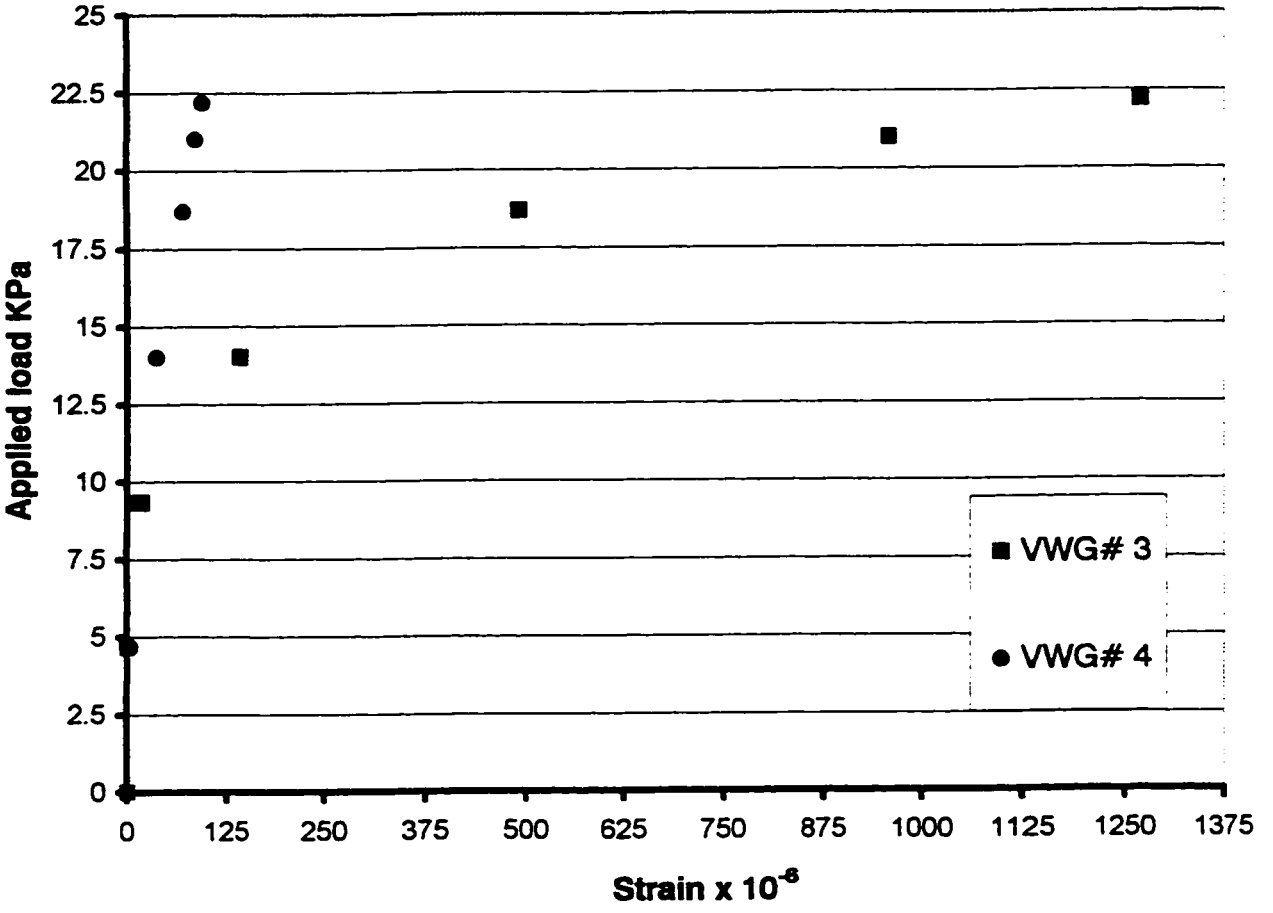

Fig. 4-10 Strain at the corner of edge column 8 in Test no. 2

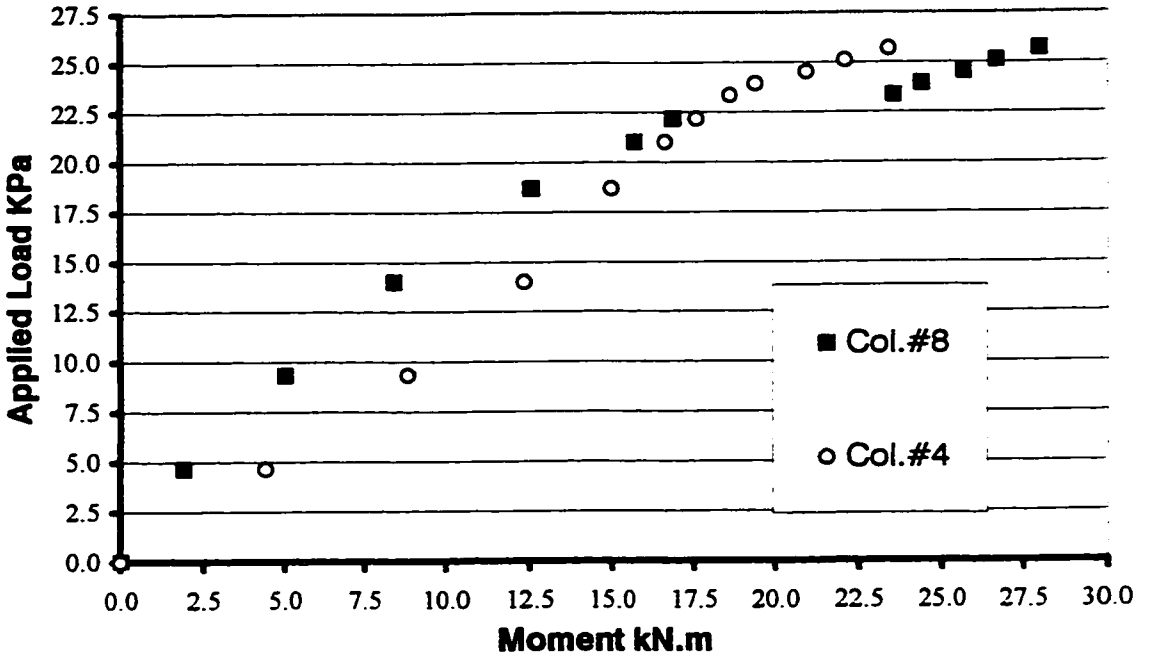

Fig. 4-11A Edge column moments in Test no. 2

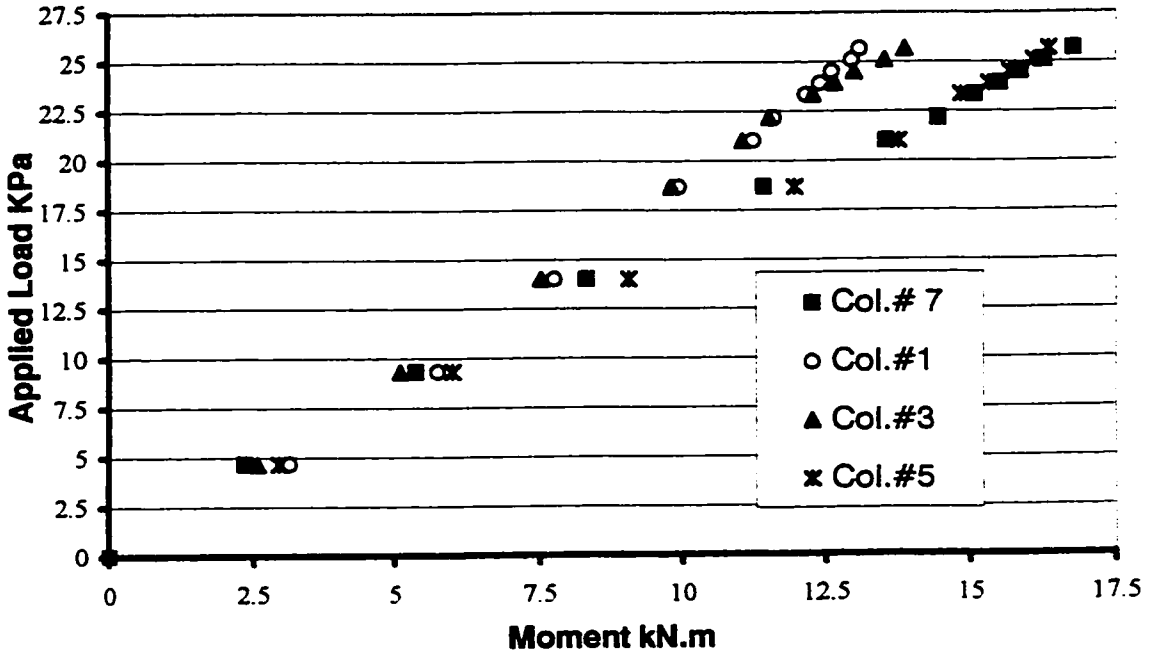

Fig. 4-11B Corner column moments in Test no.2

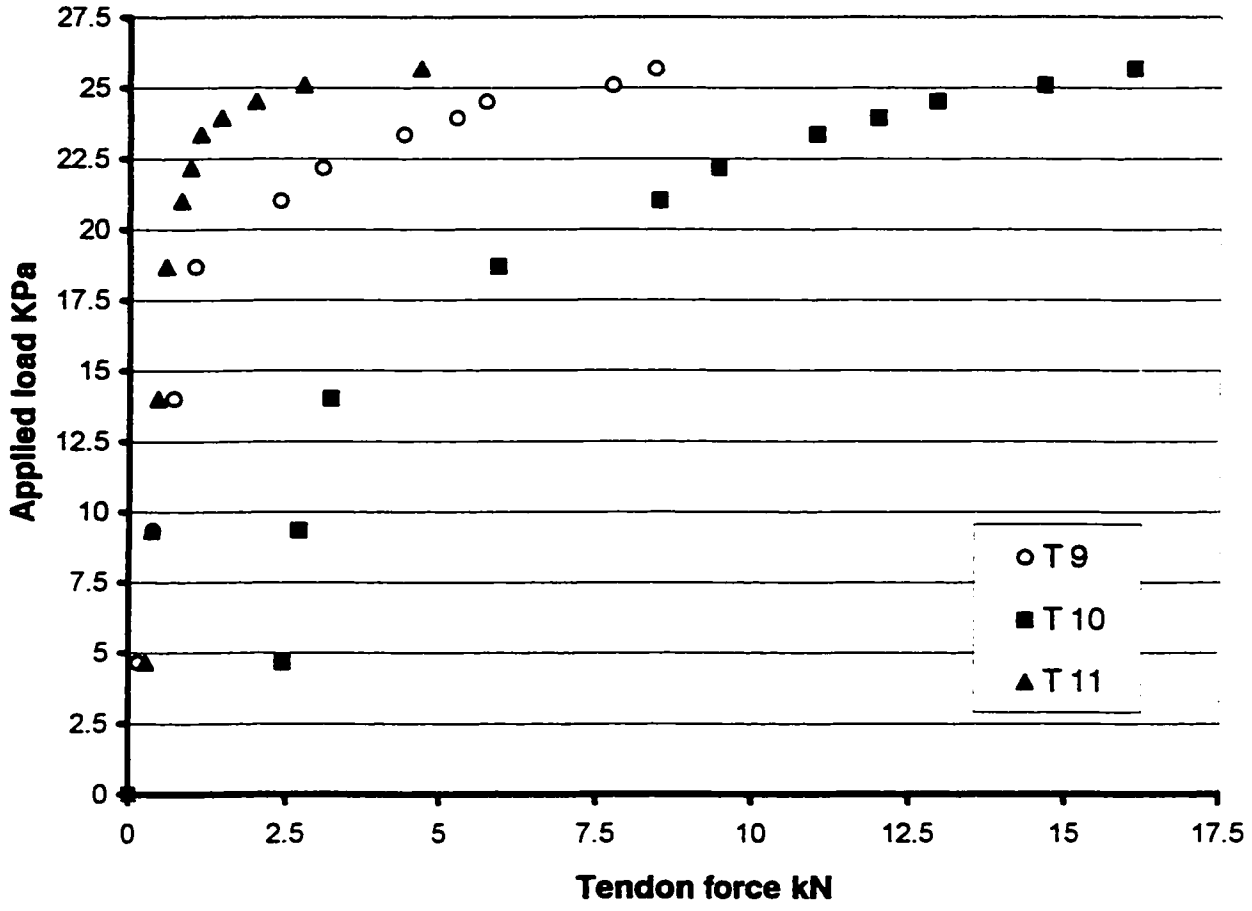

Fig. 4-12 Changes in force in N-S tendons passing through column # 8 in Test no.2

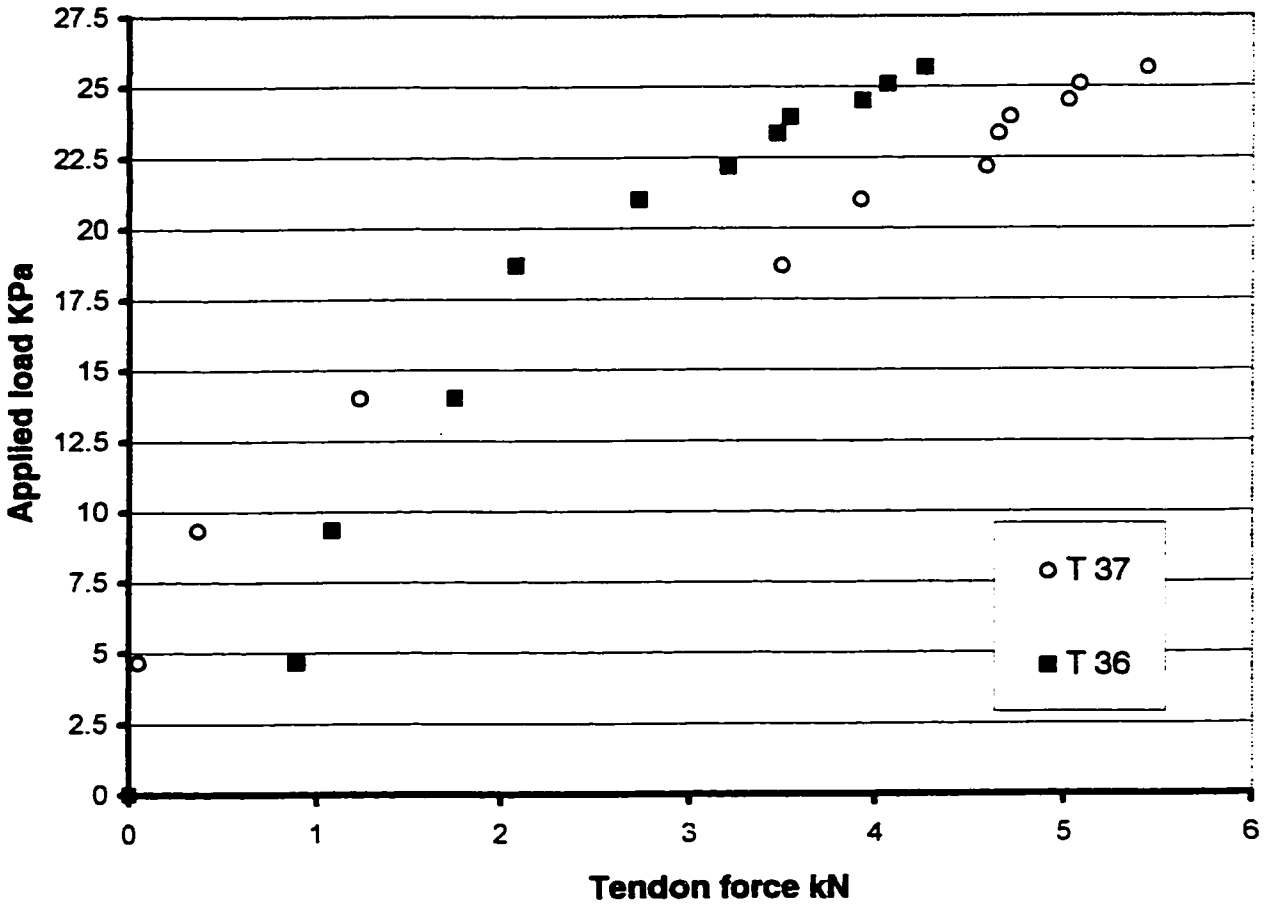

Fig. 4-13 Changes in force in E-W tendons passing through column # 8 in Test no.2

Fig. 4.14 Prior to Test no. 3, the reshored zone ready for patching

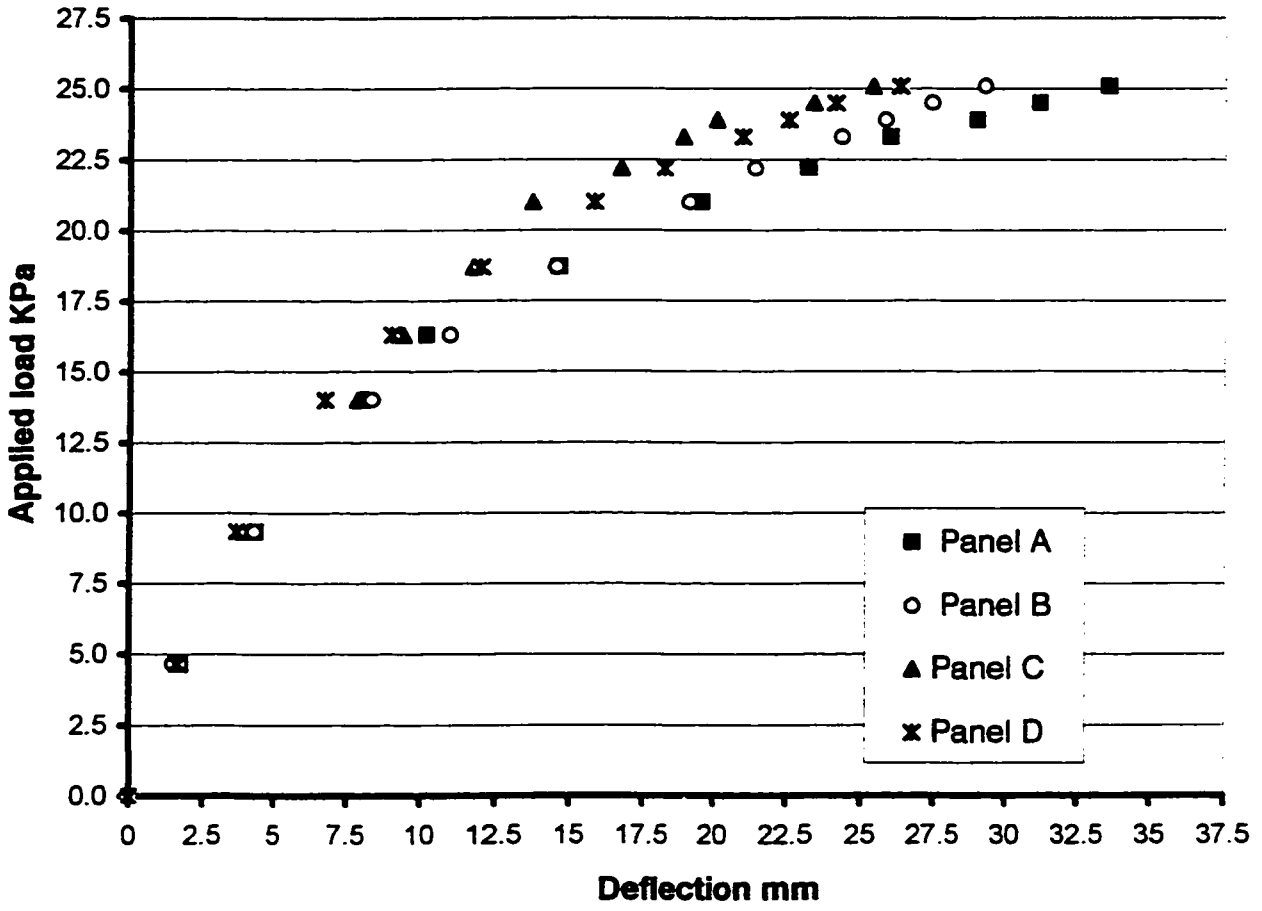

Fig. 4-15 Mid-panel deflections in Test no. 3

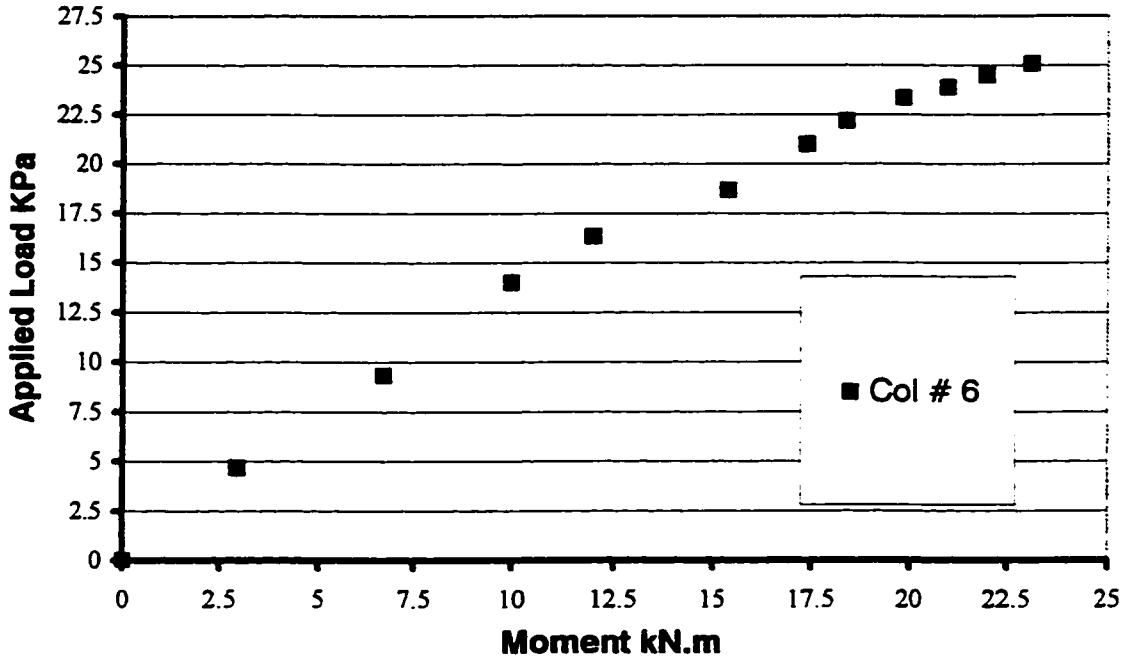

Fig. 4-16A Edge column moments in Test no. 3

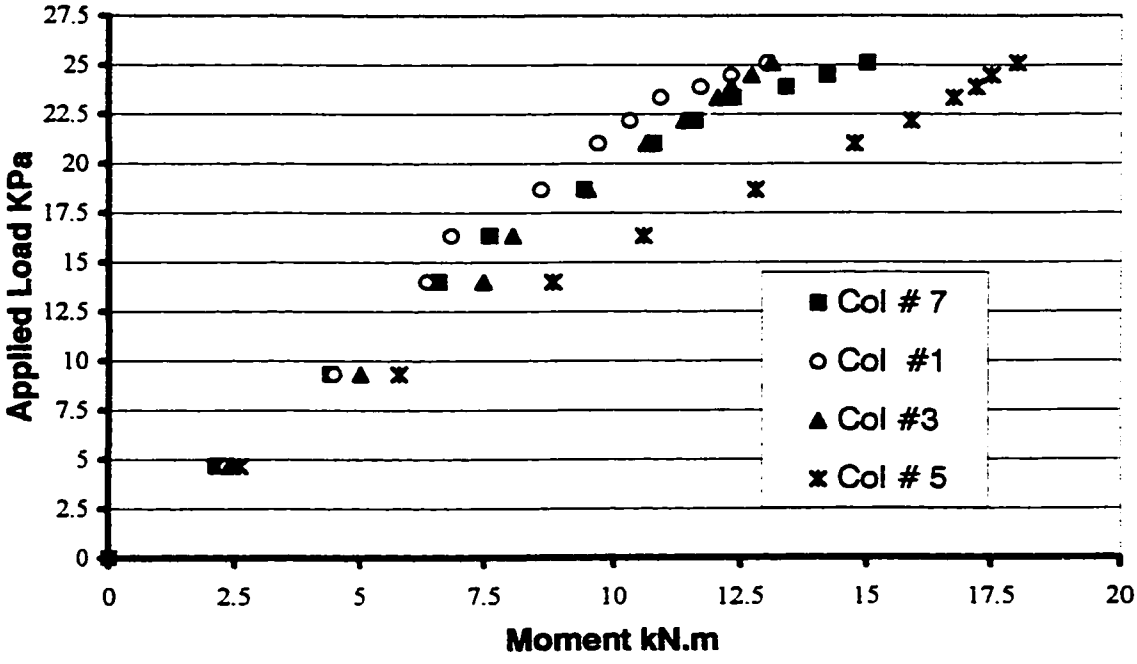

Fig. 4-16B Corner column moments in Test no. 3

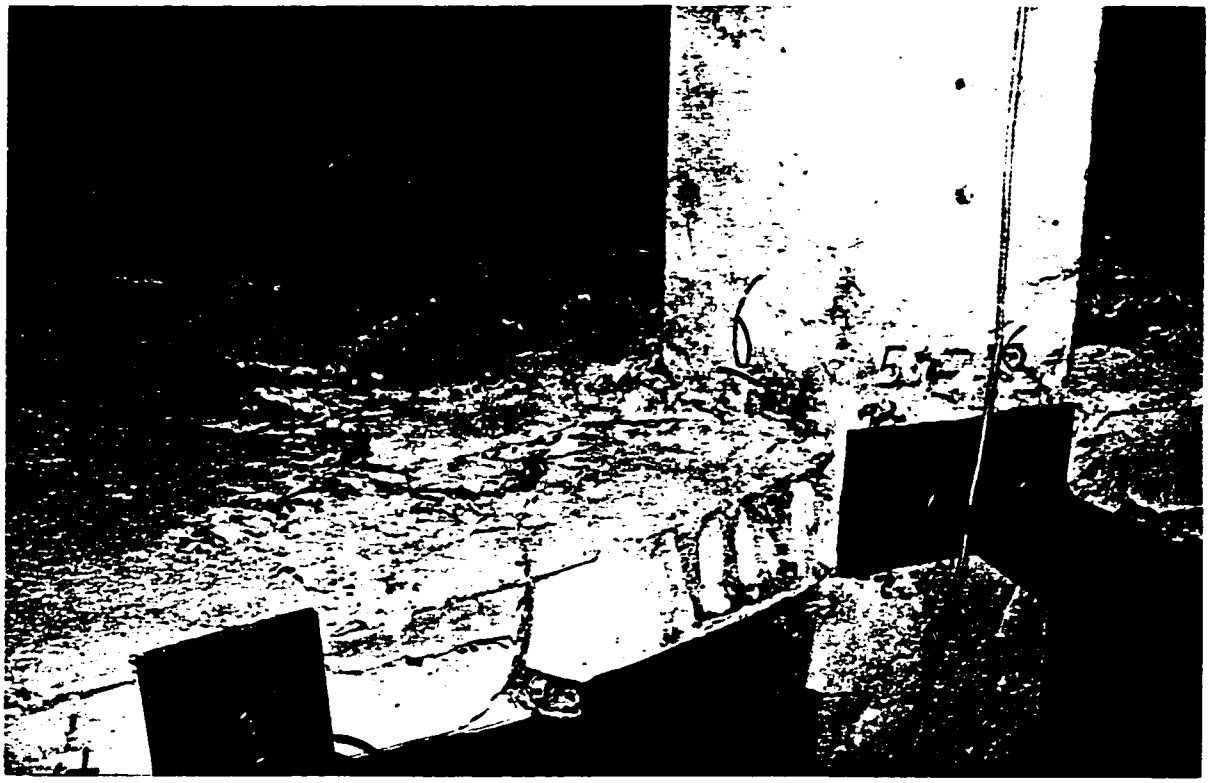

Fig. 4.17 The combination of shear and torsion failure around connection no. 6 in Test no. 3

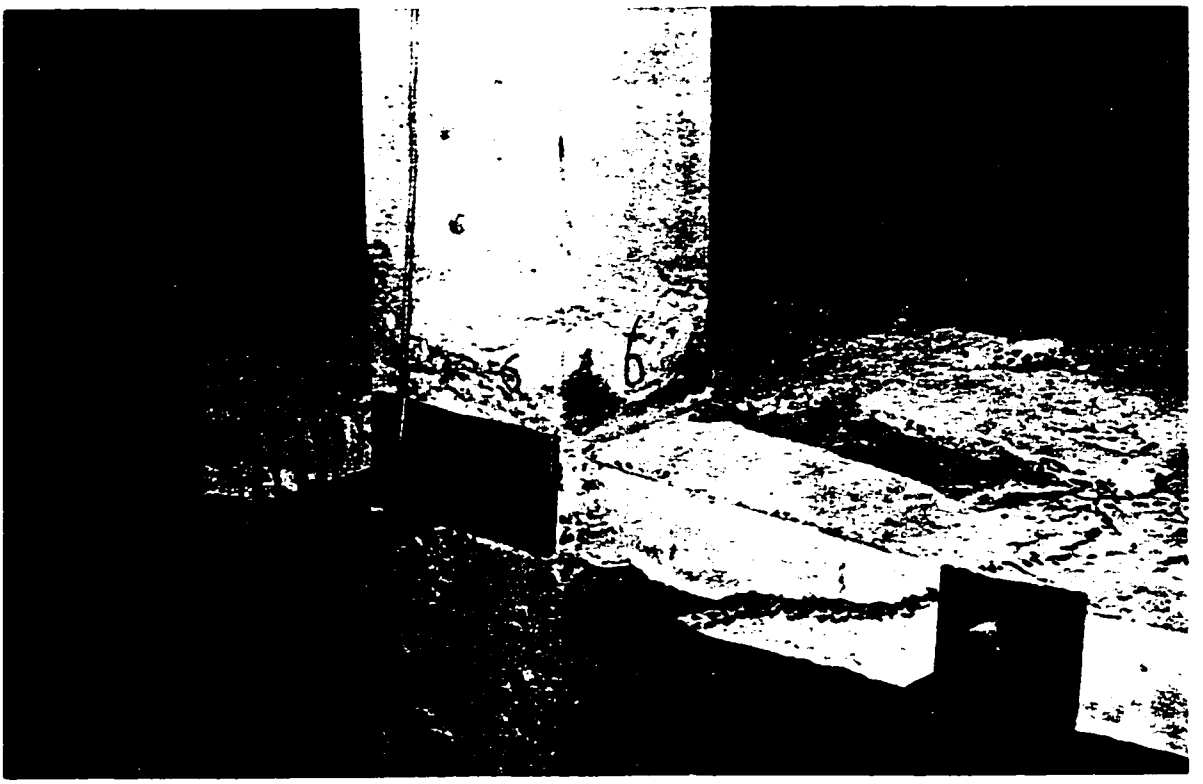

Fig. 4.18 The shear failure of connection no. 6 on the right side in Test no. 3

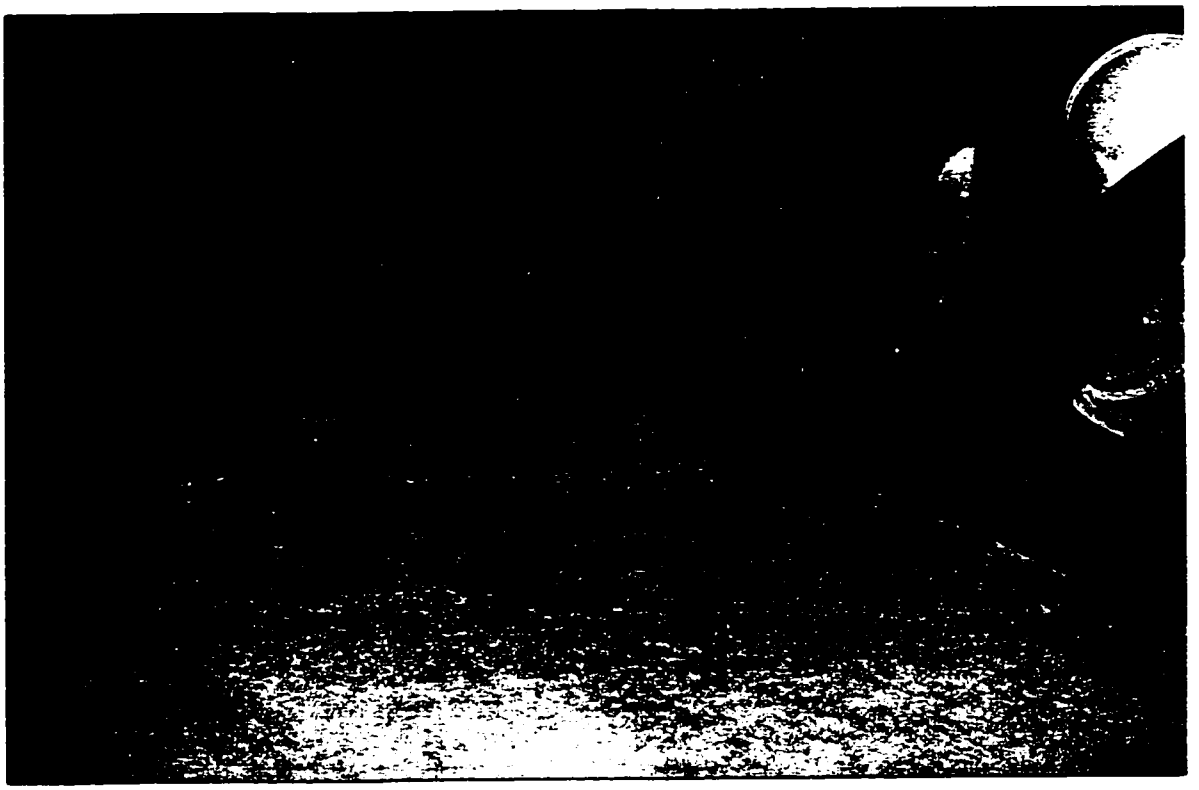

Fig. 4.19 The crushing of concrete due to moment around connection no. 6

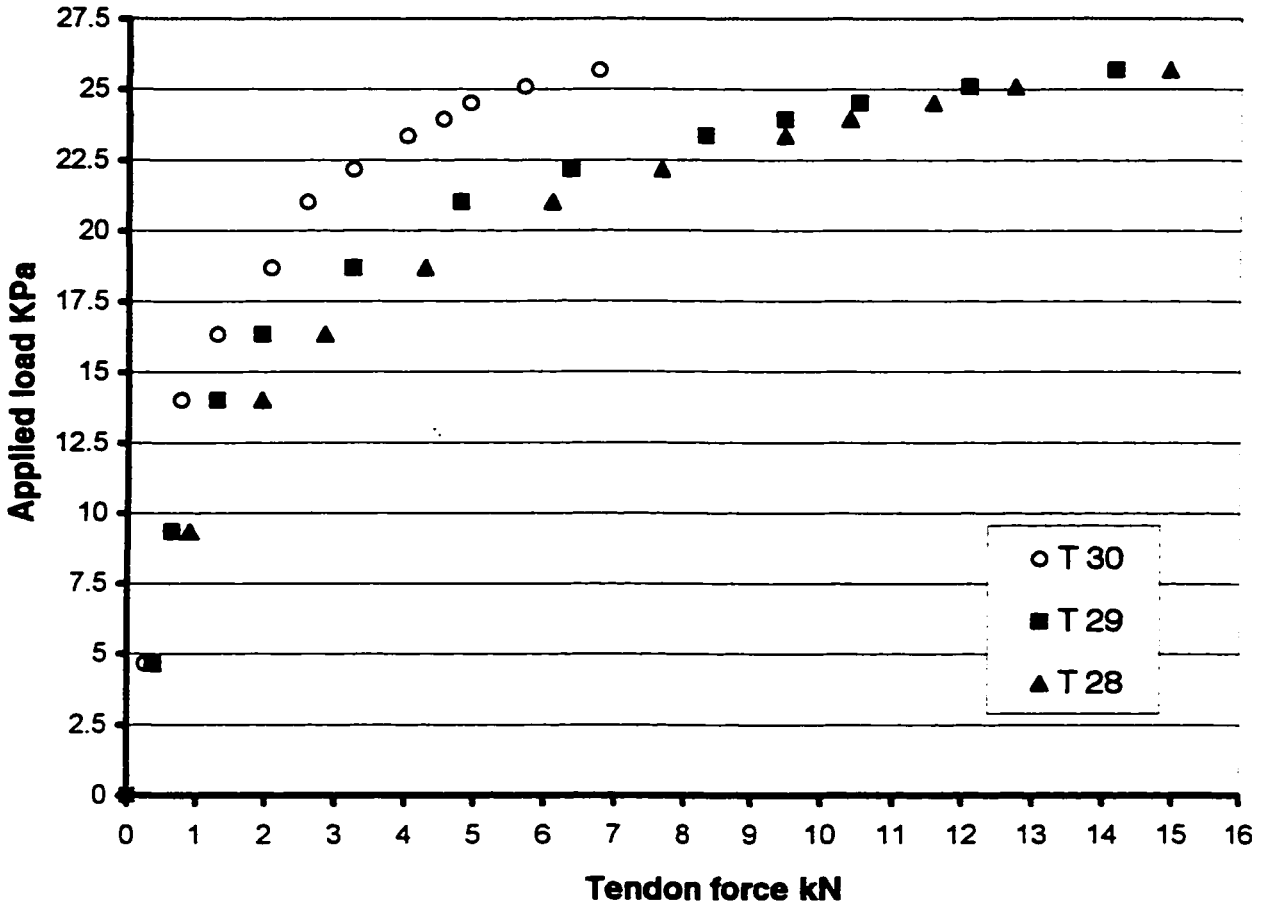

Fig. 4-20 Changes in force in E-W tendons passing through or near column # 6 in Test no.3

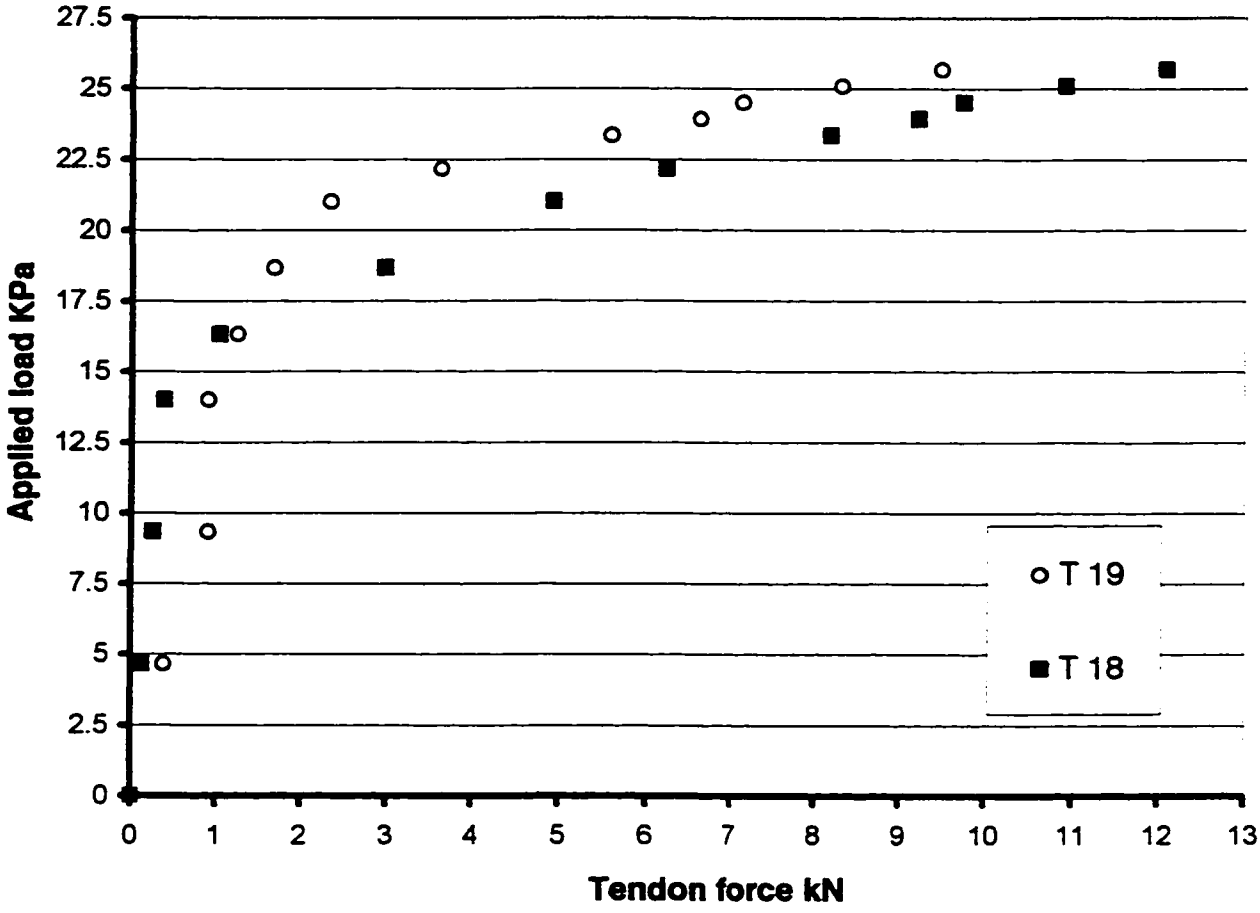

Fig. 4-21 Changes in force in N-S tendons passing through column # 6 in Test no.3

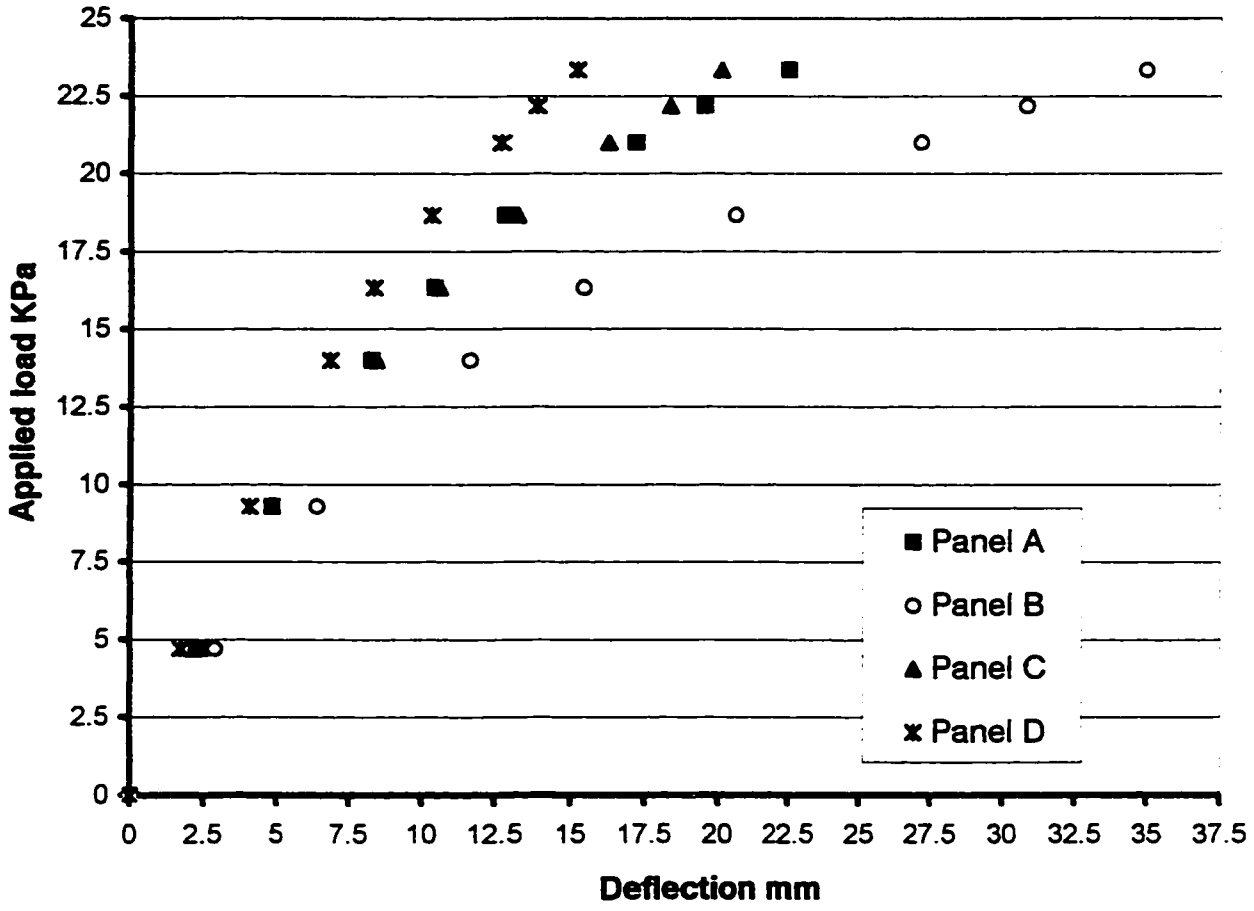

Fig. 4-22 Mid-panel deflections in Test no. 4

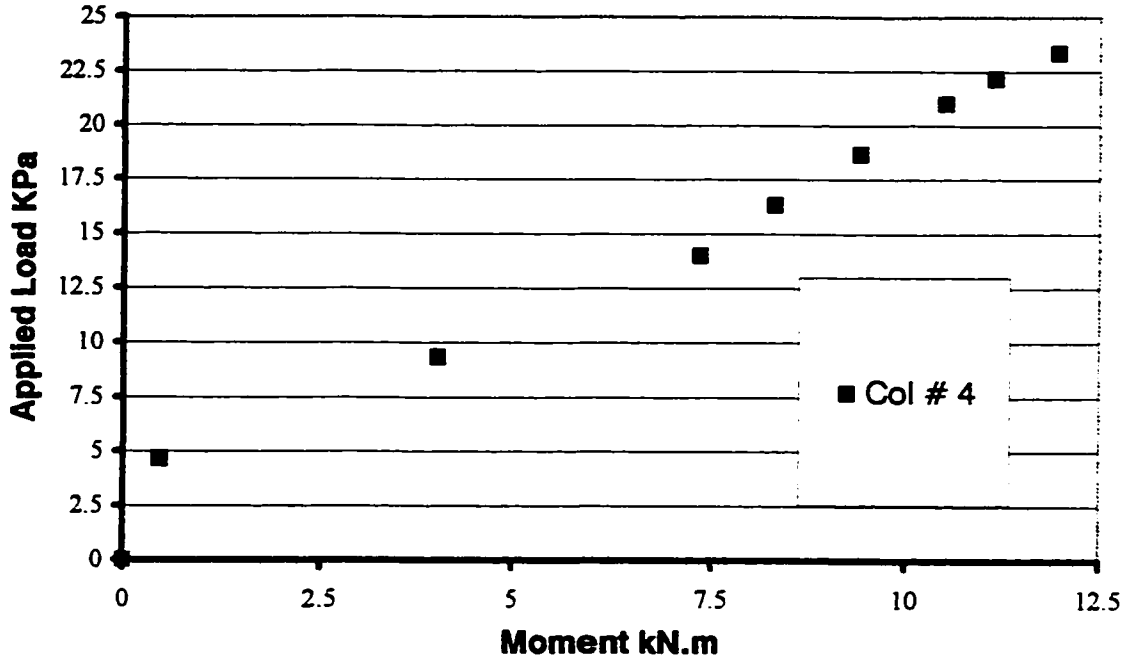

Fig. 4-23A Edge column moments in Test no. 4

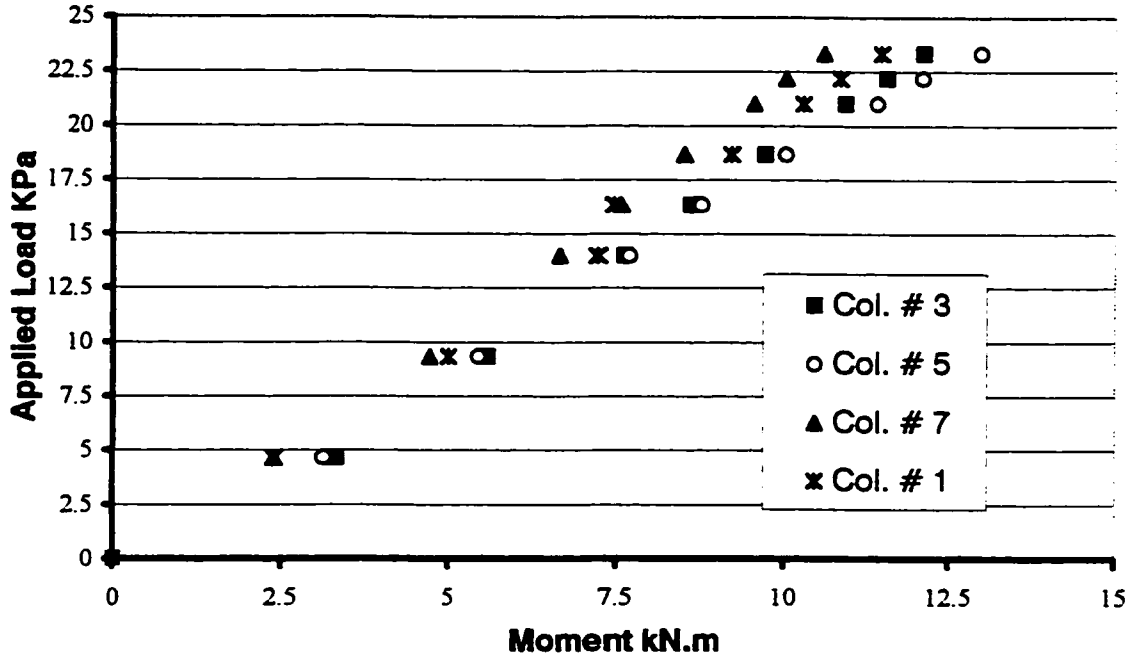

Fig. 4-23B Corner column moments in Test no. 4

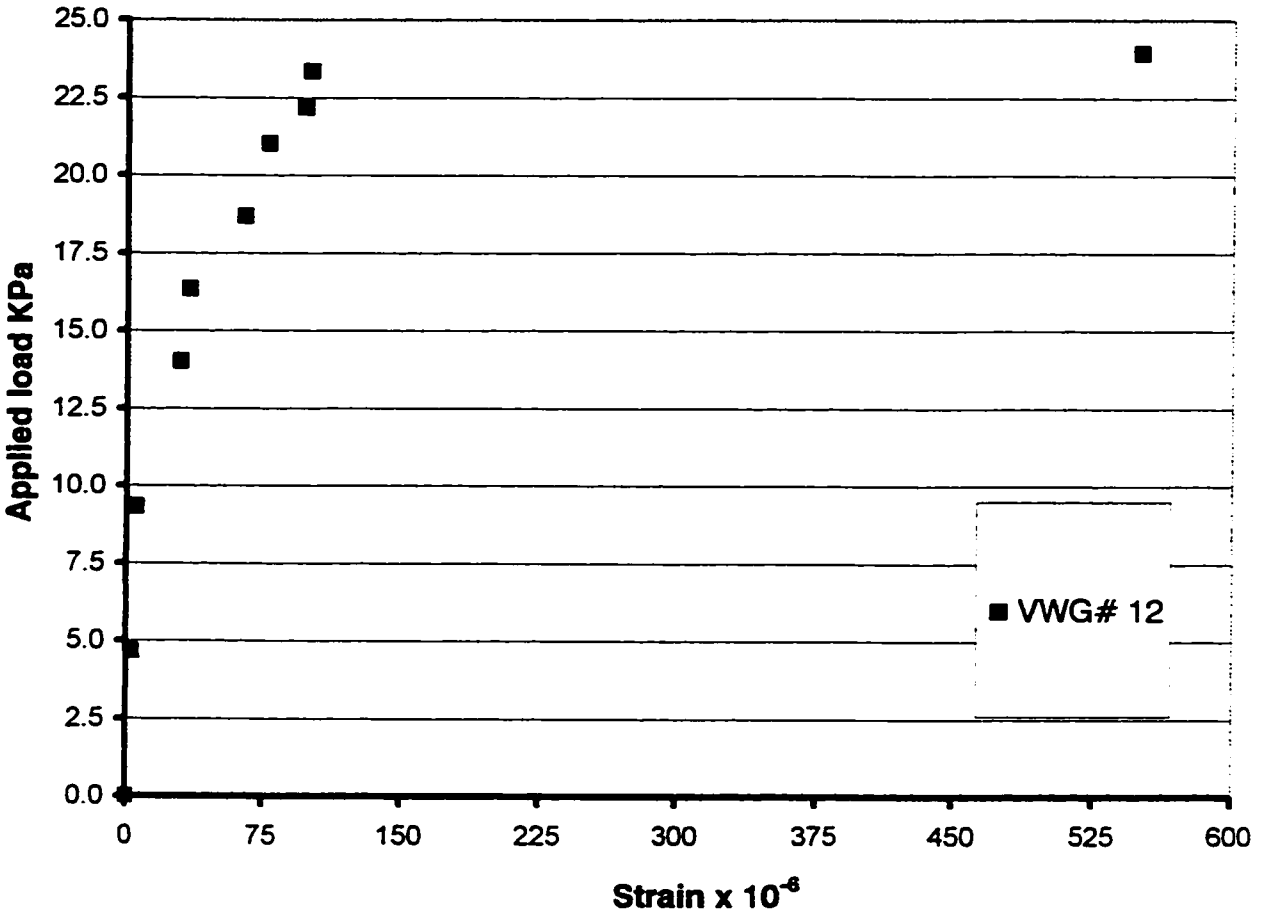

Fig. 4-24 Changes in the strain in VWG # 12
in Test no.4

Fig. 4.25 The severe damage of connection no. 4 due to punching shear failure in Test no. 4

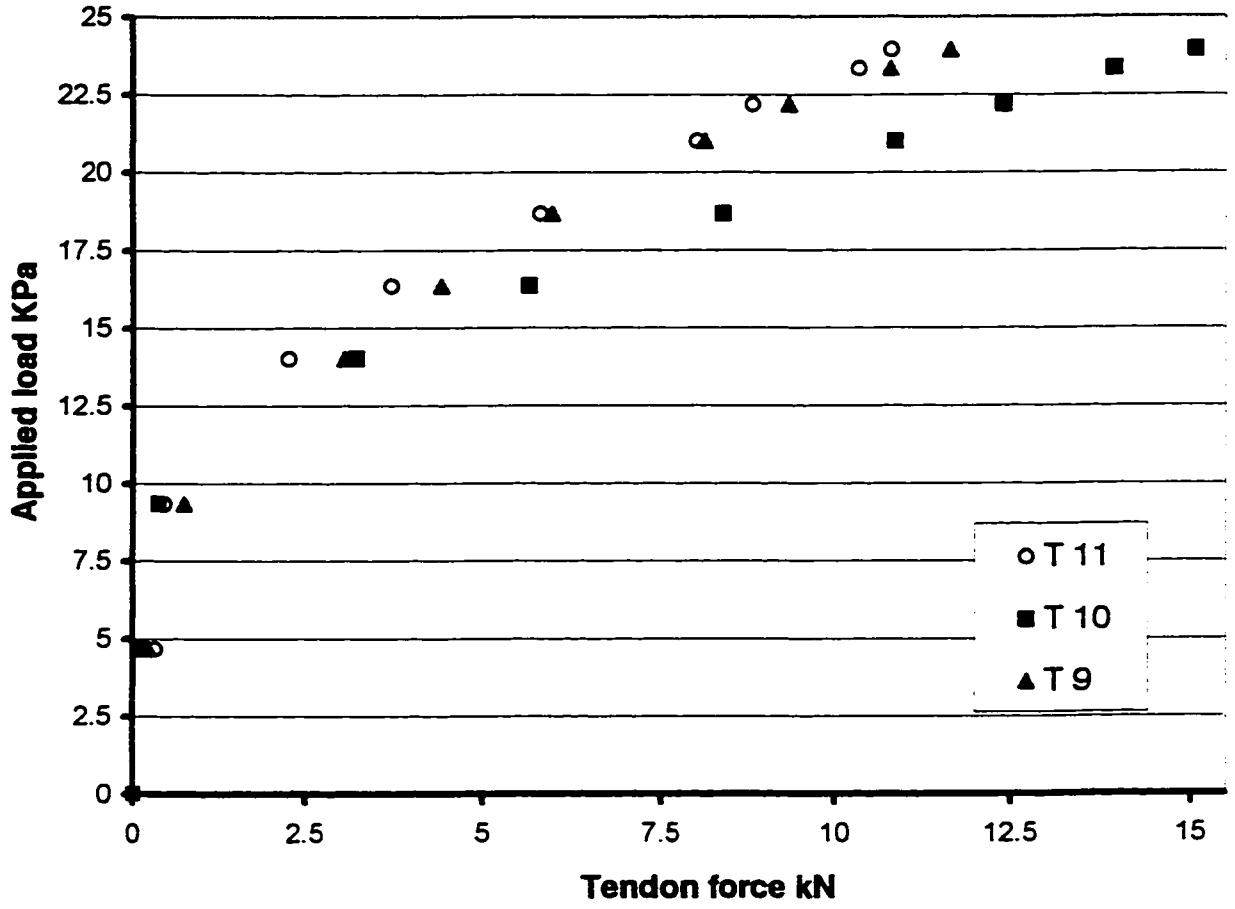

Fig. 4-26 Changes in force in N-S tendons passing through or near column # 4 in Test no.4

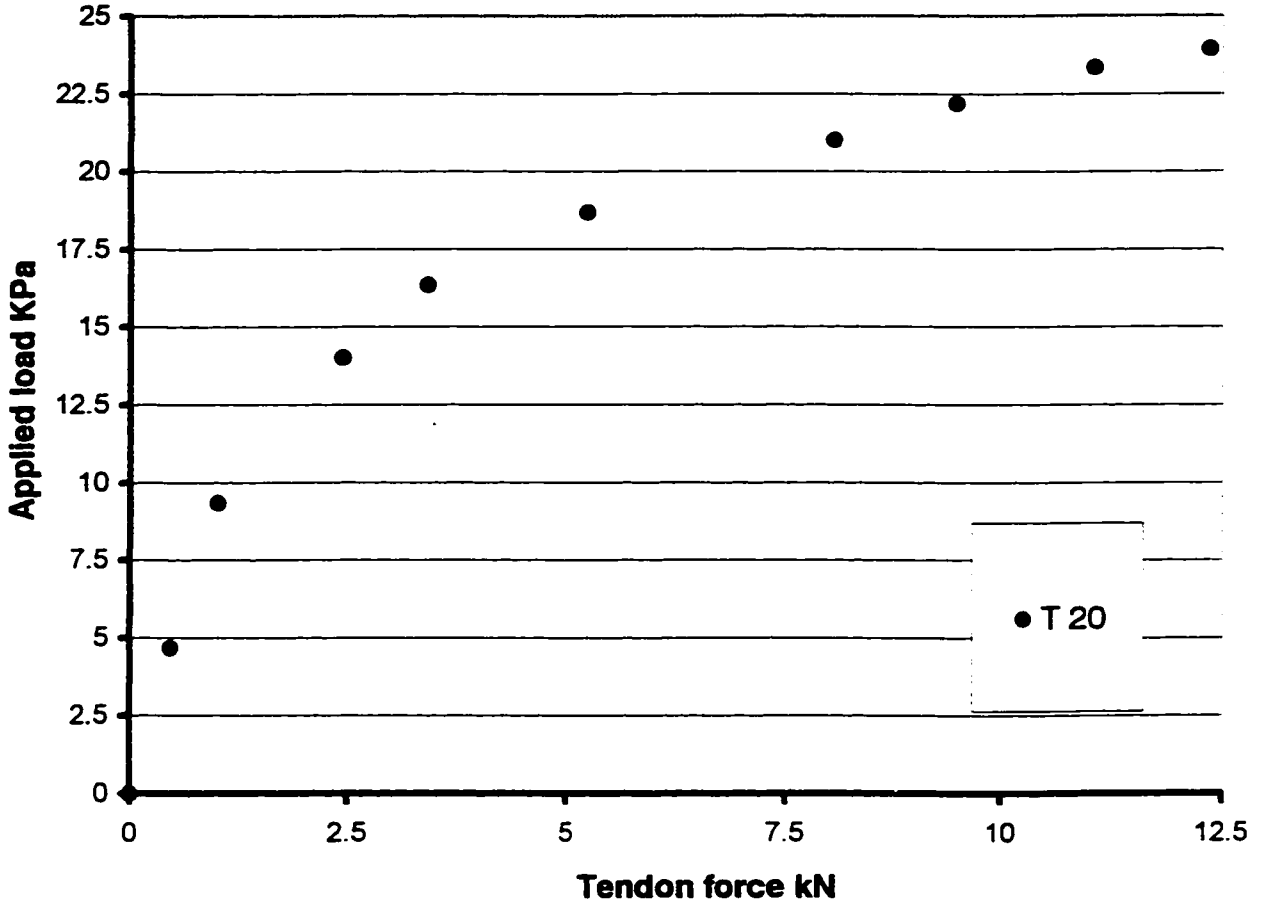

Fig. 4-27 Changes in force in E-W tendon passing through column # 4 in Test no.4

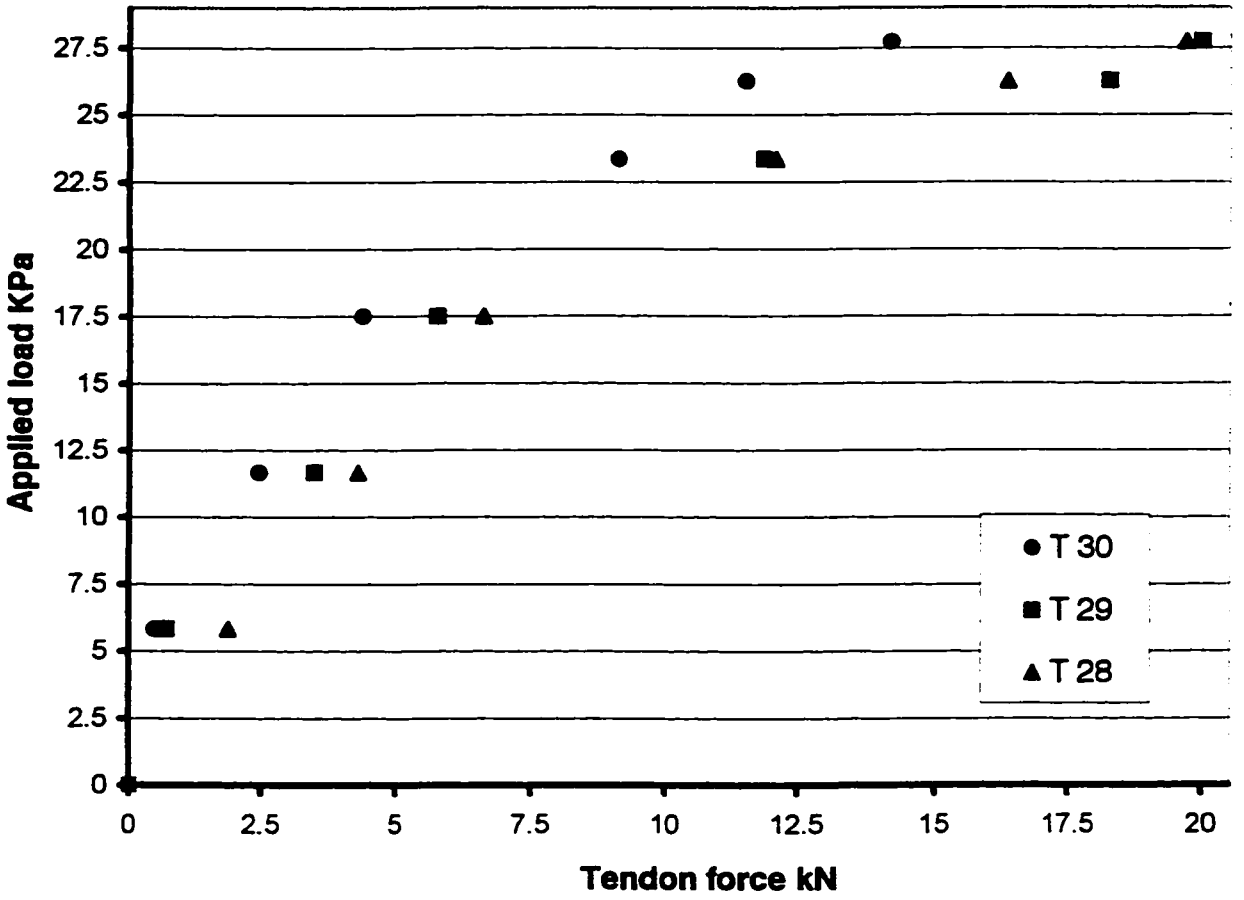

Fig. 4-28 Changes in force in E-W tendons passing through or near columns 2, 6 and 9 in Test no.5

Fig. 4.29 Deflections being taken

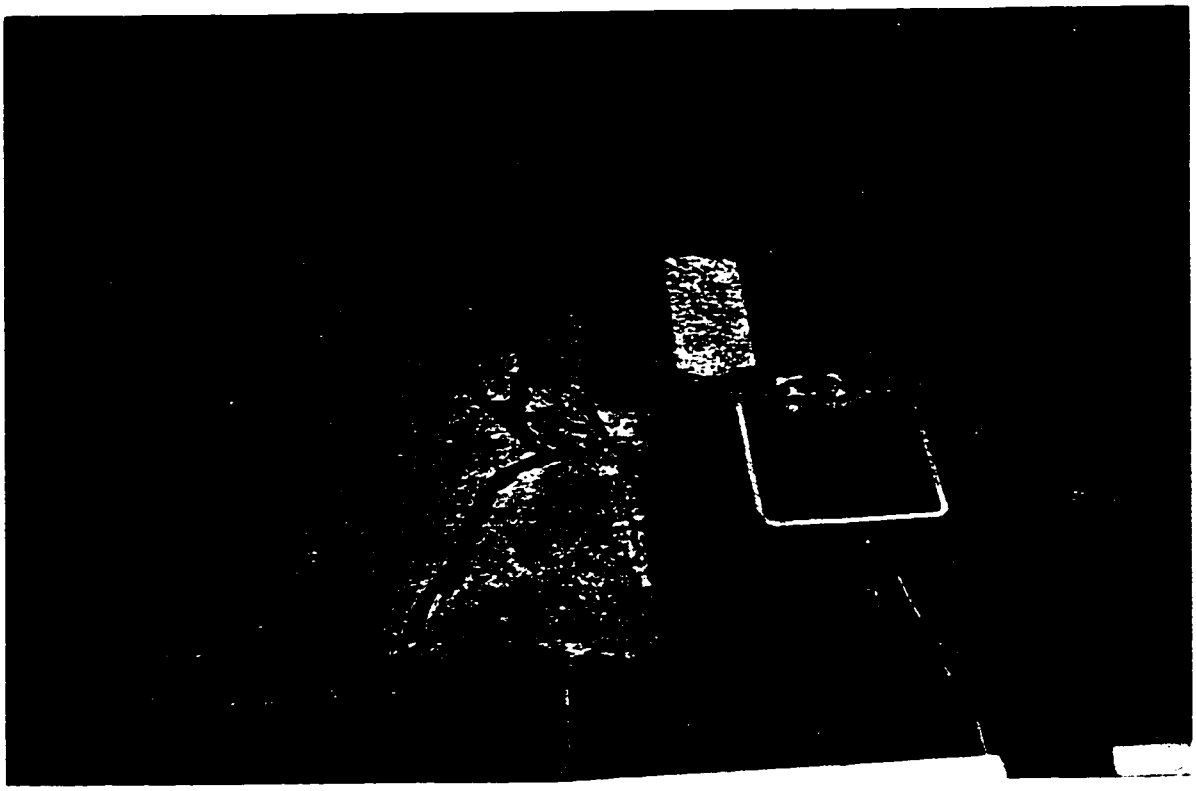

Fig. 4.30 The failure zone around column 2 in Test no. 5

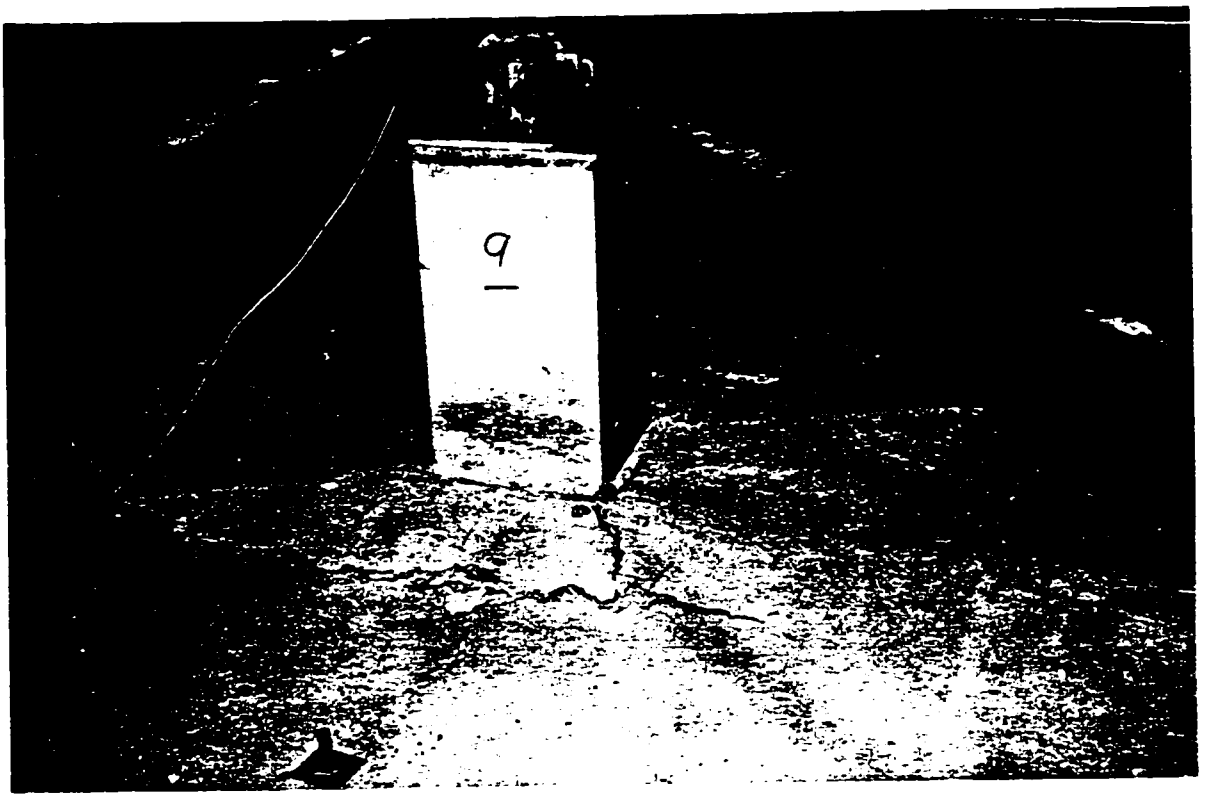

Fig. 4.31 The punching shear failure around column 9 in Test no. 5

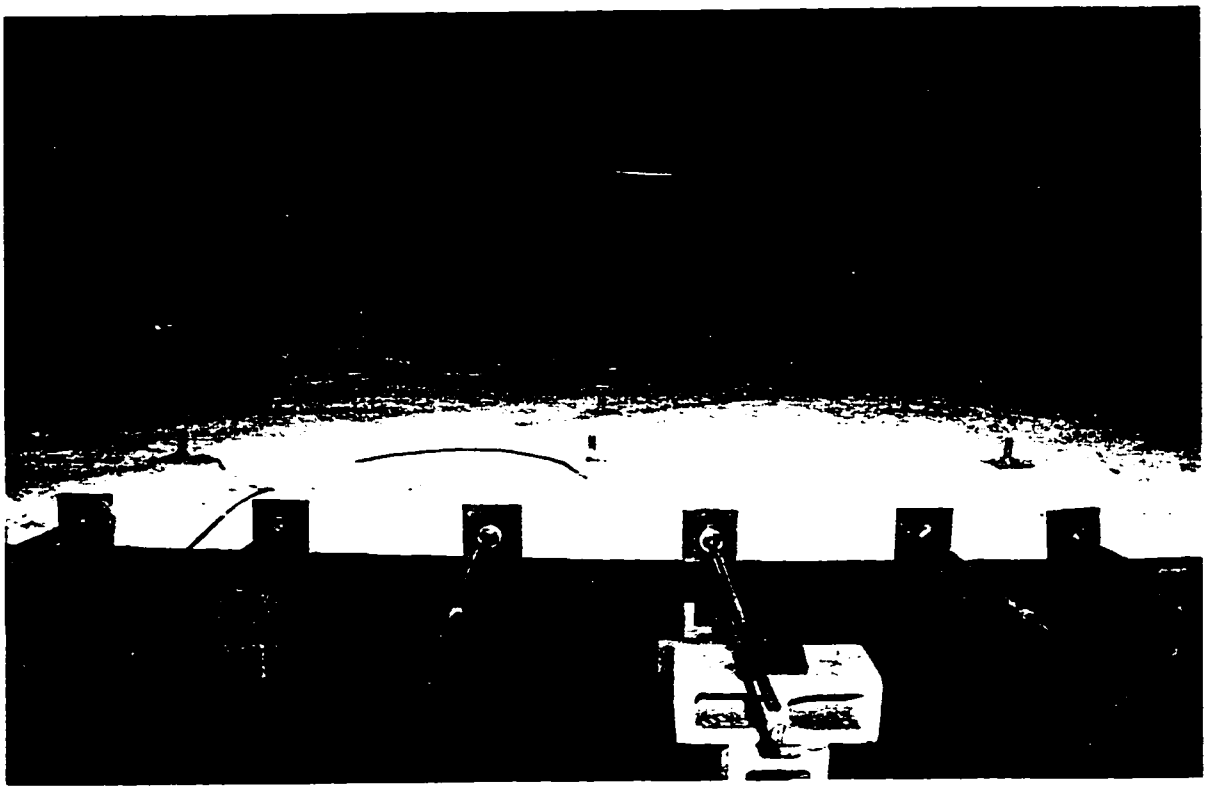

Fig. 4.32 View of the two zones failure in Test no. 5

Fig. 4.33 Column 9 and 2 connections after failure

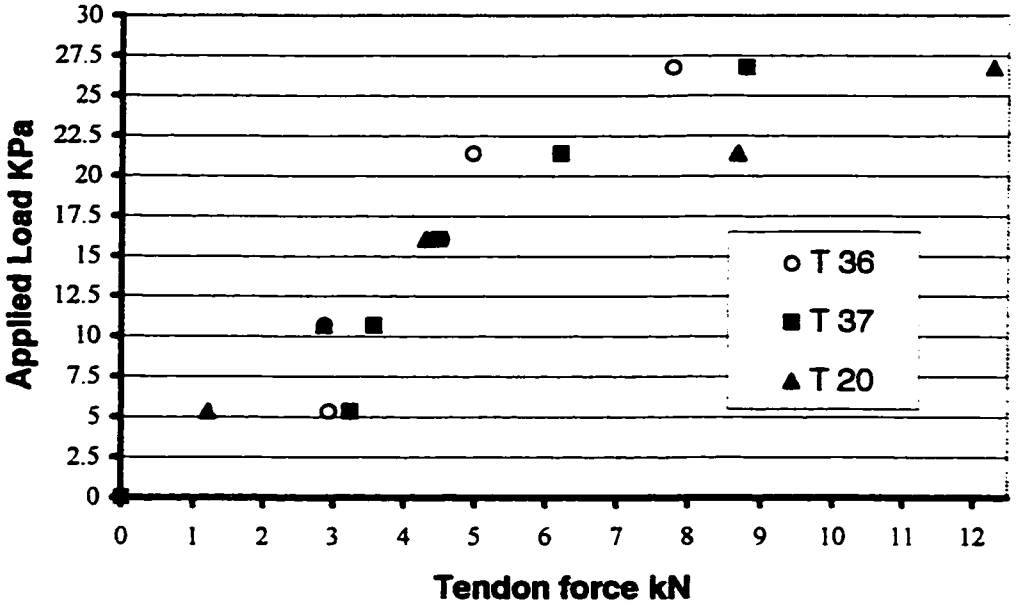

Fig. 4-34A Changes in force in E-W tendons passing through corner columns in Test no.6

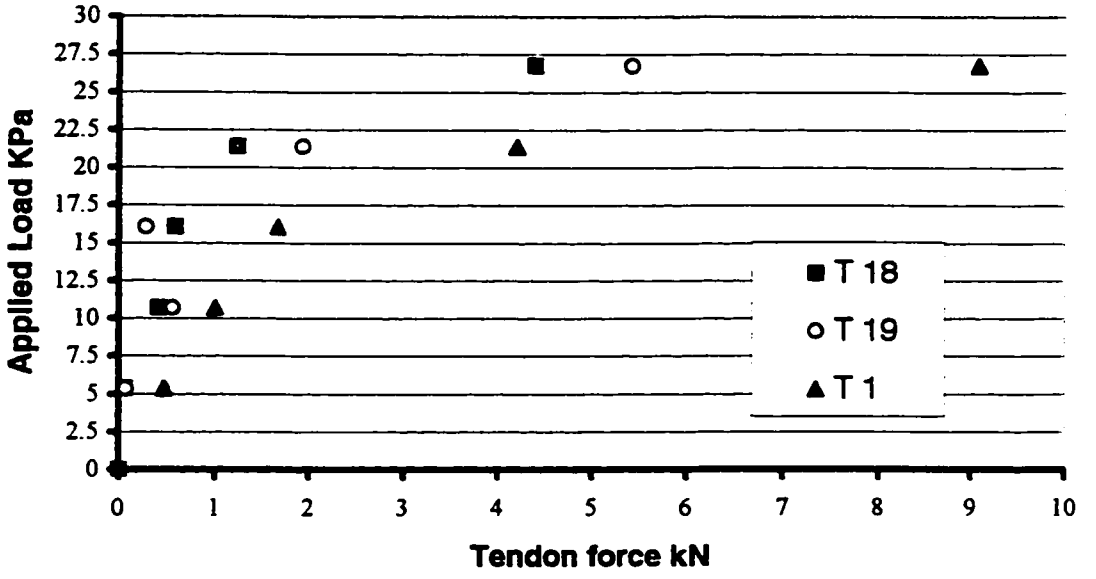

Fig. 4-34B Changes in force in N-S tendons passing through corner columns in Test no.6

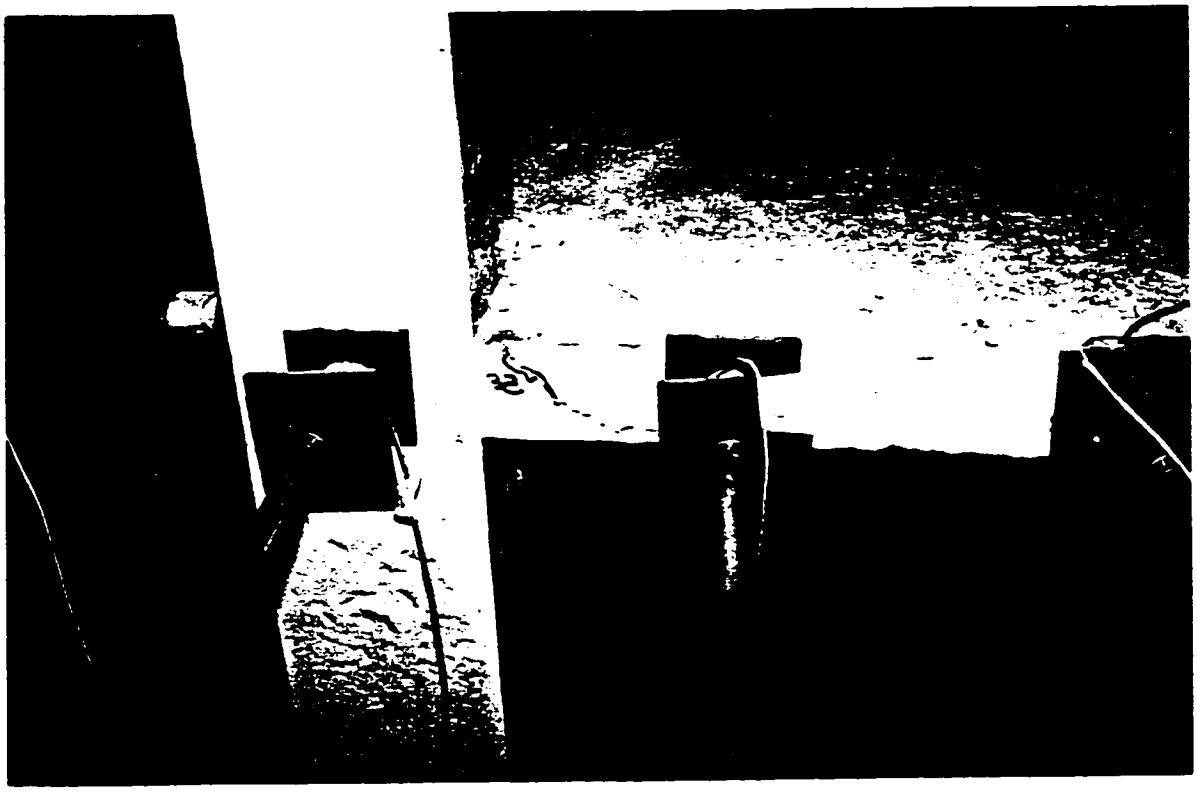

Fig. 4.35 The top and side cracks at column 3 periphery in Test no.6

Fig. 4.36 The severe cracks around column 3 from the bottom in Test no. 6

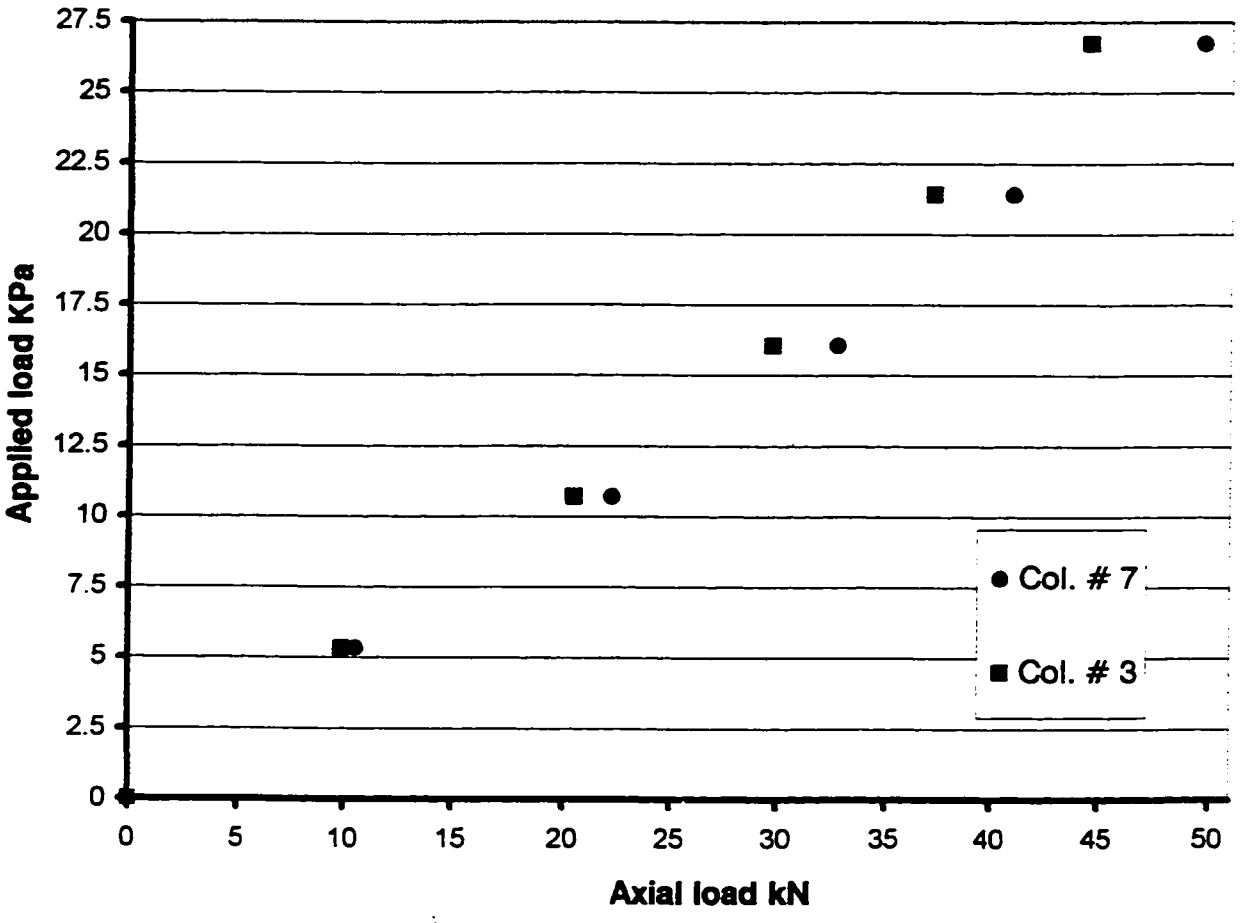

Fig. 4-37 Axial loads transferred to columns 3 & 7 in Test no. 6

Test No.	1	2	3	4
Col. No.	**2**	**8**	**6**	**4**
Load kN/m^2	**23.65**	**26.27**	**25.70**	**23.94**

Table 4-1 Failure loads for edge slab-column connections

Test No.	1	2	3	4	5
Tendon no. & Losses in kN.	**T28- 20** **T29- 20**	**T9-100%** **T10- 15** **T11- 25**	**T28-29** **T29-26**	**T9- 25.6** **T10-10.5** **T11-67.3**	**T30- 63**

Table 4-2 Losses in forces in tendons passing through the failure zone in the first five tests

Test No.	1	2	3	4	5
Load kN/m^2	22.47	25.68	25.10	23.30	26.27
	Deflection mm				
Panel A	**18.84**	**32.95**	**33.57**	**22.54**	**22.88**
Panel B	**19.88**	**33.11**	**29.29**	**34.97**	**36.32**
Panel C	**16.04**	**30.26**	**25.4**	**20.1**	**28.58**
Panel D	**15.81**	**29.76**	**26.33**	**15.22**	**19.94**

Table 4-3 Mid-panel deflections in Tests 1- 5

TEST NO.	1	2	3	4	5	6
Load kN/m^2	**23.65**	**25.70**	**25.70**	**23.94**	**27.7**	**26.80**
Column 3	**52.0**	**49.9**	**49.0**	**46.8**	**48.2**	**44.6**
Column 6	**94.2**	——	**113**	——	——	——
Column 7	**50.2**	**51.2**	**49.2**	**45.90**	**50.0**	**49.7**
Column 8	**99.7**	**122**	——	——	——	——
Column 9	**302.3**	**297**	**285.7**	**249.2**	**244**	——

Table 4-4 Loads transferred to columns 3, 6, 7, 8 and 9 in the six tests

TEST NO.	1	2	3	4
Load kN/m^2	**23.6**	**25.7**	**25.1**	**23.3**
Column 2	**22.7**	—	—	—
Column 4	**22.0**	**23.4**	—	**12.0**
Column 6	**23.0**	—	**23.1**	—
Column 8	**21.0**	**28.0**	—	—

Table 4-5 Moments transferred to edge columns

TEST NO.	1	2	3	4	5	6
Load kN/m^2	**23.6**	**25.7**	**25.1**	**23.3**	**23.3**	**26.7**
Column 1	**18.1**	**13.1**	**13.0**	**11.5**	**11.2**	**10.2**
Column 3	**18.2**	**13.9**	**13.1**	**12.1**	**12.3**	**11.7**
Column 5	**17.1**	**16.4**	**18.0**	**13.0**	**13.0**	**14.5**
Column 7	**19.0**	**16.8**	**15.0**	**10.6**	**10.4**	**12.6**

Table 4-6 Moments transferred to corner columns

CHAPTER 5

ANALYSIS OF TEST RESULTS

5.1 Behaviour of the slab :-

The slab behaved elastically up to load equal to 5.84 kN/m^2. After removing the applied load, all the deflections returned to their initial readings. From Table 4.3 it can be noted that panel B suffered the most deflection and panel D the least deflection in almost all tests. This could be explained by the number of tendons at each outside panel edge. As it can be seen from Fig. 3.8, panel D was surrounded by two tendon passing through the columns on the south and west sides. These tendons may combine with the concrete to work as hidden beams with relatively high stiffness compared to the mid panel regions of the slab. Other panels were provided with two tendons on at least one edge. Panel B had one tendon on each side and experienced the most deflection. At the same load, deflections were larger in later tests because of residual cracks and degradation of the stiffness of the slab. The maximum deflection was approximately 40 mm at panel B in Test no.5. No deflection data was gathered in Test 6. The variation of deflections can also be explained due to load redistribution between panels.

No visible cracks were seen when the slab was subjected to a load of 5.8 kN/m^2. Visible cracks were first noticed in the vicinity of edge columns at a load equal to 8.76 kN/m^2. On increasing the load, the cracks became more visible, deeper and wider. Radial cracks started to form from the corners and faces of the columns due to high stress concentrations at these locations. Prior to failure in Test no.1 the radial cracks joined,

and bottom cracks formed in the positive moment areas in the spans as shown in Fig. 4.3. These cracks followed the tendon distributions. In the successive tests the cracks formed at same areas, which were regions of high negative and positive moments. They were wider and deeper because of the decreased slab stiffness. Few cracks were observed at corner columns. Most cracks at corner columns were due to torsion caused by moments transferred to these columns in both directions.

It is difficult to determine the load at which diagonal tension cracks start forming inside the slab. However most researchers suggest that at loads equal to 50-70% of ultimate these cracks start forming, which would equal 11.8-16.5 kN/m^2 in the first test.

Comparison of the test results with the code predictions is difficult for a multi redundant structure such as a two bay by two bay flat slab as the errors in the prediction formulas may be in the calculated forces or moments or in the strength equation.

This chapter compares the measured column reactions and moments with those predicted by the analysis methods. Secondly the measured punching shear loads are compared with those calculated using the strength prediction equations.

5.2 Comparison of measured column forces and moments with EFA & RDDM :-

In this section test results will be compared with those calculated using EFA and RDDM methods. Figs. 5.1, 5.2, 5.3 compare the measured loads in corner, edge and middle columns in Test no.1 with analysis methods. Figs. 5.4, 5.5 and 5.6 show the comparison of the reactions at corner, edge and middle columns in Test no.2 with analysis methods. The EFA values in Figs. 5.2 and 5.5 are calculated using 50% of the

load from strip A and 50% from strip B; these strips are illustrated in Fig. 2.1. Figs. 5.7 and 5.8 compare the measured moments with the EFA and RDDM calculated values for the corner and edge column-slab connections respectively in Test #1. Figs. 5.9 and 5.10 compare the measured moments with EFA and RDDM calculated values in Test #2.

Sherif in his Ph.D. thesis concluded that Direct Design Method predicted column moments are in better agreement with the moments measured in his tests than those predicted by Equivalent Frame Analysis. In the current research, in general, the RDDM gives better prediction of moments except in the case of moments transferred to corner columns in test #1 where the difference between the test moments and EFA moments is 3.3% and the difference between test moments and RDDM moments is 15%. According to Corley (1970) slab moments calculated by the Equivalent Frame Method can differ from measured values by 15% at interior columns, but by much more than this at exterior columns.

5.3 Punching shear of slab-column connections :-

In a relatively thin flat slab supported on columns or the case of a large concentrated load applied on a small area and subjected to bending in two directions, shear failure may occur by punching through of the loaded area along a truncated cone or pyramid, with the failure surface sloping out in all directions.

Various code provisions such as ACI 318-95, BS 8110-85, CSA A23.3-94 and CEB FIP-90 define the critical area of punching shear strength as a fraction of the effective depth of slab away from the column face. North American codes define the critical section at a distance equal to d/2 from the column or the concentrated load. BS 8110-85 and CEB FIP-90 define the critical section at 1.5d and 2d respectively.

Equations proposed by these codes do not necessarily model the mechanism of failure or the general principles governing the true behaviour of flat slabs. They have been chosen due to their simplicity and the formulations have been chosen for their ease of use and give acceptable results.

5.3.1 Punching shear failure of the current work :-

The main concern of the current work was to investigate the punching shear resistance of edge slab-column connections and the contribution of prestress to the punching shear strength. North American codes, as mentioned in section 2.2, neglect the effect of prestress forces at the edge of the slab. Columns 3, 6, 7, 8 and 9 were provided with load cells to measure the loads transferred to them. As well all unbalanced moments transferred to external columns were measured.

Punching shear failure occurred at an applied load equal to 23.65 kN/m^2 in the first test and at a load equal to 26.27 kN/m^2 at the second test, even though the stiffness of the slab-column connection was reduced due to residual cracks from the first test. The failure zones in the first and third tests were close in area which was about 300 to 350 mm in diameter around columns 2 and 6 respectively. In the second and fourth tests, the failure areas were approximately 600 mm in diameter around columns 8 and 4 respectively. In addition, in the first and third tests, the tendons which lost part or all their initial forces were those which passed through the columns only, while in the second and fourth tests the tendons which lost their forces were those passing through column and on either side of the column. In other words, in all tests the tendons passing through the failure zone lost part or all of their initial forces.

Although the initial average prestress, f_{pc}, in the first test was almost the same for all edge columns, punching shear failure happened at column 2 on the west side. The initial prestress was higher at the face of column 2 than at columns 4 or 8 indicating that it is unsafe to use initial prestress at the face of column in calculating the punching shear strength using Equations 2.4 or 2.6.

In Test no. 1, punching shear failure happened around column 2 which had two tendons perpendicular to free edge and one tendon parallel to the free edge before connection # 6 which had two tendons in both directions. Therefore, it can be said that f_{pc} is more complicated than described by ACI 318-95and CSA A23.3-94. It is related to the tendons passing through failure zone in the two directions. However, it also can be concluded that the contribution of the prestress in the two directions is not equally divided. In all tests, no losses happened to tendon forces parallel to free edge passing through the punching shear failure zone. Therefore, their influence on the punching shear strength is less than the tendons perpendicular to free edge passing through failure zone.

In Test no. 1 the changes in tendon forces were very small. Tendon T29 experienced the biggest change which was approximately 7% of the initial load. The variation in tendon forces were more pronounced in the following tests due to the pr-existing cracks. The change was around 16% in the second test.

In the second test, punching shear failure happened at column 8 instead of column 4 even though there were 2 tendons passing through column 8 in the direction parallel to free edge comparing with one tendon at column 4. That was because of movement of columns no. 8 and 4. The unbalanced moment transferred to column 8 just prior to failure reached 28 kN.m, while at column 4 the moment was 23.4 kN.m. As illustrated in

Fig. 4.11A, in the first steps of loading, the moments at column 4 were larger than the moments at column 8. Then at few loading steps prior to failure the moment at column 8 started increasing rapidly, so slab-column 8 failed due to high moment and shear at this connection.

In Test no. 5, punching shear first happened in the vicinity of column 2 followed by a punching shear failure of the interior connection due to loss of tendon forces caused by slab-column 2 connection failure. Test no. 5 clearly demonstrated the seriousness of punching shear failure. Although it is a local phenomenon, it can lead to collapse of entire structure. In this test, first loud bang was heard around column 6, followed by punching shear of columns 2 and 9 respectively. If the applied load had not dropped, the entire slab would have collapsed.

In Test no. 6, the maximum applied load on the slab was 32.11 kN/m^2. All corner column-slab connections survived but column 3 connection experienced the biggest cracks at the bottom and top surfaces. This was because only one tendon passed through this connection in each direction, while the other connections had two tendons in at least one direction. It is concluded that the prestress is effective at corner column-slab connections despite the distance between outer face of column and slab-edge being less than the 4h required by North American codes to be considered effective.

5.3.2 Comparison of the present edge connection results with ACI & CSA:-

ACI and CSA neglect the prestress effect at edge column-slab connection. The present work showed that the precompression is effective up to the edge of the slab. In calculating the punching shear strength by the ACI 318-95 and CSA A23.3-94, Equations 2.4 and 2.6 will be used and compared with Equation 2.2 including the average calculated

prestress f_{pc}. The perimeter of the punching area is taken at a distance d/2 from the face of the column. In Equation 2.2, V and M are the values obtained from the tests.

Table 5.1A shows ratios of v_{test} / v_{ACI}, v_{ACI} is the punching shear strength given by ACI 318-95. Limiting f'_c in Equation 2.4 to be not greater than 35 MPa gives conservative values. In addition using the average prestress f_{pc} for the whole width of the slab gives high ratios of v_{test} / v_{ACI}, therefore local prestress should be used.

Although the average prestress in the two directions was similar, in the second test, column 8, resisted 30% more axial load and 23% more moment than in the first test. The contribution of the vertical component V_p did not exceed 6% of the shear resistance in any case. In Dilger's work (1989), the vertical component did not exceed 7% of the shear strength. Table 5.1B shows that CSA gives more realistic values than ACI. Using f'c equal to the mean compressive strength and d not less than 0.8h as recommended by the code gives values close to the ones obtained by the tests.

5.3.3 Experimental results for various research :-

The experimental results of various research, including the current one, will be compared with the prediction of ACI, CSA and the Gardner equation in this section. The current work is referred to as Sharifi's. In the comparison for the North American codes the vertical component is neglected because it is difficult to determine the point of inflection of the tendons passing through the shear critical section and the change of the slope in the tendon through the shear critical section.

In Burn's work (1985), a half scale model was used and the slab was loaded only at the panels surrounding the column under investigation. Table 5.2 shows the measured shear strength is lower than ACI and CSA expectation. The explanation is that the

strength of this slab was governed by the flexural strength. The slab failed in a flexural mode with very large rotation about the negative moment region before the punching shear failures occurred.

In Dilger's experimental work (1989), 6 models of post-tensioned slabs were tested to failure. Two models, S1 and S5 are included in Table 5.2, because they were the only ones that did not have shear reinforcement. In slab S1, the bonded reinforcement yielded followed by punching shear of the slab. In slab S5, the punching shear was very clear and dominant failure type. The critical section for the edge column in the slab with overhang, S5, was considered d/2 from all sides as recommended by Rice et al (1985).

In Long's work (1993), as mentioned in chapter 2, five models having the same dimensions were tested. The variables considered were: prestress level, distribution of prestressing within the panel and the tendon profile. The measure failure stresses are at least twice those predicted by the ACI-ASCE committee 423-design equation. CSA gives a better estimate than the ACI. Neither ACI nor CSA recognizes the contribution of bonded reinforcement to punching shear strength.

In Rezai's research (1993), a punching shear failure occurred around the south edge column. The column was circular in section and had the same nominal dimension as the square column in the north direction. This confirms the effect of loading area periphery on the shear resistance. The failure happened in the uniformly distributed tendons direction although the average prestress in both directions was the same.

In the present work (1997), the results of the first two tests were included in the table, because after that the average prestress was reduced by an unknown amount due to losses of force in the tendons passing through failure zones.

Even considering the effect of prestress up to the edge of the slab, the ACI provisions, except for Burn's results, are still very conservative in predicting the punching shear strength of edge column-slab connections. CSA, in some cases, gives values very close to the test values as in Rezai's and Sharifi's first test.

Some researchers, such as Saatcioglu (1997), believe that d does not reflect the effective depth from the centre of tendons to the extreme fiber, "d" is the equivalent height of the rectangular shear stress diagram equal in area to the real parabolic shear stress diagram. Here the code recommends d not to be less than 0.8h.

Most researchers suggest that the local prestress at failure should be used instead of the initial average prestress. In Table 5.3 f_{pb} is taken 10% higher than f_{pc} as recommended by Long. The variation in the results in Tables 5.2 and 5.3 does not exceed 3%.

Table 5.4 compares test results with Gardner's proposed equation 2.8 which was introduced in chapter 2. Gardner believes that d is the effective depth from the tendon center to the extreme compression fiber. Therefore in his proposed equation the values of d are smaller at the edge because of the drape of the tendon. To calculate the shear applied force, he suggests two methods: first using an eccentric shear equation in a similar way to the North American codes except that the perimeter is taken at periphery of the column instead of a distance equal to d/2 as recommended by North American

codes. The second method is derived from the British code and uses a simple multiplier to find the applied shear force.

5.3.4 Corner connections :-

In the present work, the corner connections showed very high shear and moment capacity. They were similar in size to the edge columns and the loads and moments transferred to them were less than the loads and moments transferred to edge columns. They experienced minor cracks due to loading.

In Test no. 6, the aim was to examine the behaviour of corner columns. In Figs. 5.11A, 5.11B, 5.12A and 5.12B the change in tendon forces becomes less pronounced with the distance the tendon is from the column. In Fig. 5.11A the biggest change in tendon forces at column no.1 in the east-west direction is at the tendon passing through column face. The same conclusion can be drawn for column no. 3 in Fig. 5.11B. Figs 5.12A and 5.12B show the same observation. Fig. 5.12A shows that the change in tendon T2 force is on average only 21% of the change in tendon T1 force which passes through column no.3 face.

Referring to section 4.8 summary, it was noted in Test no. 6 the corner columns experienced less moments and loads than in the previous tests. It would be due to shoring the interior and the edge columns, increasing their perimeter, attracting more load and reducing the spans.

Table 5.5A shows the comparison between Sharifi's and Rezai's test results and the ACI and CSA predictions. Table 5.5B gives the comparison with Gardner's proposed equation. In the present work, corner columns subjected to the maximum forces in Test no.1, only minor cracks were shown in that test around corner columns. Gardner's

proposed equation gives better results in the case of corner columns in Sharifis' work than Rezai's work. This is because the prestress estimated at the face of the column in Rezai's work was much larger than the average prestress calculated over the entire width of the slab.

5.4 Distribution of strain in the slab :-

Vibrating wire gauges (VWGs) were used to measure strains at mid depth of the slab. Referring, to Figs. 4.5 and 4.7, Test no. 1 the trend of these two graphs are similar, at the load where the force in the tendons started to increase, the strain in the concrete in the vicinity of that tendon started to increase as well. Table 5.6 and Fig 5.13 show the strains in the vibrating wire gauges after stressing cables to full loads.

Comparison of the various pairs of gauges is not encouraging. VWGs 3 (256 x 10^{-6}) and 6 (223 x 10^{-6}), 12 (272 x 10^{-6}) and 16 (281 x 10^{-6}), 1 (433 x 10^{-6}) and 5 (345 x 10^{-6}), 9 (243 x 10^{-6}) and 13 (213 x 10^{-6}) are in reasonable agreement but gauges 4 (282) and 8 (523) are not in agreement. The strain measured at gauges 9 (243 x 10^{-6}), 13 (213 x 10^{-6}), 12 (272 x 10^{-6}) and 16 (281 x 10^{-6}) are similar and indicate that the precompression is uniform in the slab remote from the anchorage.

As expected, VWG no. 2 experienced the highest strain because it was at the face of column 7 which had two tendons passing through it in each direction. Therefore, it is located at high stress zone. It can be concluded that precompression is effective up to the edge of the column. Comparing strains at VWGs no. 11, 10 and 9, which measured strains in the north-south direction, it is found that the strain increases with position from the free edge toward the middle of slab. The same observation can be drawn for VWGs no 15, 14 and 13 in the east-west direction. The values of strains in this direction are

less, because these VWGs were located between cables 457mm apart while VWGs no. 9, 10 and 11 were located between cables where they were 375mm apart. These results indicate that the precompression diffuses from the tendon locations at an angle of 30^{o} which is close to the commonly assumed 26^{o}. This is the first research attempt to measure the diffusion of the precompression inside two way prestressed flat slabs. However the measured strains could not be converted to stress because the modulus of elasticity is unknown.

	v_{test} / v_{ACI}							
	Test no. 1				Test no. 2			
	Column no. 2				Column no.8			
	$d = d_{eff}$		$d = 0.8h$		$d = d_{eff}$		$d = 0.8h$	
	$f'c \leq 35$	$f'c = 45$	$f'c \leq 35$	$f'c = 45$	$f'c \leq 35$	$f'c = 45$	$f'c \leq 35$	$f'c = 45$
f_{pc1}	3.36	2.96	2.17	1.91	4.23	3.73	2.74	2.41
f_{pc2}	1.86	1.73	1.24	1.16	2.21	2.10	1.48	1.38
f_{pc3}	2.15	1.98	1.41	1.30	2.73	2.51	1.75	1.61

Table 5.1A v_{test}/v_{ACI} for the current work considering the effect of the vertical component, Vp calculated using equation 2.5

	v_{test} / v_{CSA}							
	Test no. 1				Test no. 2			
	Column no. 2				Column no.8			
	$d = d_{eff}$		$d = 0.8h$		$d = d_{eff}$		$d = 0.8h$	
	$f'c \leq 35$	$f'c = 45$	$f'c \leq 35$	$f'c = 45$	$f'c \leq 35$	$f'c = 45$	$f'c \leq 35$	$f'c = 45$
f_{pc1}	2.43	2.14	1.56	1.38	3.05	2.70	1.98	1.75
f_{pc2}	1.42	1.30	0.94	0.86	1.71	1.57	1.13	1.04
f_{pc3}	1.58	1.45	1.04	0.95	2.0	1.84	1.31	1.20

Table 5.1B v_{test}/v_{CSA} for the current work considering the effect of the vertical component, Vp calculated using equation 2.5

f_{pc1} = 0 **f_{pc2}** calculated at a distance c + 6h **f_{pc3}** calculated at entire width of slab
f'_c : the compressive strength of concrete in MPa

		fcm MPa	fpc MPa	h mm	v_{test} MPa	v_{CSA} MPa	v_{test} / v_{CSA}	v_{ACI} MPa	v_{test} / v_{ACI}
Burns 1985	V209	32.75	0.932	70	1.12	2.71	0.41	1.93	0.58
	V212	32.75	0.932	70	1.19	2.71	0.44	1.93	0.62
Dilger 1989	S1	35.8	3.1	150	5.6	3.62	1.54	2.66	2.1
	S5	41.3	3.1	150	3.5	3.82	0.92	2.8	1.25
Long 1993	E1	39	2.34	50.8	5.55	3.48	1.59	2.51	2.21
	E2	39.7	2.34	50.8	5.8	3.50	1.66	2.53	2.29
	E3	39.4	3.50	50.8	6.65	3.88	1.71	2.87	2.32
	E4	39.6	1.17	50.8	4.51	3.05	1.48	2.17	2.08
	E5	36	2.34	50.8	6.37	3.37	1.89	2.51	2.54
Rezai	Test3	44	3.45	90	3.76	4.02	0.93	2.97	1.27
Sharifi	T1	45	2.7	89	3.71	3.8	0.98	2.75	1.35
	T2	45	2.8	89	4.69	3.83	1.22	2.78	1.69

Table 5.2 Comparing various research results with ACI and CSA using d=0.8h and neglecting Vp

		f_{cm} MPa	f_{pb} MPa	h mm	v_{test} MPa	v_{CSA} MPa	v_{test} / v_{CSA}	v_{ACI} MPa	v_{test} / v_{ACI}
Burns 1985	V209	32.75	1.02	70	1.12	2.75	0.41	1.97	0.57
	V212	32.75	1.02	70	1.19	2.75	0.43	1.97	0.60
Dilger 1989	S1	35.8	3.41	150	5.6	3.73	1.50	2.75	2.04
	S5	41.3	3.41	150	3.50	3.92	0.89	2.89	1.21
Long 1993	E1	39	2.57	50.8	5.55	3.56	1.56	2.58	2.15
	E2	39.7	2.57	50.8	5.8	3.59	1.62	2.60	2.23
	E3	39.4	3.85	50.8	6.65	4.0	1.66	2.97	2.23
	E4	39.6	1.29	50.8	4.51	3.1	1.45	2.21	2.04
	E5	36	2.57	50.8	6.37	3.45	1.84	2.51	2.53
Rezai	Test3	44	3.8	90	3.76	4.14	0.91	3.1	1.21
Sharifi	T1	45	2.97	89	3.71	3.89	0.95	2.84	1.31
	T2	45	3.1	89	4.69	3.94	1.19	2.87	1.63

Table 5.3 Comparing various research results with ACI and CSA using d=0.8h and neglecting Vp, $f_{pb}=1.1f_{pc}$

		fse MPa	fpc MPa	deff mm	Column Size mm	Vu kN	Mu kN.m	Test/Gar. eccentric shear	Test/Gar simple multiplier
Burns 1985	V209	1220	1.9	47	203	30.7	3.1	0.65	0.57
	V212	1220	1.9	47	203	32.04	3.4	0.7	0.65
Dilger 1989	S1	888	4.69	82.8	250	180	94	2.9	1.30
	S5	888	4.69	82.8	250	180	135	2.36	0.77
Long 1993	E1	880	4.4	34	163	46.7	4.6	1.12	0.98
	E2	990	7.0	31	163	49.8	4.9	1.15	1.01
	E3	990	10.6	29	163	56	5.5	1.13	1.0
	E4	990	3.5	33	163	40.9	4.0	1.11	0.98
	E5	990	7.0	36	163	53	5.2	1.02	0.90
Rezai	Test3	900	9.84	50	180	135	15	1.20	1.05
Sharifi	T1	859	9.84	50	203	94.1	22.7	1.12	0.71
	T2	859	4.7	50	203	122	28	2.07	1.35

Table 5.4 Comparing various research results with Gardner's proposed equation using d as the effective depth

	f_{cm} MPa	f_{pc}[1] MPa	h mm	v_{test} MPa	v_{CSA} MPa	v_{test} / v_{CSA}	v_{ACI} MPa	v_{test} / v_{ACI}
Rezai	44	3.45	90	2.98	4.02	0.74[2]	2.96	1.01
Sharifi Test #1	45	2.7	89	3.61	3.8	0.95[3]	2.76	1.31

1 average over width of slab
2 calculated moment
3 measured moment

Table 5.5A Comparing test results for corner columns with ACI and CSA, $V_p = 0$

	f_{se} MPa	f_{pc}* MPa	d_{eff} mm	Column Size mm	Vu kN	M_u kN.m	Test/Gar. eccentric shear	Test/Gar simple multiplier
Rezai	900	9.84	50	180	57.4	8.4	0.67	0.89
Sharifi	859	4.82	50	203	52	18.2	1.21	1.15

* calculated at face of column.

Table 5.5B Comparing test results for corner columns with Gardner's proposed equation

VWG	Strain x 10^{-6}	Analogue VWG
1	-433	5
2	-705	
3	-256	6
4	-282	8
5	-345	1
6	-223	3
7	-317	
8	-523	4
9	-243	13
10	-239	
11	-191	
12	-272	
13	-213	9
14	-187	
15	-107	
16	-281	12
17	-641	

Table 5.6 Strains in the VWGs after stressing of cables to full load

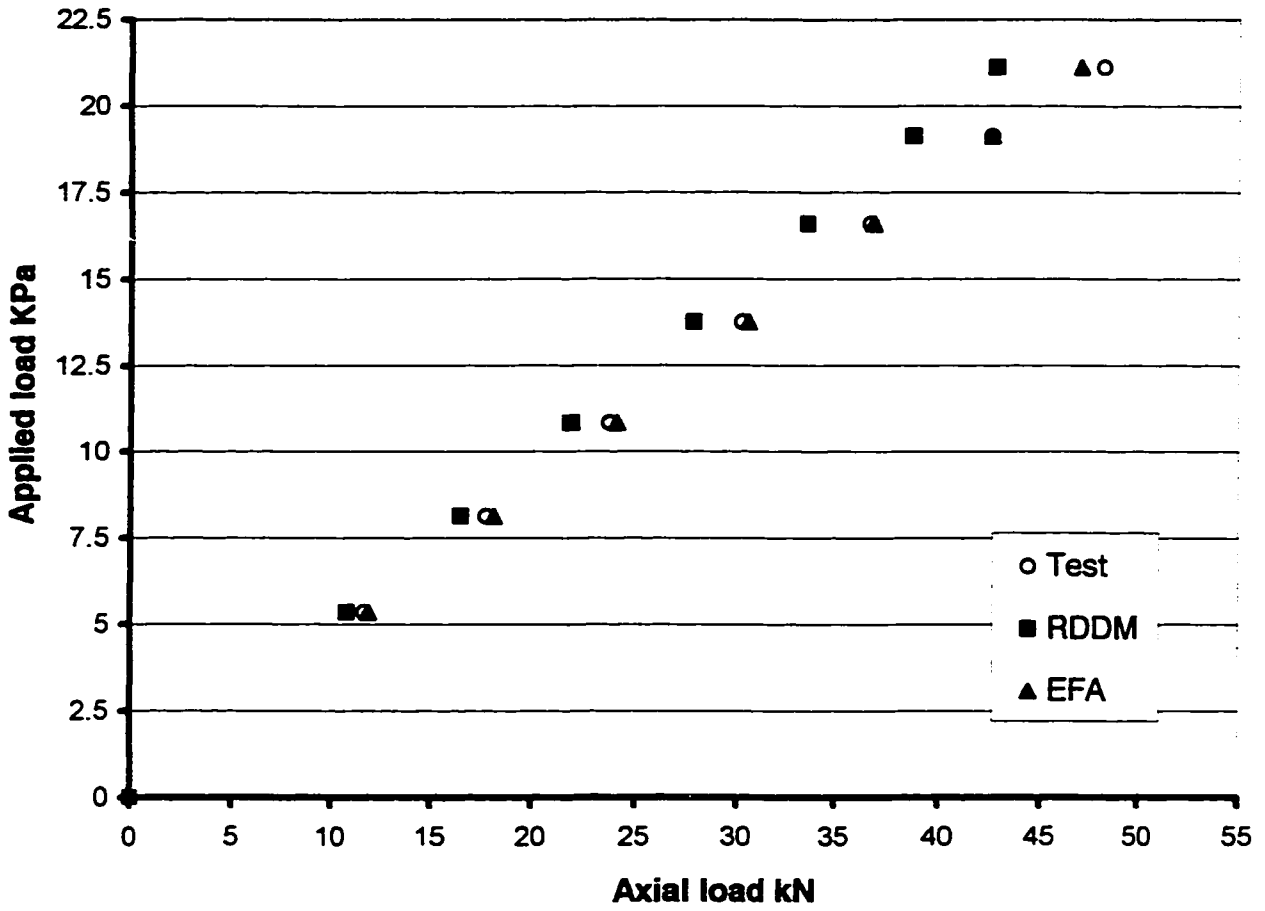

Fig. 5.1 Comparison of loads transferred to corner columns with RDDM and EFA methods in Test no. 1

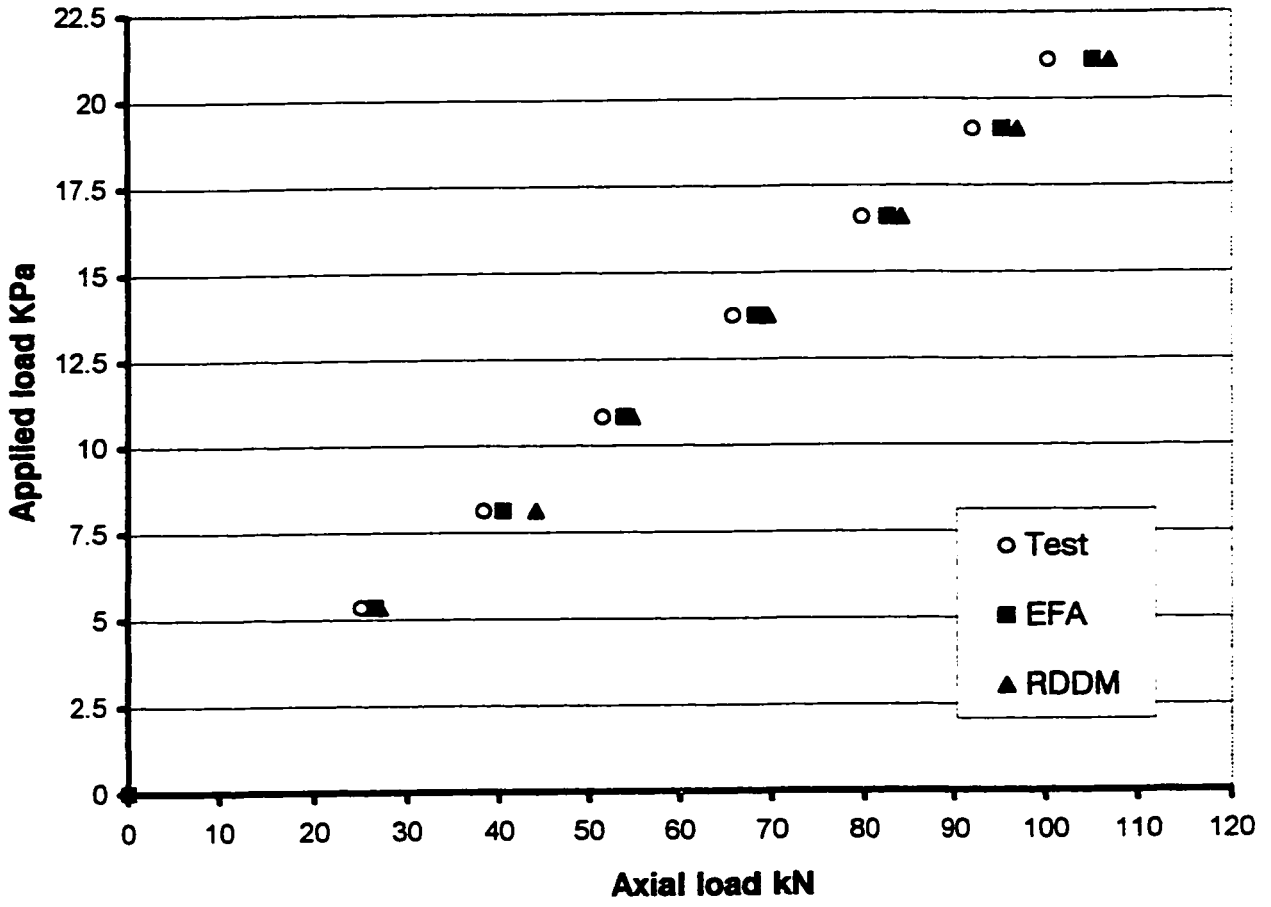

Fig. 5.2 Comparison of loads transferred to edge columns with RDDM and EFA methods in Test no. 1

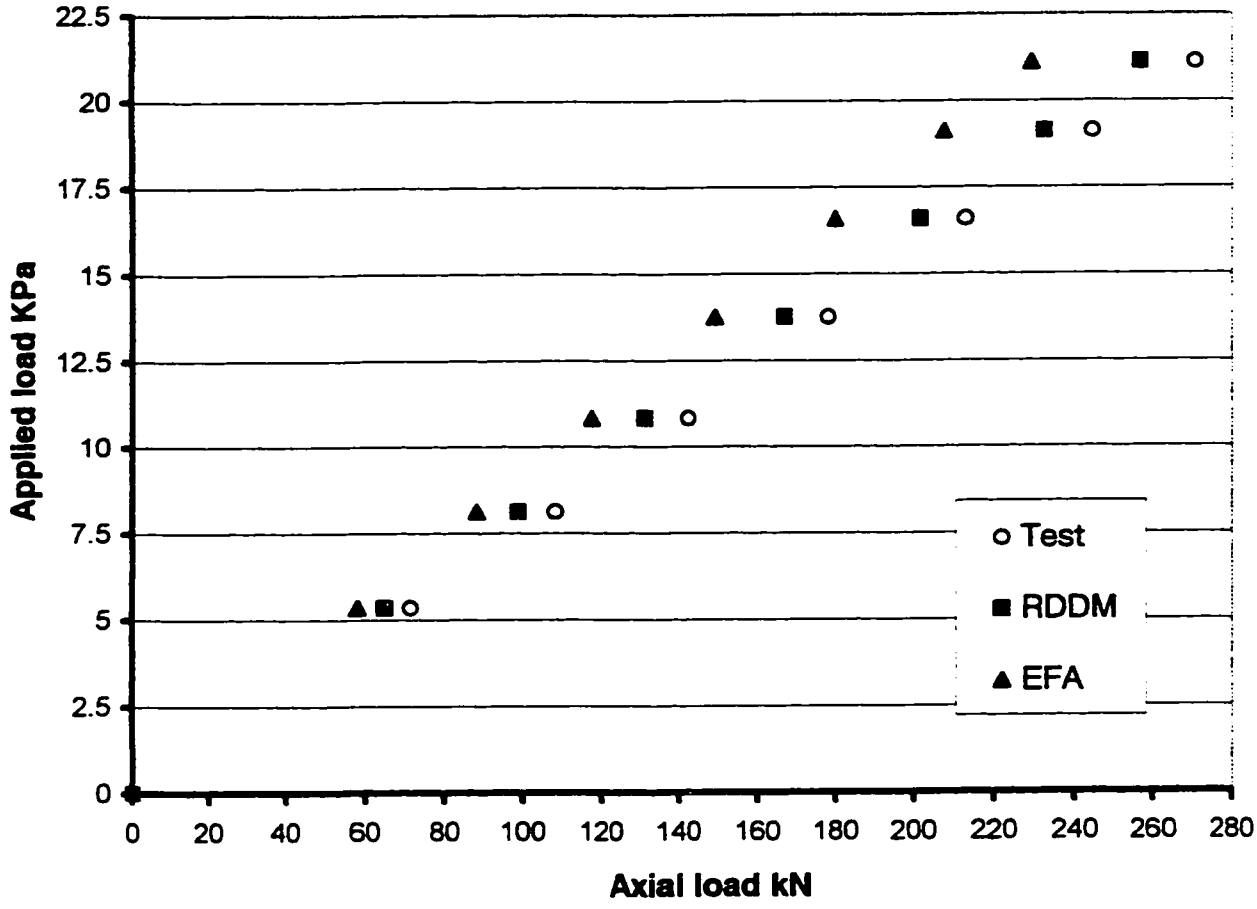

Fig. 5.3 Comparison of loads transferred to middle column with RDDM and EFA methods in Test no. 1

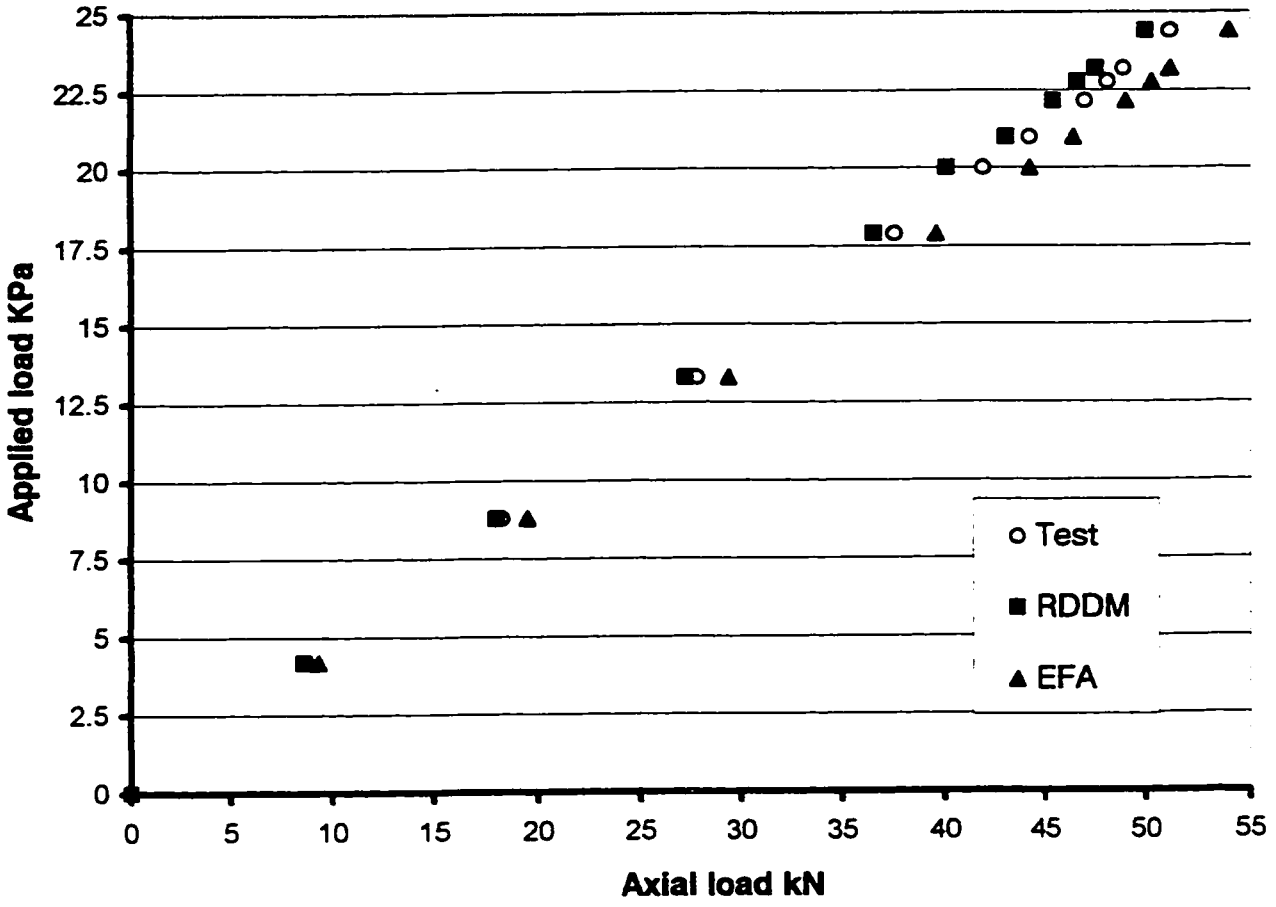

Fig. 5.4 Comparison of loads transferred to corner columns with RDDM and EFA methods in Test no. 2

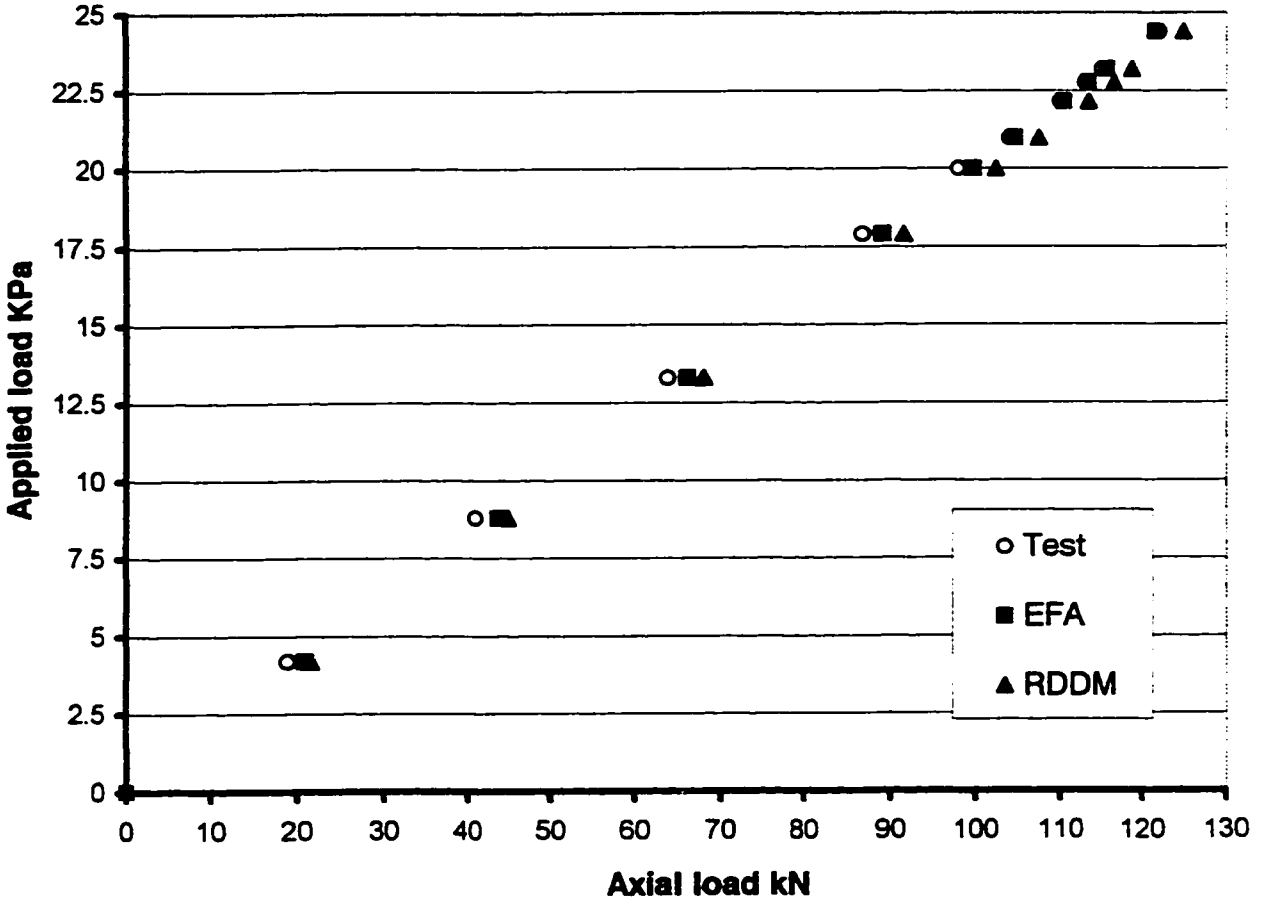

Fig. 5.5 Comparison of loads transferred to edge column with RDDM and EFA methods in Test no. 2

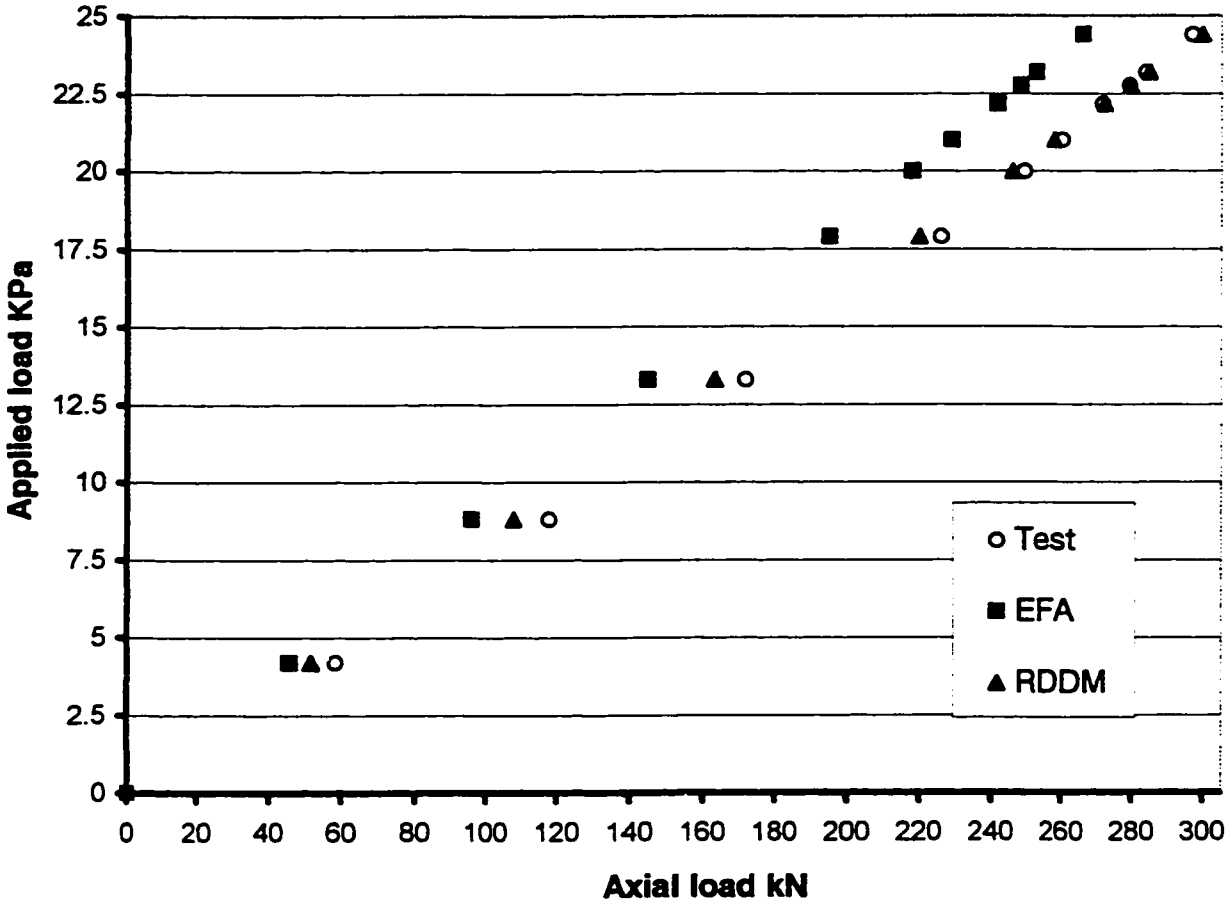

Fig. 5.6 Comparison of loads transferred to middle column with RDDM and EFA methods in Test no. 2

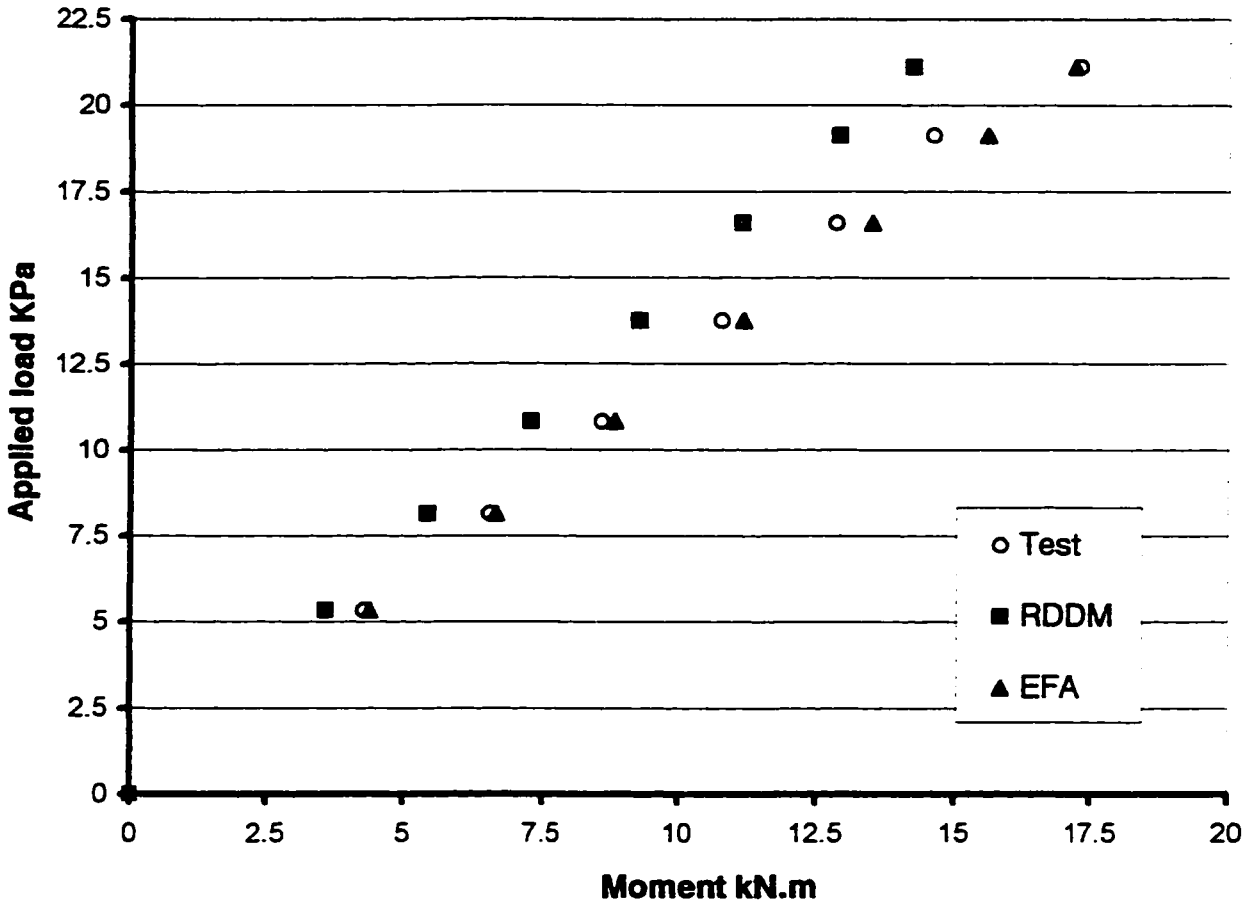

Fig. 5.7 Comparison of moments transferred to corner columns with RDDM and EFA methods in Test no. 1

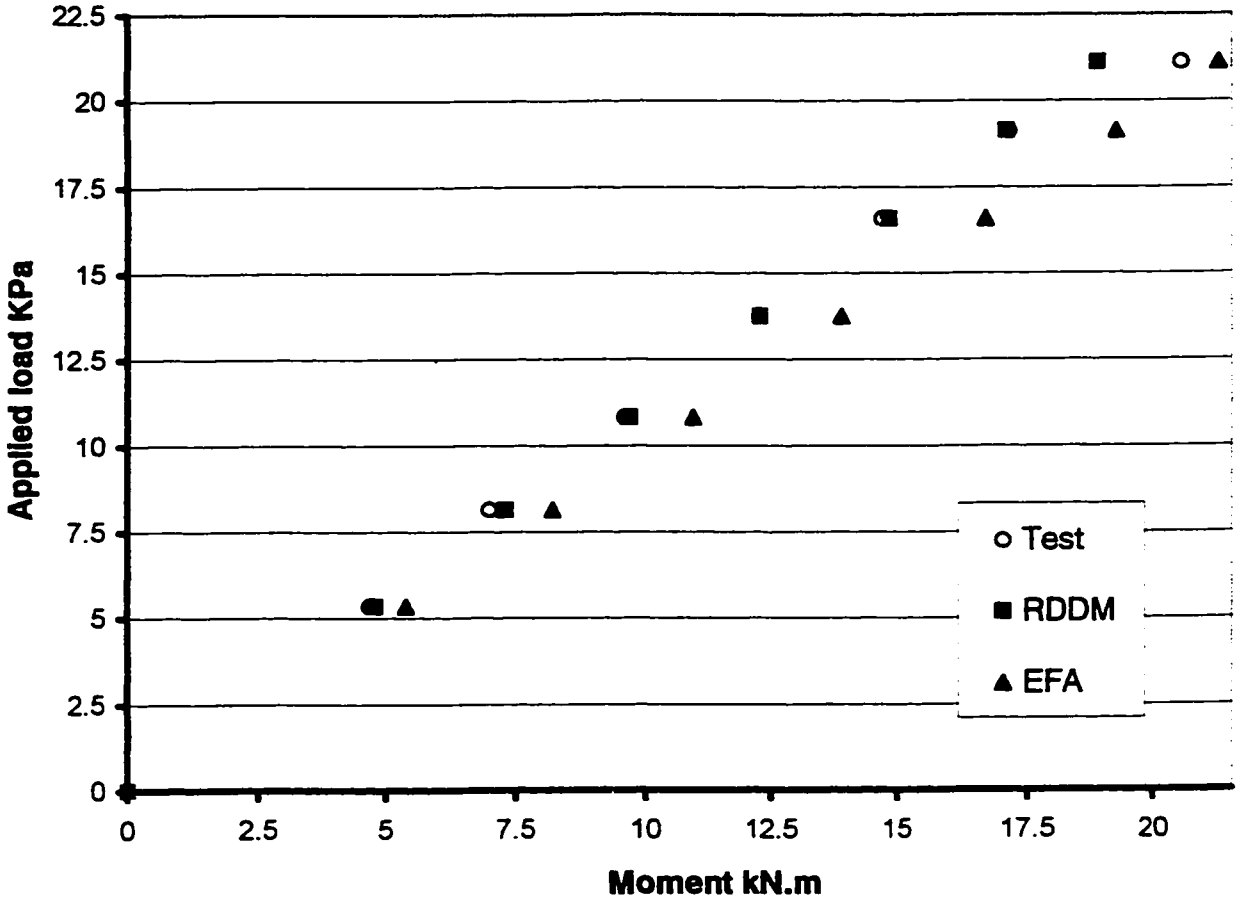

Fig. 5.8 Comparison of moments transferred to edge columns with RDDM and EFA methods in Test no. 1

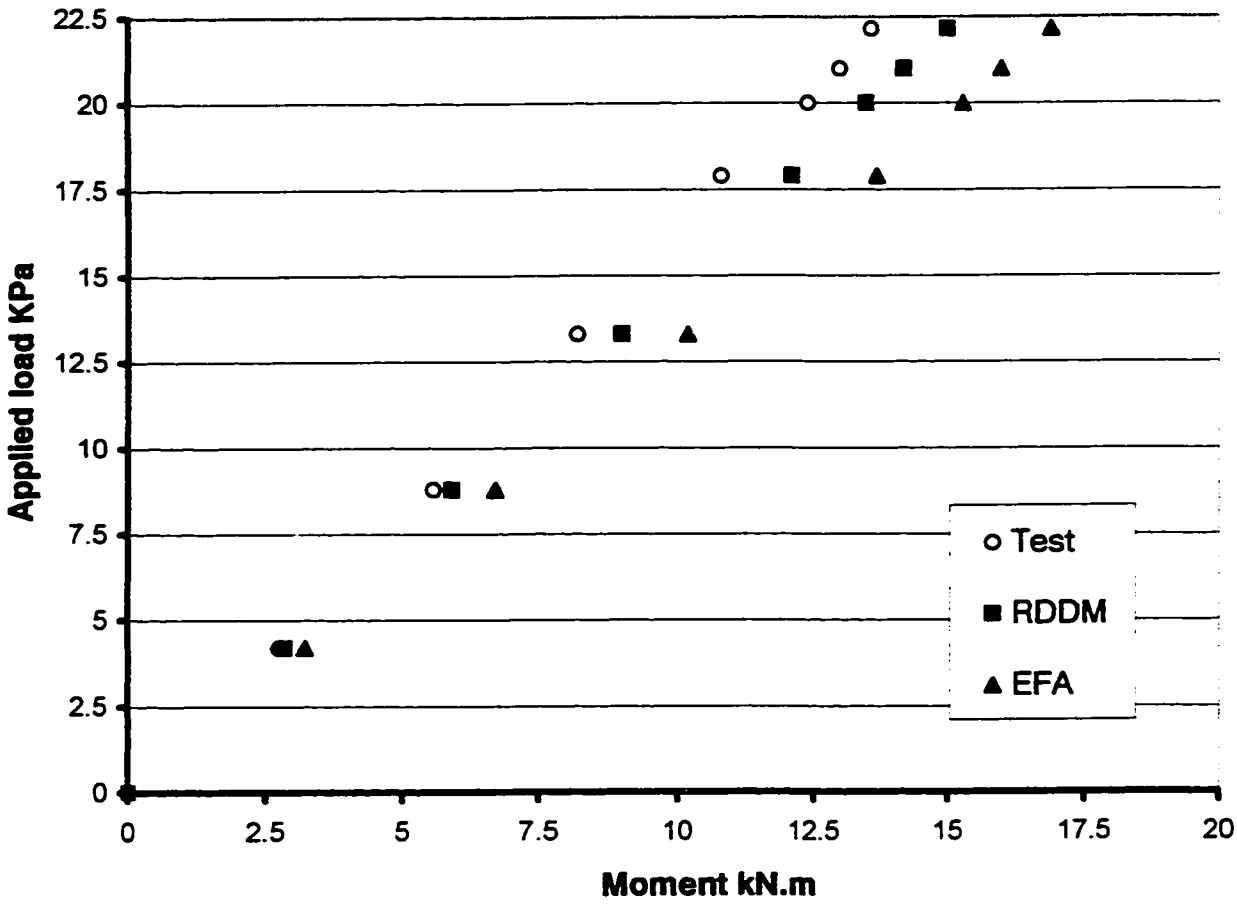

Fig. 5.9 Comparison of moments transferred to corner columns with RDDM and EFA methods in Test no. 2

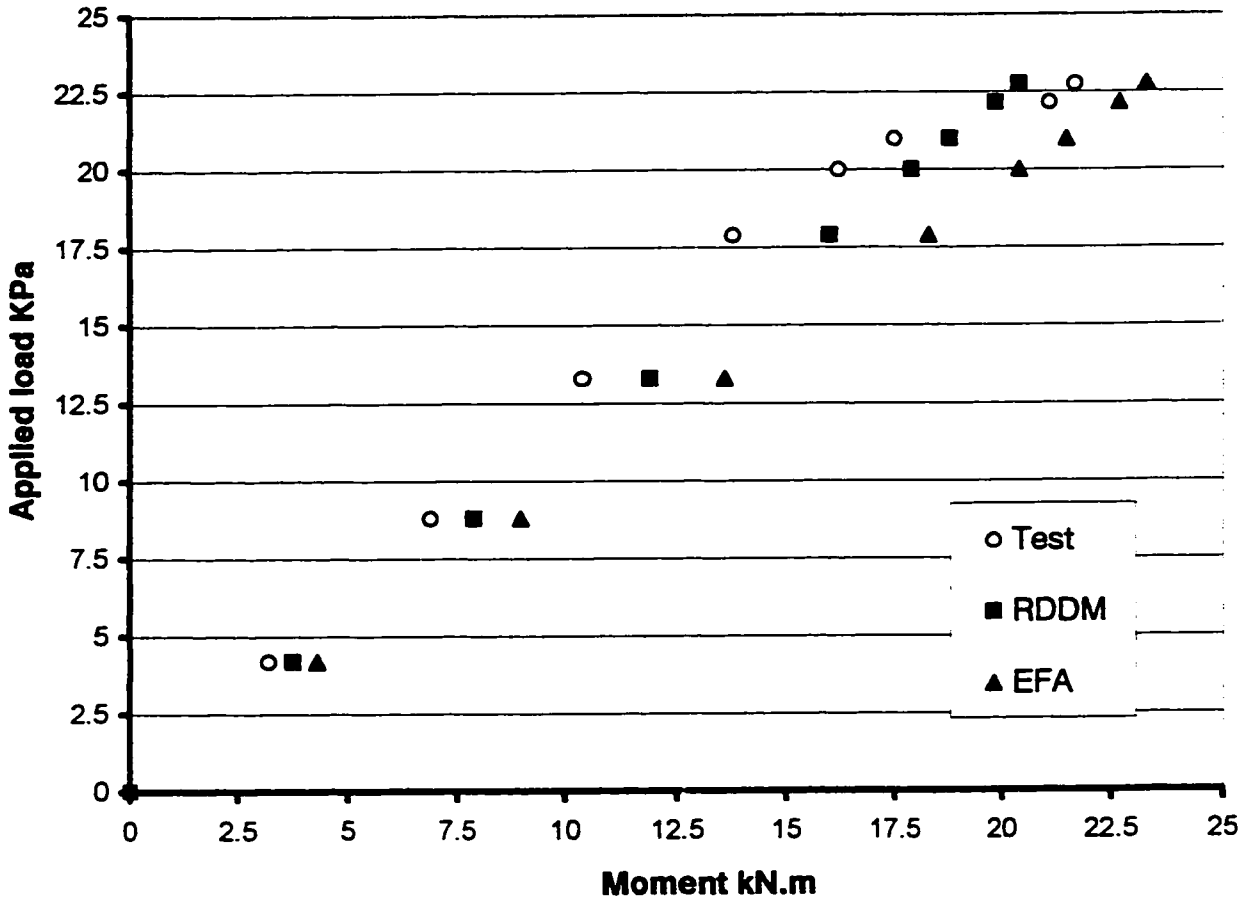

Fig. 5.10 Comparison of moments transferred to edge columns with RDDM and EFA methods in Test no. 2

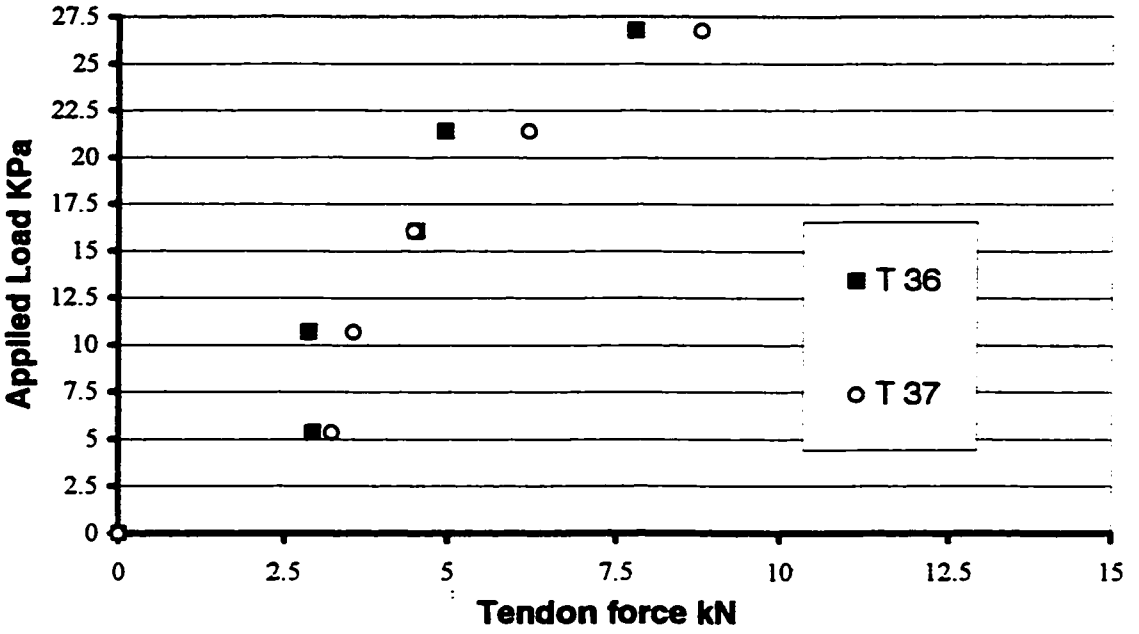

Fig. 5-11A Changes in force in E-W tendons passing through column # 1 in Test no. 6

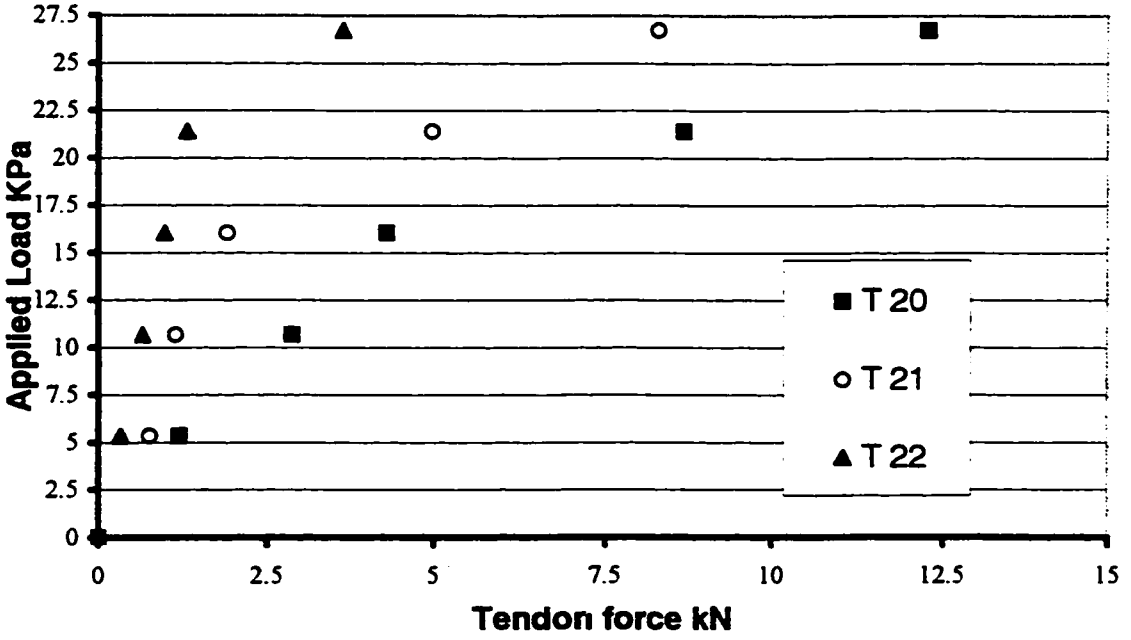

Fig. 5-11B Changes in force in E-W tendons passing through or near column # 3 in Test no. 6

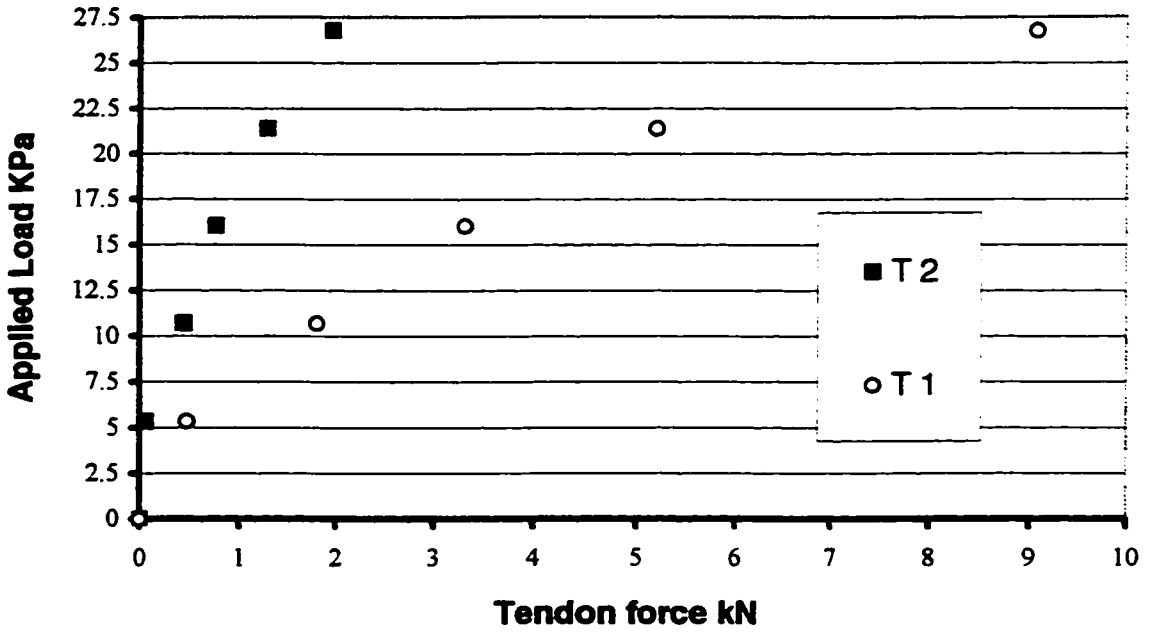

Fig. 5-12A Changes in force in N-S tendons passing through or near column # 3 in Test no. 6

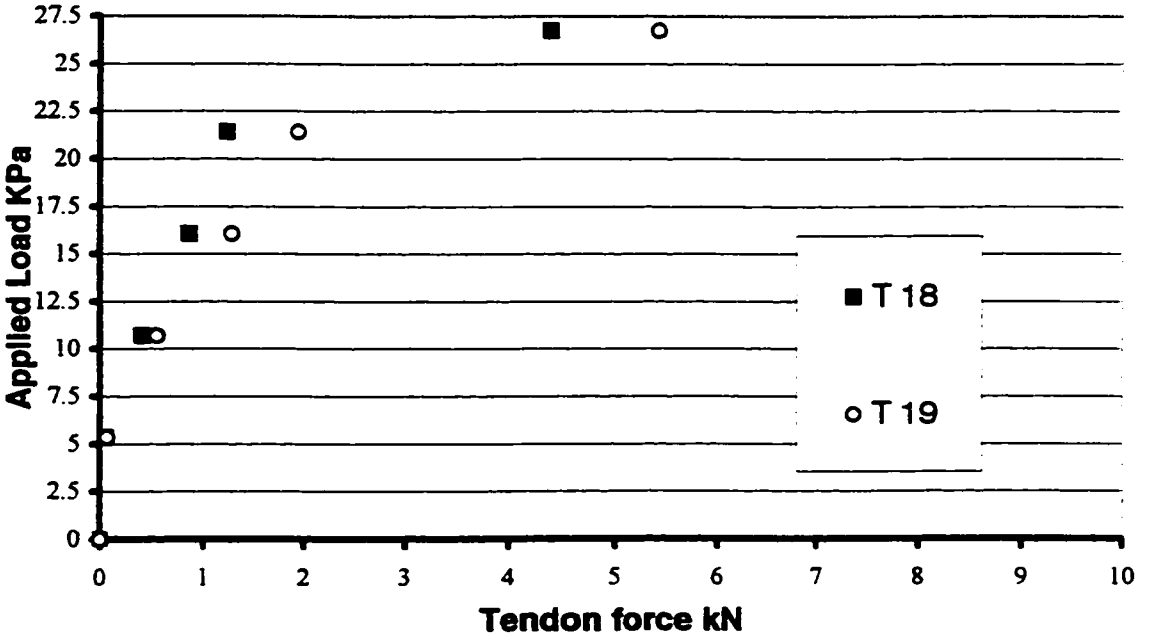

Fig. 5-12B Changes in force in N-S tendons passing through column # 5 in Test no. 6

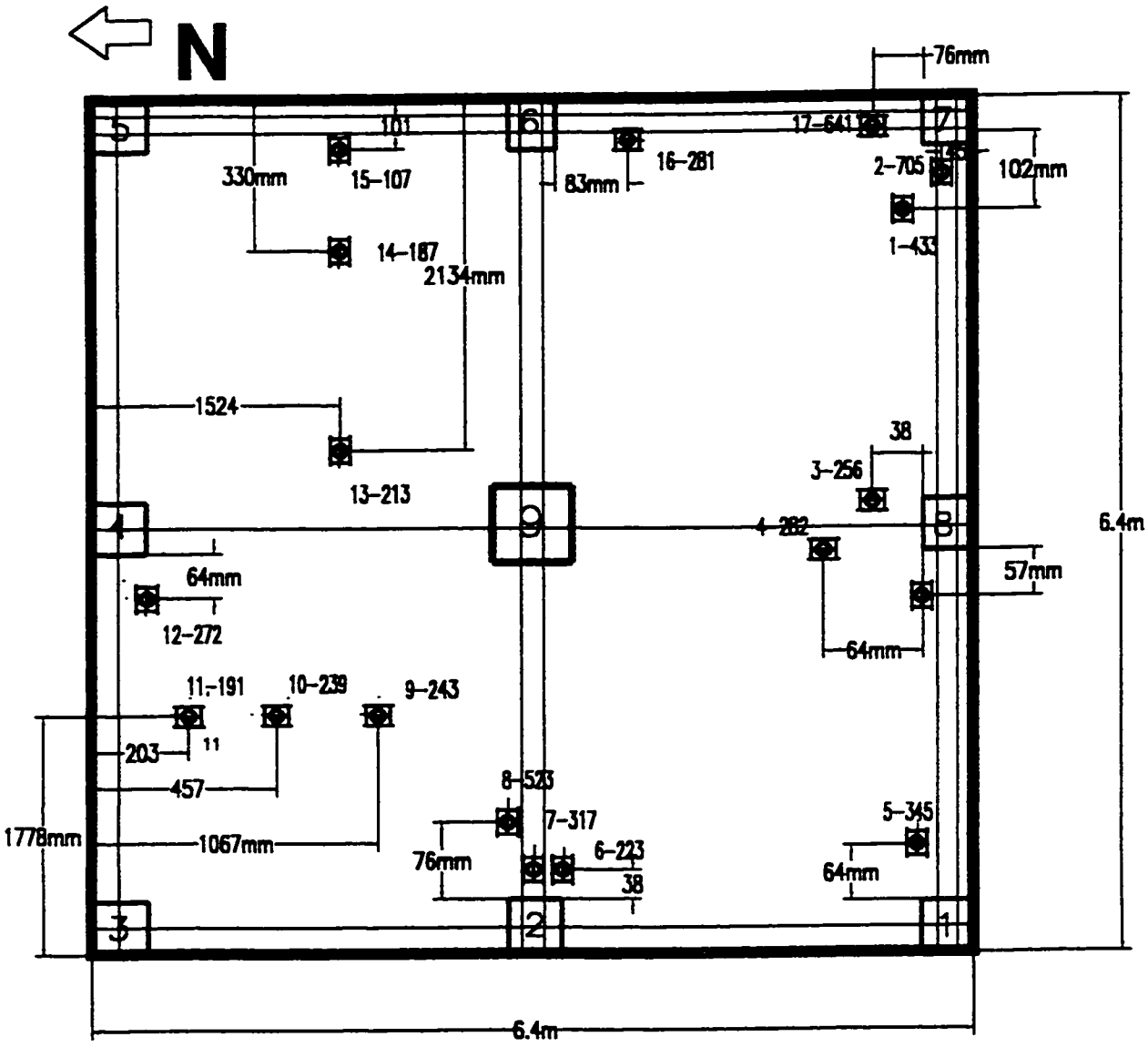

Fig. 5-13 The VWGs numbers and values after stressing of cables to full load (not to scale), showing the cables pass the columns only

CHAPTER 6

OBSERVATIONS AND RECOMMENDATIONS

6.1 Observations :-

Two-way flat plates behave in a ductile manner and experience load, and moment, redistribution in the two directions. Punching shear is the dominant mode of failure in this type of slabs, therefore caution should be spent in estimating the punching shear resistance. Repeated loads reduce the slab stiffness and reduce its ultimate strength.

In the current work the Refined Direct Design Method and the Equivalent Frame Analysis method were used to calculate the shear forces and moments transferred through the column slab connections. Generally speaking, the results of both of these methods are in good agreement with test results. Both methods gave a good estimate of the loads transferred to corner column, especially the EFA where the discrepancy with the test results did not exceed 2.5% in Test #1 and 7% in Test #2. In the EFA, to estimate the load transferred to edge columns, it was more necessary to take 50% of the load from the design strip in one direction, plus 50% of the design strip in the perpendicular direction. Again, the two methods gave reasonable estimates of the loads at the edge connections. For the case of middle columns, both methods underestimate the loads, RDDM by 7% and EFA by 17% in Test #1, and RDDM by 3% and EFA by 14 % in Test #2.

In Test no.1, moments transferred to edge connections, RDDM gave approximately identical values to test values. EFA overestimated the moments by 13%. While in Test no.2, the both methods overestimated the values up to few steps before failure when test values exceeded RDDM values. Initially the behaviour was elastic, then close to failure the load distribution changed, column 8 started absorbing more loads and moments causing this connection to fail rather than the expected no.4 connection. The discrepancy between measured moments at corner columns and calculated ones using EFA did not exceed 7% in Test no. 1.

Burn's experimental work was almost the only work used in the comparison where ACI-318.95 overestimated the punching shear strength; because the low reinforcement ratio and the failure of the slab in flexure prior to punching shear failure.

In the current work, the ACI and CSA gave better estimates of the shear strength of the first test than the second test. Therefore, f_{pc} should be modified to take the local prestress not as it is required by North American codes to be taken on the entire width of the slab.

The North American codes do not define clearly columns based on their positions, internal, edge or corner. Therefore ACI 318-95 equation 2.4 and the CSA A23.3-94 equation 2.6 must be revised to account for column position. In equation 2.4 αs must be revised to be a better representative of the column location. In the CSA provision, a similar factor should be added to take account of the column location.

Comparing Tables 5.2 and 5.3 shows that using the prestress at failure, estimated as 110% of the initial prestress instead of the initial prestress, improves the prediction by less than 3%.

Except in Burn's case due to flexural behaviour, CSA gave better agreement with the test results than ACI. Table 5.2 shows that sometimes it gave unconservative results. It is required to be more cautious when using CSA equation. Some modification might be done to the factor 0.4 in equation 2.6. Originally this factor was 0.33 in the 1977 version of CSA code, and it was converted to 0.4 in 1984 which causes some cases to be unsafe in the design.

The Gardner equation requires long calculations, but it defines the decompression component in a clear way, while calculating the vertical component is hard to determine in the North American codes. Gardner's method takes into account the prestress at the face of the column which does not reflect the local prestress. In Table 5.4, using the eccentric shear equation Gardner's equation underestimated the strength by 12% in Sharifi's first test while in the second test it underestimated by 107%. Using a simple multiplier factor caused the proposed equation to overestimate the punching shear strength of the slab at column 2 in Test no. 1 in Sherifi's work.

In analyzing the punching shear strength of corner columns, in Table 5.5A, CSA A23.3-94 overestimated the punching shear strength in Rezai's work, while it gave relatively close values to the maximum load applied in Sharifi's experimental work but failure did not occur. In Rezai's experimental tests, the moments were calculated using Finite Element Method. These moments were relatively small comparing with moments measured during the current and other research.

The precompression in both directions has an impact on the punching shear strength of the slab-column connection. The direction perpendicular to the free edge has more influence than the direction parallel to the free edge. So the tendons perpendicular

to the free edge lost part or all of their forces when punching shear failure happened, while the tendons parallel to the free edge did not lose any force due to punching shear failure.

The measured strain in the VWGs indicated that the strain diffuses at an angle of 30^0 with the tendon layout. With zero stress at the edge and increases gradually until it gets uniform at a certain distance from the edge. In the current research it was found that the strain becomes uniform at a distance equal to almost 350mm which is at 5% from the slab width. Therefore it can be concluded that the strain is uniform in the entire slab except at or close to the anchorage plates where stress concentration is high. A high concentration of stress was found at the connections, which indicates that the precompression is effective at the edge and corner connections. This precompression increases the punching shear strength of these connections.

6.2 Recommendations :-

The prestress is effective to the edge of the slab and can be used in calculations of punching shear strength of unbonded, post-tensioned, concrete slabs. The provision of North American codes which neglects precompression if the distance between the outer face of the column and the edge is less than 4h, should be eliminated to obtain economical design.

Using the initial prestress on the entire width of the slab underestimates the punching shear strength, while using the prestress at the face of the column overestimates the punching shear strength. Therefore, the suggested width should be between these two values.

The requirement of the concrete compressive strength not to exceed 35 MPa can be eliminated. All the recent research had compressive strengths exceeding 40 MPa.

The unbalanced moment transferred by shear eccentricity has a significant effect on the overall punching shear strength of the connection. Comparison between the fraction of the unbalanced moment to be transferred by flexure suggested by CSA and ACI codes and the one suggested by Rangan and Hall, indicates that the elastic model adopted by the ACI and CSA may result in underestimation of the moment transferred by shear at edge columns. More research is required to determine the percentage to be transferred by flexure, torsion and shear.

To use the eccentric shear equation requires use of a parameter called J. This J is an ambiguous term defined by the code as analogous to the polar moment of inertia. Ghali says "when the critical section has shape other than rectangle, it is not obvious how J can be calculated". Therefore, this parameter should be modified in the code.

The use of effective depth not less than 0.8h, especially at edge columns, is an acceptable measure and simplifies calculations and gives estimation of the punching shear strength close to the measured ones during various tests.

The Refined Direct Design Method for two bay square slabs can be adopted by North American codes because it is a simple and effective tool to determine the moments in 2 bay x 2 bay flat plates.

More research is needed to study the shape effect on these kind of slabs. Close to full scale rectangular slabs need to be investigated to analyze their behavior and the effect of supporting area shape on punching shear resistance especially for edge columns.

More research is needed to investigate the punching shear strength of prestressed unbonded flat slabs under seismic loads. Punching shear phenomena is local and brittle, therefore more understanding is required for these slabs behaviour under cyclic loading.

Appendix A

Calibration of Load Cells at columns and tendons, Vibrating Wire Gauges, Rods and Jacks.

	Col.#3	Col.# 7	Col.#9			Col.#6	Col.#8
Load kN	Reading	Reading	Load kN	Reading	Load kN	Reading	Reading
0	0	0	0	0	0	0	0
5	372	349	20	-118	10	10	10
10	718	700	40	-217	20	20	20
15	1083	1055	60	-327	30	30	30
20	1432	1411	80	-437	40	40	40
25	1810	1790	100	-546	50	50	50
30	2162	2140	120	-654	60	60	60
35	2523	2495	140	-763	70	70	70
40	2887	2844	160	-870	80	80	80
45	3254	3200	180	-972	90	90	90
50	3616	3540	200	-1073	100	100	100
55	3981	3893	220	-1186	110	110	110
60	4347	4247	240	-1292	120	120	120
65	4709	4602	260	-1400	130	130	130
70	5067	4952	280	-1509	140	140	140
75	5422	5299			150	150	150
80	5785	5635			160	160	160
85	6144	5980					
90	6506	6318					
95	6851	6667					
100	7218	7008					

Calibration of Load Cells under columns no. 3, 6, 7, 8 and 9

Load kN	0	10	20	30	40	50	60
με	2571	2545	2536	2520	2503	2485	2466
Load kN	70	80	90	100	110	120	130
με	2449	2432	2414	2396	2379	2362	2345
Load kN	140	150	160	170	180	190	200
με	2328	2311	2293	2275	2258	2242	2224

Calibration of the Vibrating Wire Gauges embedded in the concrete cylinder on April 17, 1997

Load kN	0	20	40	60	80	100
με	2475	2441	2404	2366	2328	2291
Load kN	120	140	160	180	200	220
με	2253	2219	2184	2149	2114	2080
Load kN	240	260	280	300	320	340
με	2046	2011	1977	1945	1909	1872

Calibration of the Vibrating Wire Gauges embedded in the concrete cylinder on June 19, 1997

Big Jack # 202		Jack # 195		Jack # 130	
Pressure psi	Load kN	Pressure psi	Load kN	Pressure psi	Load kN
1000	32	1000	12.5	1000	13.5
2000	62.5	2000	26	2000	25
3000	92.5	3000	38	3000	35.75
3200	96	4000	50	4000	47.5
3300	100	5000	62.25	5000	61.25
3400	104	6000	74.25	6000	73.25
3500	108			7000	85

Calibration of Jacks

Rod # 1		Rod # 5		Rod # 9		Rod # 11	
Load kN	Strain	Load kN	Strain	Load kN	Strain	Load kN	Strain
0	5	0	1	0	-4	0	-35
5	200	5	194	5	184	5	155
10	385	10	379	10	363	10	344
15	554	15	570	15	530	15	534
20	744	20	766	20	703	20	711
25	936	25	951	25	882	25	904
30	1110	30	1146	30	1059	30	1097
35	1295	35	1329	35	1237	35	1290
40	1491	40	1530	40	1416	40	1476
45	1679	45	1771	45	1603	45	1642
50	2022	50	2020	50	1899	50	1973
55	2556	55	2555	55	2380	55	2296

Calibration of the Threaded Rods

Tube # 2		Tube # 4		Tube # 6		Tube # 8	
Load kN	Strain	Load kN	Strain	Load kN	Strain	Load kN	Strain
0	4	0	1	0	-3	0	0
5	210	5	76	5	172	5	176
10	368	10	285	10	329	10	333
15	490	15	844	15	494	15	500
20	664	20	1216	20	652	20	653
25	883	25	1477	25	817	25	865
30	1001	30	1608	30	982	30	1185
35	1205	35	1804	35	1167	35	1571
40	6479	40	2297	40	1394	40	9602
45	1529	45	4700	45	1785	45	11320
50	1821	50	14700	50	2465	50	17130
55		55		55	3589	55	16616

Calibration of the Tubes

# 1	Loading	Unloading	# 2	Loading	Unloading	# 9	Loading	Unloading
0	-131	-136	0	5	-10	0	0	-14
10	-279	-289	10	-110	-136	10	-223	-143
20	-432	-435	20	-226	-252	20	-360	-272
30	-574	-568	30	-373	-392	30	-486	-394
40	-717	-708	40	-521	-541	40	-614	-530
50	-877	-858	50	-668	-680	50	-741	-683
60	-1020	-1004	60	-825	-836	60	-872	-809
70	-1175	-1157	70	-990	-980	70	-1005	-945
80	-1328	-1303	80	-1147	-1120	80	-1091	-1082
90	-1477	-1448	90	-1292	-1272	90	-1231	-1219
100	-1630		100	-1447		100	-1366	
# 10	Loading	Unloading	# 11	Loading	Unloading	# 18	Loading	Unloading
0	-15	-21	0	0	-66	0	-500	-516
10	-147	-150	10	-188	-199	10	-683	-623
20	-288	-309	20	-331	-346	20	-864	-810
30	-462	-471	30	-472	-479	30	-1050	-1025
40	-616	-625	40	-615	-608	40	-1245	-1225
50	-781	-789	50	-757	-761	50	-1433	-1419
60	-933	-942	60	-914	-906	60	-1627	-1610
70	-1091	-1100	70	-1057	-1058	70	-1799	-1787
80	-1257	-1251	80	-1218	-1206	80	-1966	-1936
90	-1411	-1397	90	-1369	-1372	90	-2117	-2092
100	-1568		100	-1523		100	-2270	
# 19	Loading	Unloading	# 20	Loading	Unloading	# 21	Loading	Unloading
0	0	-5	0	0	-3	0	-5	-20
10	-263	-271	10	-166	-142	10	-148	-199
20	-443	-469	20	-309	-293	20	-302	-320
30	-621	-640	30	-450	-438	30	-454	-497
40	-787	-812	40	-596	-572	40	-620	-644
50	-950	-974	50	-738	-703	50	-782	-796
60	-1125	-1129	60	-881	-852	60	-940	-948
70	-1276	-1278	70	-1028	-1020	70	-1096	-1109
80	-1443	-1439	80	-1173	-1166	80	-1241	-1254
90	-1602	-1592	90	-1330	-1324	90	-1404	-1396
100	-1753		100	-1486		100	-1567	
# 22	Loading	Unloading	# 28	Loading	Unloading	# 29	Loading	Unloading
0	-33	-60	0	0	-11	0	0	-20
10	-212	-233	10	-167	-172	10	-200	-202
20	-394	-418	20	-327	-344	20	-403	-386
30	-570	-588	30	-505	-532	30	-560	-563
40	-730	-749	40	-607	-669	40	-726	-724
50	-883	-905	50	-840	-836	50	-880	-873

60	-1056	-1058	60	-990	-1008	60	-1036	-1025
70	-1210	-1208	70	-1152	-1170	70	-1183	-1179
80	-1364	-1366	80	-1327	-1319	80	-1346	-1334
90	-1519	-1512	90	-1493	-1473	90	-1500	-1483
100	-1676		100	-1634		100	-1657	
# 30	Loading	Unloading	**# 35**	Loading	Unloading	**# 36**	Loading	Unloading
0	-52	-95	0	-8	-52	0	-42	-62
10	-222	-259	10	-93	-84	10	-209	-248
20	-398	-434	20	-178	-173	20	-394	-391
30	-566	-602	30	-303	-284	30	-543	-533
40	-746	-766	40	-420	-397	40	-691	-660
50	-900	-926	50	-524	-517	50	-832	-820
60	-1065	-1083	60	-646	-639	60	-985	-967
70	-1227	-1239	70	-770	-769	70	-1141	-1120
80	-1385	-1390	80	-898	-886	80	-1285	-1260
90	-1550	-1540	90	-1030	-1032	90	-1423	-1405
100	-1710		100	-1153		100	-1570	
# 37	Loading	Unloading	**#5 A**	Loading	Unloading	**#5 B**	Loading	Unloading
0	15	-29	0	2198	2202	0	2067	2018
10	-144	-140	10	2113		10	1959	1889
20	-310	-314	20	2023	2056	20	1823	1747
30	-483	-480	30	1937	1965	30	1680	1617
40	-650	-646	40	1859	1890	40	1553	1511
50	-816	-815	50	1781	1802	50	1446	1415
60	-986	-980	60	1703	1715	60	1343	1329
70	-1138	-1139	70	1621	1637	70	1249	1242
80	-1298	-1283	80	1538	1547	80	1156	1159
90	-1455	-1429	90	1455	1462	90	1065	1068
100	-1608		100	1369		100	982	

Calibration of Load Cells at Tendons

The Least-Sequares method was used to interpolate the values, which were not in the tables. There was no error in reading the loads, so that the errors were in the strain measurements.
The following normal equations was used :

$$a\Sigma x_i^2 + b\Sigma x_i = \Sigma x_i Y_i,$$

$$a\Sigma x_i + bN = \Sigma Y_i.$$

Solving theses equations simultaneously gave the values for slope and intercept a and b.

Load Cell No.	a	B	Initial
1	-14.98	-127.27	-131.0
2	-14.81	50.05	5.0
5A	-8.20	2191.54	2198
5B	-10.98	2032.73	2067
9	-13.05	-73.95	0.0
10	-15.73	7.50	-15.0
11	-14.97	-19.04	0.0
15	-12.80	-80.23	-2.0
18	-18.06	-7.10	0.0
19	-17.06	-79.86	0.0
20	-14.65	-8.86	0.0
21	-15.69	6.23	-5.0
22	-16.32	-61.10	-33.0
28	-16.45	-5.14	0.0
29	-15.75	3.91	7.0
30	-16.55	-65.36	-52.0
35	-11.63	41.95	0.0
36	-15.14	-71.41	-42.0
37	-16.34	10.14	15.0
Col. #3	70.21	0.0	0.0
Col. #7	72.27	0.0	0.0
Col. #9	-5.37	0.0	0.0
Threaded Rod	38	0.0	0.0
Tube	33	0.0	0.0

REFERENCES

ACI Committee 318, Building Code Requirements for Reinforced Concrete (ACI 318-95) and Commentary, American Concrete Institute, Detroit, 1995.

ACI - ASCE Committee 426, Recommendations for Concrete Members Prestressed with Unbonded Tendons, ACI Structural Journal, Vol. 86, No. 3, May-June 1989, pp.301-318.

BS 8110-85, Structural Use of Concrete, Handbook to British Standard, 1985.

Burns N. H. and Hemakom R., Test of Post-Tensioned Flat Plate with Banded Tendons, Journal of Structural Engineering, ASCE, Vol. 111, No. 9, 1985, pp. 1899-1915.

Corley W. G. and Jirsa J. O., Equivalent Frame Analysis for Slab Design, ACI Structural Journal, Vol. 67, No. 11, Nov. 1970, pp. 875-884.

CSA Standard A23.3-94, Design of Concrete Structures for Buildings, Canadian Portland Cement Association, Ottawa, 1994.

CSA Standard A23.3-M84, Design of Concrete Structures for Buildings, Canadian Portland Association, Ottawa, 1984.

Dilger W. H. and Shatila M., Shear Strength of Prestressed Concrete Edge Slab-Column Connections with and without Shear Stud Reinforcement, Canadian Journal of Civil Engineering, Vol. 16, 1989, pp. 807-819.

Desayi P. and Seshadri H. K., Punching Shear Strength of Flat Slab Corner Column Connections, The British Journal of Structures and Buildings, Vol. 122, No. 1, Feb. 1997, pp. 21-26.

Design of Prestressed Concrete Flat Slabs, Report No. 2, The South African Institution of Civil Engineers, 1994.

Elgabry A., Shear and Moment Transfer of Concrete Flat Plates, Thesis presented to the University of Calgary, in partial fulfillment of the requirements for the degree of Ph.D., Calgary Alberta in 1991.

Elgabry A. and Ghali A., Transfer of Moments between Columns and Slabs, ACI Structural Journal, Vol. 93, No. 5, January-February 1996, pp. 56-61.

Foutch D. A., Gamble W. L., Sunidja H., Tests of Post-Tensioned Concrete Slab-Edge Column Connections, ACI Structural Journal, Vol. 87, No. 2, March-April 1990, pp. 167-179.

Franklin S.O. and Long A.E., The Punching Behaviour of Unbonded Post-Tensioned Flat Plates, Proc. Inst. Civil Engineers, Part 2, 73, September 1982, pp. 609-631.

Gardner N. J., Punching Shear Provisions for reinforced and prestressed concrete flat slabs, Canadian Journal of Civil Engineering, Vol. 23, No. 2, 1996, pp. 502-510.

Gardner N. J. and Rezai Kallage M., Punching Shear Strength of Continuous Post-Tensioned Concrete Flat Plates, ACI Structural Journal, In Press.

Gardner N. J. and Shao Xiao-Yun, Punching Shear of Continuous Flat Reinforced Concrete Slabs, ACI Structural Journal, Vol. 93, No. 2, March-April 1996, pp. 218-228.

Gerber L.L. and Burns N.H., Ultimate Strength Tests of Post-Tensioned Flat Plates, PCI Journal, Vol. 16, No. 6, November-December 1971, pp. 40-58.

Ghali A. and Megally S., Design for Punching Shear in Concrete: Critical Review of Canadian Standard CSA-A23.3-94, Canadian Journal of Civil Engineering; Vol. 23, No. 2, April 1996, pp. 444-456.

Grira M., A Critical Review of The Symmetric Punching Shear of Reinforced Concrete Flat Slabs, Thesis presented to the University of Ottawa, in partial fulfillment of the requirements for the degree of Master of Applied Science, Ottawa in 1990.

Kosut M., Burns N. H., and Winter V., Test of Post-Tensioned Flat Plate, Journal of Structural Engineering, Vol. 111, No. 9, Sept. 1985, pp.1916-1929.

Long A. E. and Cleland D. J., Post-Tensioned Concrete Flat Slabs at Edge Columns, ACI Materials Journal, Vol. 90, No. 3, May-June 1993, pp. 207-213.

Post-Tensioned Concrete Floors Design Handbook, The British Concrete Society, Technical Report No. 43, 1994.

Precast And Prestressed Concrete, Design Manual, Third Edition, Ottawa, Ontario, 1996.

Rangan B. V. and Hall A. S., Moment and shear transfer between slab and edge column, Journal of the ACI, Vol. 80, No. 3, 1983, pp. 183-191.

Regan P. E., The Punching Resistance of Prestressed Concrete Slabs, Proceeding of the Institute of Civil Engineers, Part 2, December 1985, pp. 657-680.

Rezai Kallage M., Punching Shear Strength of Continuous Post-Tensioned Concrete Flat Plate, Thesis presented to the University of Ottawa, in partial fulfillment of the requirements for the degree of Master of Applied Science, Ottawa in 1993.

Rice P. F., Hoffman E. S., Gustafson D. P. and Gouwens A. J., Structural Design Guide to the ACI Building Code, 3rd ed., 1985, pp. 134-135.

Saatcioglu M., Private communication, 1997.

Shehata Ibrahim A.E.M., Simplified method for estimating the punching resistance of reinforced concrete slabs, Materials and Structures, Vol. 23 No. 137, 1990, pp. 364-371.

Shehata Ibrahim A.E.M. and Regan P.E., Punching in reinforced concrete slabs, Journal of Structural Engineering, Vol. 115 No. 7, 1989, pp. 1726-1740.

Shehata Ibrahim A.E.M. and Shehata Lidia, Compressive strength of concrete elements with variable dimensions, Materials and Structures, Vol.22, No. 137, 1989, pp.264-268

Sherif A. G., Behaviour of Reinforce Concrete Flat Slabs, Thesis presented to the University of Calgary, in partial fulfillment of the requirements for the degree of Ph.D., Calgary Alberta in 1996.

Sherif A. G. and Dilger W. H., Critical Review of The CSA 23.3 - 94 Punching Shear Strength Provisions for Interior Columns, Canadian Journal of Civil Engineering, Vol. 23, No. 5, Oct. 1996, pp. 998-1011.

Technical Notes, Post-Tensioning Institute, Issue No. 4, Phoenix Arizona, March 1994.

IMAGE EVALUATION
TEST TARGET (QA-3)

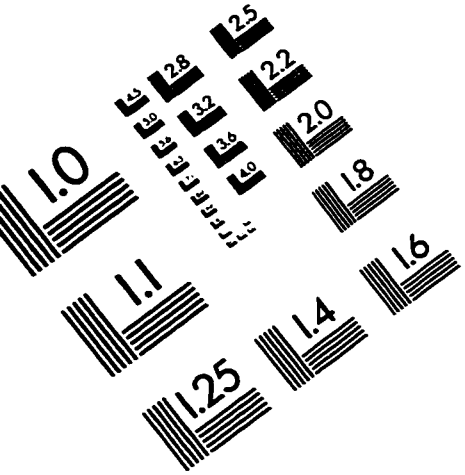

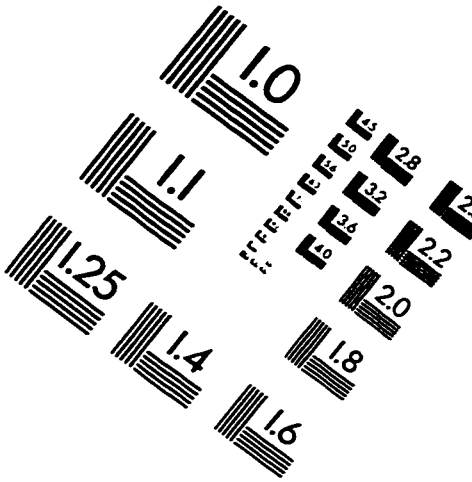

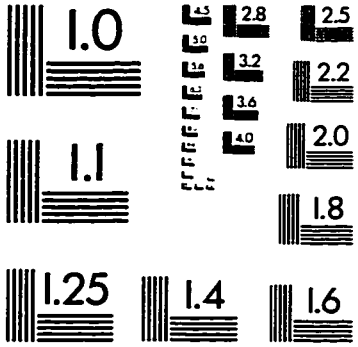

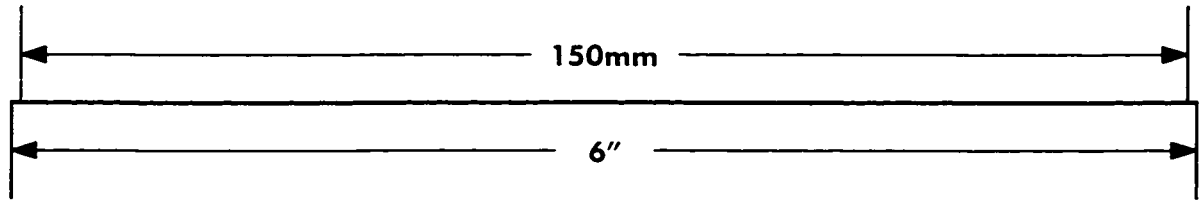

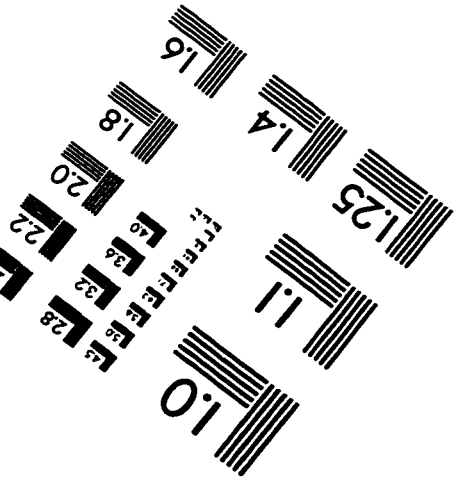

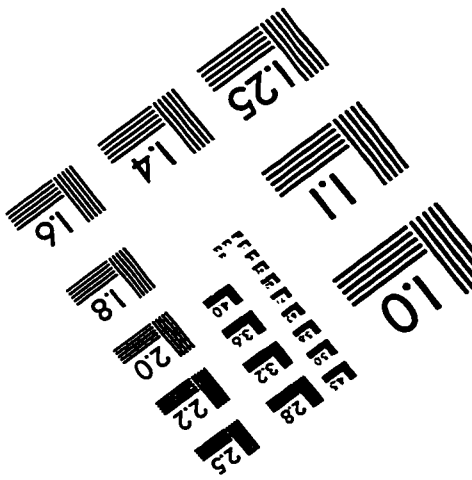

APPLIED IMAGE, Inc
1653 East Main Street
Rochester, NY 14609 USA
Phone: 716/482-0300
Fax: 716/288-5989